Modeling of bending-torsion couplings in active-bending structures. Application to the design of elastic gridshell.

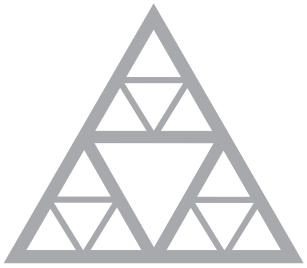

École des Ponts

ParisTech

Thèse n. xxxxx
présenté le 01 décembre 2017
à l'Ecole des Ponts ParisTech
laboratoire Navier
Université Paris-Est

pour l'obtention du grade de Docteur ès Sciences
par

Lionel du Peloux

acceptée sur proposition du jury:

Prof Name Surname, président du jury
Prof Name Surname, directeur de thèse
Prof Name Surname, rapporteur
Prof Name Surname, rapporteur
Prof Name Surname, rapporteur

Paris, Ecole des Ponts ParisTech, 2016

Contents

Index of notation

Geometry of curves

$\boldsymbol{t}$	The unit tangent vector.
$\boldsymbol{n}$	The unit normal vector.
$\boldsymbol{b}$	The unit binormal vector.
τ_f	The torsion of Frenet.
$\boldsymbol{\kappa b}$	The curvature binormal vector.
$\boldsymbol{\Omega}$	The darboux vector.

Mechanics of rods

$\gamma, \overline{\gamma}$	Centerline curve – reference configuration.
γ	The centerline curve – actual configuration.
s	The arc length of the centerline – reference configuration.
s_t	The arc length of the centerline – actual configuration.
$\overline{\boldsymbol{x}}$	The centerline position vector – reference configuration.
$\boldsymbol{x}$	The centerline position vector – actual configuration.
$\overline{\boldsymbol{\nu}}$	The force strain vector – reference configuration.
$\boldsymbol{\nu}$	The force strain vector – actual configuration.
$\overline{\boldsymbol{\varkappa}}$	The material curvature (or moment strain) vector – reference configuration.
$\boldsymbol{\varkappa}$	The material curvature (or moment strain) vector – actual configuration.
$\mathcal{E}_s$	The streching energy.
$\mathcal{E}_b$	The bending energy.
$\mathcal{E}_t$	The twisting energy.

Elastic gridshells Part I

1 A neat way to build free-form architecture

2 Experimenting elastic gridshells

Rich Kirchhoff beam model Part II

3 Geometry of smooth and discrete space curves

3.1 Introduction

idée : Rapprocher l'étude des courbes continues et des discrétisées avec le concept de modèle de la «courbe polygone» de Leibniz et de ses successeurs, une infinité de côtés infiniment petits. [Del11, p.235]

Voir aussi que la geometry des space curves semble intimement liée à celle des surface. [Coo13, Del11]

> Car les courbes n'étant que des polygones d'une infinité de côtés, et ne différent entre elles que par la différence des angles que ces côtés infiniment petits font entre eux; il n'appartient qu'à l'Analyse des infiniment petits de déterminer la position de ces cotés pour avoir la courbure qu'ils forment [...] [, Liebniz].

Attention à la terminologie smooth vs. continious :

> A smooth curve is a curve which is a smooth function, where the word "curve" is interpreted in the analytic geometry context. In particular, a smooth curve is a continuous map f from a one-dimensional space to an n-dimensional space which on its domain has continuous derivatives up to a desired order.[1]

3.1.1 Goals and contributions

Dans ce chapitre, après un bref rappel sur le cadre mathématique d'étude des courbes paramétrique de l'espace, on présente les notions de courbures et de torsion géométrique associées au repère de Frenet. On montre ensuite le cas plus général d'un repère mobile

[1] Definition of a smooth curve from mathworld : http://mathworld.wolfram.com/SmoothCurve.html

quelconque attaché à une courbe gamma. On définit enfin la particularité d'un repère mobile adapté à un courbe, et on présente, en sus du repère de Frenet, une approche différente pour accrocher des repères le long d'une courbe (Bishop / RMF / Zéro-twisting frame)

Contributions : présentation et comparaison de différentes façons d'estimer la courbure discrete

3.1.2 Related work

(author?) [Bis75] [Bis75] **(author?) (year?)**

[Bis75] [BWR+08] [Hof08] [**?**] [Fre52] [Del07] [FGSS14] [Gug89] [Klo86]

3.1.3 Overview

3.2 Parametric curves

3.2.1 Definition

Let I be an interval of $\mathbb{R}$ and $F\colon t \mapsto F(t)$ be a map of $\mathcal{C}(I, \mathbb{R}^3)$. Then $\gamma = (I, F)$ is called a *parametric curve* and :

- The 2-uplet (I, F) is called a *parametrization* of γ
- $\gamma = F(I) = \{F(t), t \in I\}$ is called the *graph* or *trace* of γ
- γ is said to be $\mathcal{C}^k$ if $F \in \mathcal{C}^k(I, \mathbb{R}^3)$

Note that for a given graph in $\mathbb{R}^3$ they may be different possible parameterizations. Thereafter γ will simply refers to its graph $F(I)$.

3.2.2 Regularity

Let $\gamma = (I, F)$ be a parametric curve, and $t_0 \in I$ be a parameter.

- A point of parameter t_0 is called *regular* if $F'(t_0) \neq 0$.
  The curve γ is called *regular* if γ is $\mathcal{C}^1$ and $F'(t) \neq 0, \forall t \in I$
- A point of parameter t_0 is called *biregular* if $F'(t_0)$ and $F''(t_0)$ are not collinear
  The curve γ is called *biregular* if γ is $\mathcal{C}^2$ and $F'(t) \cdot F''(t) \neq 0, \forall t \in I$

3.2.3 Reparametrization

Let $\gamma = (I, F)$ be a parametric curve of class $\mathcal{C}^k$, $J \in \mathbb{R}^3$ an interval, and $\varphi \colon I \mapsto J$ be a $\mathcal{C}^k$ diffeomorphisme. Lets define $G = F \circ \varphi$. Then :

- $G \in \mathcal{C}^k(J, \mathbb{R}^3)$
- $G(J) = F(I)$
- φ is said to be an admissible *change of parameter* for γ
- (J, G) is said to be another *admissible parametrization* for γ

3.2.4 Natural parametrization

Let γ be a space curve of class $\mathcal{C}^1$. A parametrization (I, F) of γ is called *natural* if $\|F'(t)\| = 1, \forall t \in I$. Thus :

- The curve is necessarily regular
- F is strictly monotonic

3.2.5 Curve length

Let $\gamma = (I, F)$ be a parametric curve of class $\mathcal{C}^1$. The length of γ is define as :

$$L = \int_I \|F'(t)\| dt \tag{3.1}$$

Note that the length of γ is invariant under reparametrization.

3.2.6 Arc length parametrization

Let $\gamma = (I, F)$ be a regular parametric curve. Let $t_0 \in I$ be a given parameter. The following map is said to be the *arc length of origin* t_0 of γ :

$$s \colon t \mapsto \int_{t_0}^{t} \|F'(u)\| du \quad , \quad s \in I \times \mathbb{R} \tag{3.2}$$

The arc length $s \colon I \mapsto s(I)$ is an admissible change of parameter for γ. Indeed, s is a $\mathcal{C}^1$ diffeomorphisme because it is bijective ($s' > 0$).

Lets define $G = F \circ s^{-1}$ and $J = s(I)$. Thus (J, G) is a natural reparametrization of γ and $\|G'(s)\| = 1, \forall s \in J$. This parametrization is preferred because the natural parameter s traverses the image of γ at unit speed ($\|G'\| = 1$).[2]

[2] Regular curves are also known as *unit speed* curves.

Thereafter, for a regular curve γ : $\gamma(t)$ will denote the point $F(t)$ of parameter $t \in I$; while $\gamma(s)$ will denote the point $G(s)$ of arc length $s \in J = [0, L]$.

3.3 Frenet trihedron

The Frenet trihedron is a fundamental mathematical tool from the field of differential geometry to study local characterization of planar and non-planar space curves. It is a direct orthonormal basis attached to any point P, of parameter $t \in I$, on a parametric curve γ. This basis is composed of three unit vectors $\{\boldsymbol{t}(t), \boldsymbol{n}(t), \boldsymbol{b}(t)\}$ called respectively the *tangent*, the *normal*, and the *binormal* unit vectors.[3]

Introduced by Frenet in 1847 in his thesis "Courbes à Double Courbure" [Fre52], it brings out intrinsic local properties of space curves : the curvature (κ) which evaluates the deviance of γ from being a straight line (see §3.4.1) ; and the torsion (τ_f) which evaluates the deviance of γ from being a planar curve (see §3.4.2).

These quantities, also known as "generalized curvatures" in modern differential geometry, are essential to understand the geometry of space curves. As stated by the *Fundamental Theorem of Space Curves*[4], a curve is fully determined by its curvature and torsion up to a solid movement in space (see §3.4.3).

3.3.1 Tangent vector

The first component of the Frenet trihedron is called the *unit tangent vector*. Let $\gamma = (I, F)$ be a regular parametric curve. Let $t \in I$ be a parameter. The *unit tangent vector* is defined as :

$$\boldsymbol{t}(t) = \frac{\gamma'(t)}{\|\gamma'(t)\|} \quad , \quad \|\boldsymbol{t}(t)\| = 1 \tag{3.3}$$

For a curve parametrized by arc length, this expression simply becomes :

$$\boldsymbol{t}(s) = \gamma'(s) \quad , \quad s \in [0, L] \tag{3.4}$$

In differential geometry, the unit tangente to the curve γ at point P_0 is obtained as the limit of the (normalized) vector $\overrightarrow{P_0P}$, as P approches P_0 on the path γ (fig. 3.1). For a regular curve, the left-sided and right-sided limits coïncide as P^- and P^+ approche P_0 respectively from its left and right sides :

$$\boldsymbol{t}(P_0) = \lim_{P \to P_0} \frac{\overrightarrow{P_0P}}{\|\overrightarrow{P_0P}\|} = \lim_{P^- \to P_0} \frac{\overrightarrow{P_0P^-}}{\|\overrightarrow{P_0P^-}\|} = \lim_{P^+ \to P_0} \frac{\overrightarrow{P_0P^+}}{\|\overrightarrow{P_0P^+}\|} \tag{3.5}$$

[3] Strictly speaking, the map $\boldsymbol{t} : t \longmapsto \boldsymbol{t}(t)$ is a *vector field* while $\boldsymbol{t}(t)$ is a *vector* of $\mathbb{R}^3$. For the sake of simplicity, and if there is no ambiguity, these two notions will not be explicitly distinguished hereinafter.

[4] The full demonstration of this theorem is attributed to Darboux in [Del07, p.11].

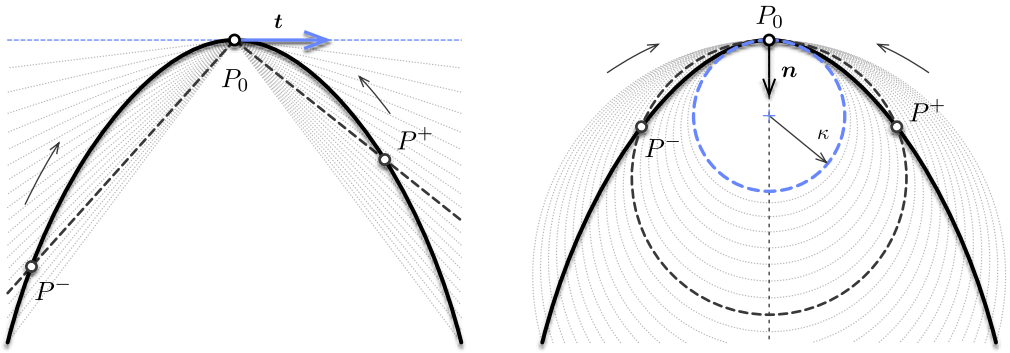

(a) Curve's tangent.

(b) Curve's normal and osculating circle.

Figure 3.1 – Differential definition of Frenet's trihedron at given point P_0.

3.3.2 Normal vector

The second component of the Frenet trihedron is called the *unit normal vector*. It is constructed from $\boldsymbol{t}'$ which is necessarily orthogonal to $\boldsymbol{t}$. Indeed :

$$\|\boldsymbol{t}\| = 1 \Rightarrow \boldsymbol{t}' \cdot \boldsymbol{t} = 0 \Leftrightarrow \boldsymbol{t}' \perp \boldsymbol{t} \tag{3.6}$$

Let $\gamma = (I, F)$ be a biregular parametric curve.[5] Let $t \in I$ be a parameter. The *unit normal vector* is defined as :

$$\boldsymbol{n}(t) = \frac{\boldsymbol{t}'(t)}{\|\boldsymbol{t}'(t)\|} = \frac{\gamma'(t) \times (\gamma''(t) \times \gamma'(t))}{\|\gamma'(t)\|^3} \quad , \quad \|\boldsymbol{n}(t)\| = 1 \tag{3.7}$$

For a curve parametrized by arc length, this expression simply becomes :

$$\boldsymbol{n}(s) = \frac{\boldsymbol{t}'(s)}{\|\boldsymbol{t}'(s)\|} = \gamma'(s) \times (\gamma''(s) \times \gamma'(s)) \quad , \quad s \in [0, L] \tag{3.8}$$

In differential geometry, the unit normal to the curve γ at point P_0 is obtained as the limit of the (normalized) vector $\overrightarrow{P_0P^+} - \overrightarrow{P_0P^-}$, as P^- and P^+ approche P_0 respectively from its left and right sides (fig. 3.1) :

$$\boldsymbol{n}(P_0) = \lim \frac{\overrightarrow{P_0P^+} - \overrightarrow{P_0P^-}}{\|\overrightarrow{P_0P^+} - \overrightarrow{P_0P^-}\|} \tag{3.9}$$

Remark that the notion of *normal vector* is ambiguous for non-planar curves as there is an infinite number of possible normal vectors lying in the plane orthogonal to the curve's tangent. In practice, the tangent derivative is a convenient choice as it allows to extend the notion of curvature from planar to non-planar space curves. However, we will see (§3.5.6) that other kind of trihedron can be constructed regarding this choice and that one of them is especially suitable for the study of slender beams.

[5] Note that $\boldsymbol{n}$ exists if only γ is biregular, that is $\boldsymbol{t}'$ never vanishes or, equivalently, γ is never locally a straight line.

3.3.3 Binormal vector

The third vector of Frenet's trihedron is called the *unit binormal vector*. It is constructed from $\boldsymbol{t}$ and $\boldsymbol{n}$ to form an orthonormal direct basis of $\mathbb{R}^3$. Let $\gamma = (I, F)$ be a biregular parametric curve. Let $t \in I$ be a parameter. The *unit binormal vector* is defined as :

$$\boldsymbol{b}(t) = \boldsymbol{t}(t) \times \boldsymbol{n}(t) = \frac{\gamma'(t) \times \gamma''(t)}{\|\gamma'(t) \times \gamma''(t)\|} \quad , \quad \|\boldsymbol{b}(t)\| = 1 \tag{3.10}$$

For a curve parametrized by arc length, this expression simply becomes :

$$\boldsymbol{b}(s) = \boldsymbol{t}(s) \times \boldsymbol{n}(s) = \gamma'(s) \times \gamma''(s) \quad , \quad s \in [0, L] \tag{3.11}$$

3.3.4 Osculating plane

The tangent and normal unit vectors $\{\boldsymbol{t}, \boldsymbol{n}\}$ form an orthonormal basis of the so-called *osculating plane*, whereas the binormal vector ($\boldsymbol{b}$) is orthogonal to it. This plane is of prime importance because it is the plane in which the curve takes its curvature (see §3.4.1).

As reported in [Del07, p.45], the osculating plane seems to have been first introduced by Bernoulli as the plane passing through three infinitely near points on a curve.[6] Likewise, in modern differential geometry, the osculating plane is defined as the limit of the plane passing through the points P^-, P_0 and P^+ while P^- and P^+ approche P_0 respectively from its left and right side (fig. 3.1).

Note that the normal unit vector and the binormal unit vector $\{\boldsymbol{n}, \boldsymbol{b}\}$ define the so-called *normal plane*, while the normal tangent vector and the binormal unit vector $\{\boldsymbol{t}, \boldsymbol{b}\}$ define the so-called *rectifying plane*. This planes are secondary for the present study.

3.4 Curves of double curvature

The study of space curves belongs to the field of differential geometry. According to [Del07, p.28], the terminology *curve of double curvature* is attributed to Pitot around 1724.[7] However, as stated in [Coo13, p.321] curvature and torsion where probably first thought by Monge around 1771.[8] It is also interesting to note that, at that time, "curvature" was

[6] "Voco autem planum osculans, quod transit per tria curvae quaesitae puncta infinite sibi invicem propinqua" [Ber28, p.113].

[7] "Les Anciens ont nommé cette courbe Spirale ou Hélice ; parce que la formation sur le cylindre suit la même analogie que la formation d'une spirale ordinaire sur un plan; mais elle est bien différente de la spirale ordinaire, étant une des courbes à double courbure, ou une des lignes qu'on conçoit tracée sur la surface des Solides. Peut-être que ces sortes de courbes à double courbure, ou prises sur la surface des Solides, feront un jour l'objet des recherches des géomètres. Celle que nous venons d'examiner est, je crois, la plus simple de toutes. " [Pit26, p.28]

[8] "On appelle point d'inflexion, dans une courbe plane, le point où cette ligne, après avoir été concave dans un sens, cesse de l'être pour devenir concave dans l'autre sens. Il est évident que dans ce point, la courbe perd sa courbure, et que les deux élémens consécutifs sont en ligne droite. Mais une courbe à double courbure peut perdre chacune de ses courbures en particulier, ou les perdre toutes deux dans le même point ; c'est-à-dire, qu'il peut arriver ou que trois élémens consécutifs d'une même courbe à double courbure se trouvent dans un même plan, ou que deux de ces élémens soient en ligne droite. Il suit de là que les

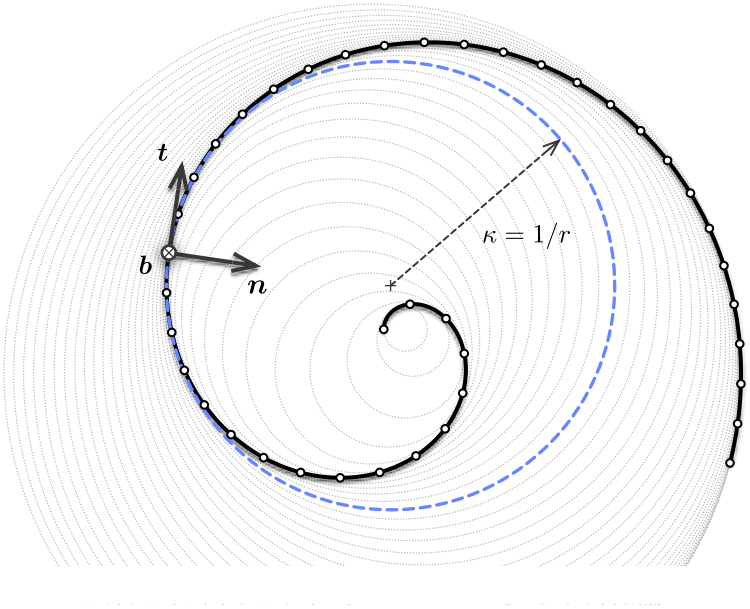

Figure 3.2 – Osculating circles for a spiral curve at different parameters.

also referred to as "flexure", reflecting that the study of physical problems (e.g. *elastica*) and the study of curves of double curvature were intimately related to each other.

Space curves were historically understood as *curves of double curvature* by extension to the case of planar curves, where the curvature measures the deviance of a curve from being a straight line. The second curvature, nowadays known as the "torsion" or "second generalized curvature", measures the deviance of a curve from being plane.

3.4.1 First invariant : the curvature

In differential geometry, the *osculating circle* is defined as the limit of the circle passing through the points P^-, P_0 and P^+ while P^- and P^+ approche P_0 (fig. 3.1). This circle lies on the osculating plane and its radius is nothing but the inverse of the local curvature of a curve.[9] While the tangent gives the best local approximation of the curve as a straight line, the osculating circle gives the best local approximation of that curve as an arc.

The curvature is also known to be the *gradient of arc length* (see [Vou14, p.4]) and calculated as : $\nabla L = \kappa \boldsymbol{n}$. Thus, the curvature gives the first-order variation in arc length when deforming a curve γ in a closed enough curve $\gamma + \epsilon\delta\gamma$:

$$L(\gamma + \epsilon\delta\gamma) = L(\gamma) + \epsilon(\nabla L \cdot \delta\gamma) + o(\epsilon) \quad , \quad \nabla L \cdot \delta\gamma = \frac{d}{d\epsilon} L(\gamma + \epsilon\delta\gamma)\Big|_{\epsilon=0} \tag{3.12}$$

courbes à double courbure peuvent avoir deux espèces d'inflexions; la première a lieu lorsque la courbe devient plane, et nous l'appellerons simple inflexion; la seconde, que nous appellerons double inflexion, a lieu lorsque la courbe devient droite dans un de ses points." [Mon09, p.363].

[9] As explained by Euler itself, at a given arc length parameter (s), the osculating plane is the plane in which a curve takes its curvature : "in quo bina fili elementa proxima in curvantur" [Eul75, p.364].

This is easily understood in the case of a circle of radius r extended to a circle of radius $r + dr$, where the total arc length variation is given by : $L(r + dr) - L(r) = \kappa dr L(r)$.

Note that due to the inner product with the normal vector, only the normal component of the deformation results in an effective extension of the curve. This point is worth to note as it will be related to the *inextensibility assumption* made later in our beam model.

Curvature

Let γ be a regular arc length parametrized curve. Let $s \in [0, L]$ be an arc length parameter. The *curvature* is a positive scalar quantity defined as :

$$\kappa(s) = \|\boldsymbol{t}'(s)\| \geq 0 \quad , \quad \boldsymbol{t}'(s) = \kappa(s)\boldsymbol{n}(s) \tag{3.13}$$

The curvature is *independent* regarding the choice of parametrization. This makes the curvature an *intrinsic property* of a given curve and that is why it is also referred to as a *geometric invariant*. Following [GAS06, pp.203-204] it can be computed for any parametrization (I, F) of γ as :

$$\kappa(t) = \frac{\|\gamma'(t) \times \gamma''(t)\|}{\|\gamma'(t)\|^3} \quad , \quad \boldsymbol{t}'(t) = \|\gamma'(t)\|\kappa(t)\boldsymbol{n}(t) \tag{3.14}$$

Note that in eq. (3.13) the prime denotes the derivative regarding the natural parameter (s) while it denotes the derivative regarding any parameter (t) in eq. (3.14). Consequently, the *speed* of the curve's parametrization appears in the latter equation :

$$v(t) = \frac{ds}{dt} = \|\gamma'(t)\| = s'(t) \tag{3.15}$$

The curvature measures how much a curve *bends instantaneously* in its osculating plane, that is how fast the tangent vector is rotating in the osculating plane around the binormal vector. In differential geometry this is expressed as :

$$\kappa(s) = \lim_{ds \to 0} \frac{\angle(\boldsymbol{t}(s), \boldsymbol{t}(s + ds))}{ds} = \lim_{ds \to 0} \frac{(\boldsymbol{t}(s + ds) - \boldsymbol{t}(s)) \cdot \boldsymbol{n}(s)}{ds} \tag{3.16}$$

This is equivalent as measuring how fast the osculating plane itself is rotating around the binormal vector. Consequently a curve is locally a *straight line* when its curvature vanishes $(\kappa(s) = 0)$.

Radius of curvature

The *radius of curvature* is defined as the inverse of the curvature $(r = 1/\kappa)$. From a geometric point of view, one can demonstrate that it is the radius of the osculating circle (fig. 3.2). Remark that where the curvature vanishes the radius of curvature goes to infinity ; that is the osculating circle becomes a line, a circle of infinite radius.

Center of curvature

The *center of curvature* is defined as the center of the osculating circle (fig. 3.2). The locus of all the centers of curvature of a curve is called the *evolute*.

Curvature binormal vector

Finally, following [BWR+08] we define the *curvature binormal vector*. Let γ be a biregular arc length parametrized curve. Let $s \in [0, L]$ be an arc length parameter. The *curvature binormal vector* is defined as :

$$\boldsymbol{\kappa b}(s) = \boldsymbol{t}(s) \times \boldsymbol{t}'(s) = \kappa(s) \cdot \boldsymbol{b}(s) \quad , \quad \|\boldsymbol{\kappa b}(s)\| = \kappa(s) \tag{3.17}$$

This vector will be useful as it embed all the necessary information on the curve's curvature. We will see (§3.5.6) that this vector is associated to the angular velocity of a specific adapted moving frame attached to the curve and called the *Bishop frame*.

3.4.2 Second invariant : the torsion

Let γ be a biregular arc length parametrized curve. Let $s \in [0, L]$ be an arc length parameter. The *torsion* is a scalar quantity defined as :

$$\tau_f(s) = \boldsymbol{n}'(s) \cdot \boldsymbol{b}(s) = -\boldsymbol{b}'(s) \cdot \boldsymbol{n}(s) \tag{3.18}$$

The torsion is *independent* regarding the choice of parametrization. This makes the torsion an *intrinsic property* of a given curve and that is why it is also referred to as a *geometric invariant*. Following [GAS06, p.204] it can be computed for any parametrization (I, F) of γ as :

$$\tau_f(t) = \frac{(\gamma'(t) \times \gamma'(t)) \cdot \gamma''(t)}{\|\gamma'(t) \times \gamma''(t)\|^2} \quad when \quad \kappa(t) > 0 \tag{3.19}$$

The torsion measures how much a curve goes *instantaneously out of its plane*, that is to say how fast the normal or binormal vectors are rotating in the normal plane around the tangent vector. In differential geometry this is expressed as :

$$\tau_f(s) = \lim_{ds \to 0} \frac{\angle(\boldsymbol{n}(s), \boldsymbol{n}(s+ds))}{ds} = \lim_{ds \to 0} \frac{(\boldsymbol{n}(s+ds) - \boldsymbol{n}(s)) \cdot \boldsymbol{b}(s)}{ds} \tag{3.20}$$

This is equivalent as measuring how fast the osculating plane is rotating around the tangent vector. Consequently a curve is locally *plane* when its torsion vanishes ($\tau_f(s) = 0$).

Remark that the *torsion* is denoted "τ_f" and not simply "τ" as the latter will be reserved to denote any angular velocity of a moving adapted frame around its tangent vector. Thus, τ_f refers to the particular angular velocity of the Frenet trihedron around it's tangent vector. This torsion, which is a geometric property of the curve, will be indifferently referred to as the *Frenet torsion* or the *geometric torsion*.

3.4.3 Fundamental theorem of space curves

This two *generalized curvatures*, respectively the curvature (κ) and the torsion (τ_f), are *invariant* regarding the choice of parametrization and under *euclidean motions*. The *Fundamental theorem of space curves* states that a curve is fully described, up to a Euclidean motion of $\mathbb{R}^3$, by its positive curvature ($\kappa > 0$) and torsion (τ) [GAS06, p.229].

3.4.4 Serret-Frenet formulas

The *Fundamental theorem of space curves* is somehow a consequence of the *Serret-Frenet formulas*, which is the first-order system of differential equations satisfied by the Frenet trihedron. Let γ be a biregular arc length parametrized curve. Let $s \in [0, L]$ be an arc length parameter. Then, the Frenet trihedron satisfies the following formulas :

$$\begin{cases} \boldsymbol{t}'(s) = \kappa(s)\boldsymbol{n}(s) \\ \boldsymbol{n}'(s) = -\kappa(s)\boldsymbol{t}(s) + \tau_f(s)\boldsymbol{b}(s) \\ \boldsymbol{b}'(s) = -\tau_f(s)\boldsymbol{n}(s) \end{cases} \tag{3.21}$$

This system can be seen as the *equations of motion* of the Frenet trihedron moving along the curve γ at unit speed ($\|\gamma'\| = 1$). Indeed, introducing its *angular velocity vector* also known as the *Darboux vector* ($\boldsymbol{\Omega_f}$), the previous system is expressed as :

$$\begin{bmatrix} \boldsymbol{t}'(s) \\ \boldsymbol{n}'(s) \\ \boldsymbol{b}'(s) \end{bmatrix} = \boldsymbol{\Omega_f}(s) \times \begin{bmatrix} \boldsymbol{t}(s) \\ \boldsymbol{n}(s) \\ \boldsymbol{b}(s) \end{bmatrix} \quad where \quad \boldsymbol{\Omega_f}(s) = \begin{bmatrix} \tau_f(s) \\ 0 \\ \kappa(s) \end{bmatrix} \tag{3.22}$$

Because the Frenet trihedron satisfies a first-order system of differential equations of parameters κ and τ_f it is possible, by integration, to reconstruct the trace of the moving frame and thus the curve, up to a constant of integration (a trihedron in this case).

Finally, those formulas can be generalized to any non unit-speed parametrization of a curve[10]. Let $\gamma = (I, F)$ be a biregular parametric curve. Let $t \in I$ be a parameter. Then the following *generalized Serret-Frenet formulas* hold :

$$\begin{cases} \boldsymbol{t}'(t) = v(t)\kappa(t)\boldsymbol{n}(t) \\ \boldsymbol{n}'(t) = -v(t)\kappa(t)\boldsymbol{t}(t) + v(t)\tau_f(s)\boldsymbol{b}(t) \\ \boldsymbol{b}'(t) = -v(t)\tau_f(t)\boldsymbol{n}(t) \end{cases} \tag{3.23}$$

Again, this system can be seen as the *equations of motion* of the Frenet trihedron moving along the curve γ at non unit-speed ($v(t) = \|\gamma'(t)\|$). This time the *angular velocity vector* ($\boldsymbol{\Omega}$) is distinct from the *Darboux vector* ($\boldsymbol{\Omega_f}$) and the previous system is expressed as :

$$\begin{bmatrix} \boldsymbol{t}'(t) \\ \boldsymbol{n}'(t) \\ \boldsymbol{b}'(t) \end{bmatrix} = \boldsymbol{\Omega}(t) \times \begin{bmatrix} \boldsymbol{t}(t) \\ \boldsymbol{n}(t) \\ \boldsymbol{b}(t) \end{bmatrix} \quad where \quad \boldsymbol{\Omega}(t) = v(t) \begin{bmatrix} \tau_f(t) \\ 0 \\ \kappa(t) \end{bmatrix} \tag{3.24}$$

[10] See [GAS06, p.203] for a complete proof.

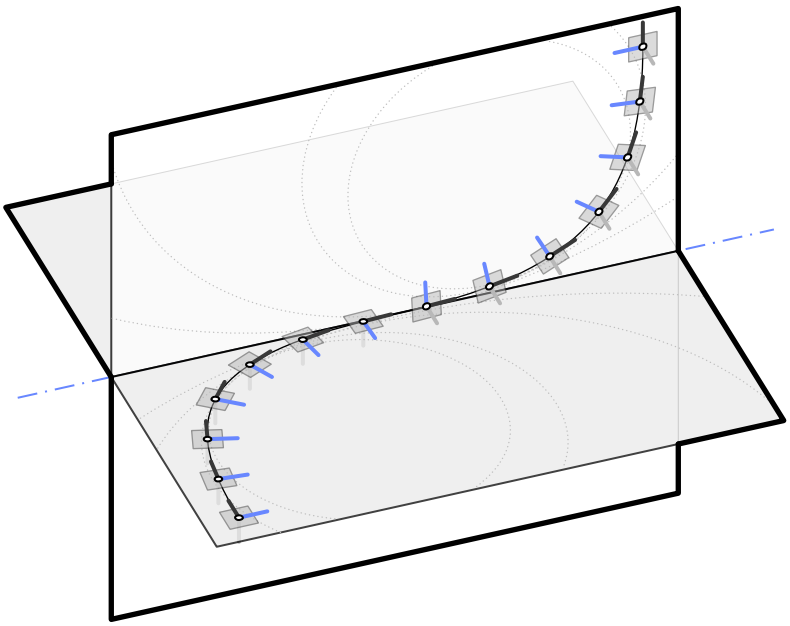

Figure 3.3 – Geometric torsion and rotation of the osculating plane. Note the existence of an inflexion point with a vanishing curvature and a discontinuity of both τ_f and the osculating plane.

3.5 Curve framing

While the Frenet trihedron "has long been the standard vehicle for analysing properties of the curve invariant[11] under euclidean motions" [Bis75, p.1], a curve can be potentially framed with any arbitrary *moving frame*, understood as an *orthonormal basis field*. Thus, the Frenet frame is not the only way to frame a curve and other frames may or may not exhibit some interesting properties.[12]

In his paper [Bis75] Bishop establishes the differential equation that a moving frame must satisfy and remarks that, because of the orthnormality condition, the first derivatives of the frame components can be expressed in terms of themselves through a skew-symmetric coefficient matrix. For such a frame, the understanding of its motion along the curve is thus reduced to the knowledge of only three scalar coefficient functions. He remarks that most of the interesting properties that the Frenet frame exhibits are due to the fact that one of this coefficient function is vanishing everywhere on the curve (that is the frame is *rotation-minimizing* regarding one of its components) ; and that the Frenet frame is *adapted* to the curve (that is one of its components is nothing but the unit tangent vector).

In this section we introduce the *moving frame* notion and two properties of interest such a frame can exhibit in addition, that is : to be *adapted* to the curve ; and to be *rotation-minimizing* regrading a given direction. We then reconsider the case of the Frenet frame

[11] Namely the curvature (κ) and the Frenet torsion (τ_f).
[12] Recall the title of Bishop's paper : "There is more than one way to frame a curve" [Bis75].

regrading this mathematical framework. Finally, we introduce the *zero-twisting* frame also known as the *bishop* frame.[13] This tool will be fundamental for our futur study of slender beams.

3.5.1 Moving frame

Let γ be a curve parametrized by arc length. A map F which associates to each point of arc length parameter s a direct orthonormal trihedron is said toi be a *moving frame* :

$$\begin{array}{rccl} F: & [0,L] & \longrightarrow & \mathcal{SO}_3(\mathbb{R}) \\ & s & \longmapsto & F(s) = \{\boldsymbol{e}_3(s), \boldsymbol{e}_1(s), \boldsymbol{e}_2(s)\} \end{array} \tag{3.25}$$

Consequently, a moving frame F attached to γ satisfies for all $s \in [0, L]$:

$$\begin{cases} \|\boldsymbol{e}_i(s)\| = 1 \\ \boldsymbol{e}_i(s) \cdot \boldsymbol{e}_j(s) = 0 \quad , \quad i \neq j \end{cases} \tag{3.26}$$

The term "moving frame" will refer indifferently to the map itself (denoted $F = \{\boldsymbol{e}_3, \boldsymbol{e}_1, \boldsymbol{e}_2\}$), or to a specific evaluation of the map (denoted $F(s) = \{\boldsymbol{e}_3(s), \boldsymbol{e}_1(s), \boldsymbol{e}_2(s)\}$).

Governing equations

Computing the derivatives of the previous relationships leads to the following system of differential equations that the frame must satisfy for all $s \in [0, L]$:

$$\begin{cases} \boldsymbol{e}_i'(s) \cdot \boldsymbol{e}_i(s) = 0 \\ \boldsymbol{e}_i'(s) \cdot \boldsymbol{e}_j(s) = -\boldsymbol{e}_i(s) \cdot \boldsymbol{e}_j'(s) \quad , \quad i \neq j \end{cases} \tag{3.27}$$

Thus, there exists 3 scalar functions (τ, k_1, k_2) such that $\{\boldsymbol{e}_3', \boldsymbol{e}_1', \boldsymbol{e}_2'\}$ can be expressed in the basis $\{\boldsymbol{e}_3, \boldsymbol{e}_1, \boldsymbol{e}_2\}$:

$$\begin{cases} \boldsymbol{e}_3'(s) = k_2(s)\boldsymbol{e}_1(s) - k_1(s)\boldsymbol{e}_2(s) \\ \boldsymbol{e}_1'(s) = -k_2(s)\boldsymbol{e}_3(s) + \tau(s)\boldsymbol{e}_2(s) \\ \boldsymbol{e}_2'(s) = k_1(s)\boldsymbol{e}_3(s) - \tau(s)\boldsymbol{e}_1(s) \end{cases} \tag{3.28}$$

It is common to rewrite this first-order linear system of differential equations as a matrix equation : [14,15]

$$\begin{bmatrix} \boldsymbol{e}_3'(s) \\ \boldsymbol{e}_1'(s) \\ \boldsymbol{e}_2'(s) \end{bmatrix} = \begin{bmatrix} 0 & k_2(s) & -k_1(s) \\ -k_2(s) & 0 & \tau(s) \\ k_1(s) & -\tau(s) & 0 \end{bmatrix} \begin{bmatrix} \boldsymbol{e}_3(s) \\ \boldsymbol{e}_1(s) \\ \boldsymbol{e}_2(s) \end{bmatrix} \tag{3.29}$$

[13] Named after Bishop who introduced it.

[14] In the case of a space curve, where $\boldsymbol{e}_3$ is chosen to be the curve tangent unit vector and $\boldsymbol{e}_1$ is chosen to be the curve normal unit vector, this set of equations is known as the *Serret-Frenet formulas*.

[15] In the case of a space curve drawn on a surface, where $\boldsymbol{e}_3$ is chosen to be the curve tangent unit vector and $\boldsymbol{e}_1$ is chosen to be the surface normal unit vector, this set of equations is known as the *Darboux-Ribaucour formulas*.

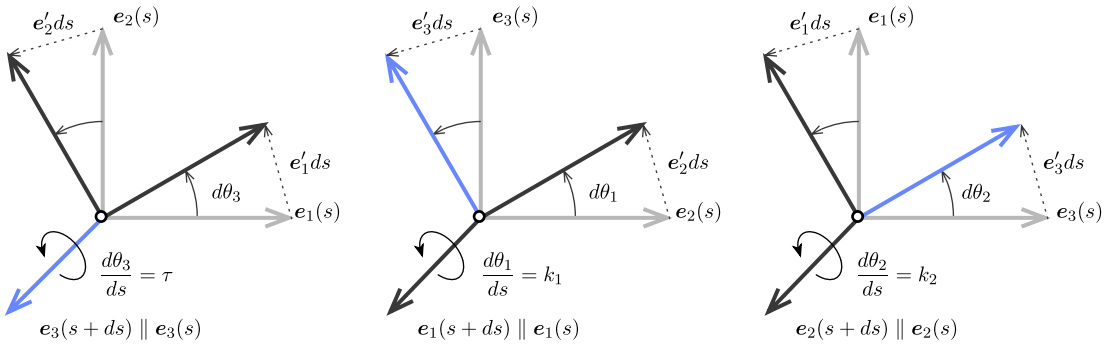

Figure 3.4 – Geometric interpretation of the angular velocity vector of a moving frame.

Since the progression of any moving frame along γ is ruled by a first-order system of differential equations, a unique triplet $\{\tau, k_1, k_2\}$ leads to a set of moving frames equal to each other within a constant of integration.[16] Basically, with a given triplet $\{\tau, k_1, k_2\}$, one can propagate a given initial direct orthonormal trihedron (at $s = 0$ for instance) through the whole curve by integrating the system of differential equations. In general, a moving frame will be fully determined by τ, k_1 and k_2 together with the initial condition $\{\boldsymbol{e}_3(s=0), \boldsymbol{e}_1(s=0), \boldsymbol{e}_2(s=0)\}$.

Angular velocity

This system can be seen as the *equations of motion* of the frame moving along the curve γ at unit speed ($\|\gamma'\| = 1$). Indeed, introducing its *angular velocity vector* ($\boldsymbol{\Omega}$), the previous system is expressed as :

$$\boldsymbol{e}_i'(s) = \boldsymbol{\Omega}(s) \times \boldsymbol{e}_i(s) \quad avec \quad \boldsymbol{\Omega}(s) = \begin{bmatrix} \tau(s) \\ k_1(s) \\ k_2(s) \end{bmatrix} \tag{3.30}$$

This result is straightforward deduced from eq. (3.29). Note that the cross product reveals the skew-symmetric nature of the system, which could already be seen in eq. (3.29). Geometrically, decomposing the infinitesimal rotation of the moving frame around its directors between arc length s and $s+ds$ (fig. 3.4) shows that the scalar functions τ, k_1 and k_2 effectively correspond to the angular speed of the frame moving along γ, respectively around $\boldsymbol{e}_3$, $\boldsymbol{e}_1$ and $\boldsymbol{e}_2$:

$$\frac{d\theta_3}{ds}(s) = \tau(s) \quad , \quad \frac{d\theta_1}{ds}(s) = k_1(s) \quad , \quad \frac{d\theta_2}{ds}(s) = k_2(s) \tag{3.31}$$

[16] This assumption reminds the *Fundamental theorem of space curves* (§3.4.3).

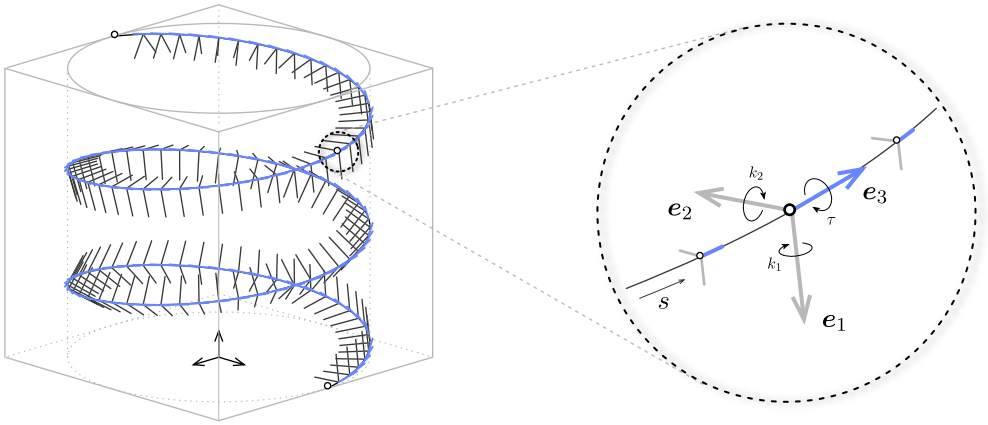

Figure 3.5 – Adapted moving frame $F(s) = \{\boldsymbol{e}_3(s), \boldsymbol{e}_1(s), \boldsymbol{e}_2(s)\}$ where $\boldsymbol{e}_3(s) = \boldsymbol{t}(s)$.

3.5.2 Adapted moving frame

Let F be a moving frame as defined in the previous section. F is said to be *adapted* to γ if at each point $\gamma(s)$, $\boldsymbol{e}_3(s)$ is the unit tangent vector of γ (fig. 3.5) :

$$\boldsymbol{e_3}(s) = \boldsymbol{t}(s) = \frac{\gamma'(s)}{\|\gamma'(s)\|} \tag{3.32}$$

For an adapted frame, the components k_1 and k_2 of the angular velocity vector are related to the curvature of γ[17] :

$$\kappa(s) = \|\boldsymbol{e}_3'(s)\| = \|k_2(s)\boldsymbol{e}_1(s) + k_1(s)\boldsymbol{e}_2(s)\| = \sqrt{k_1(s)^2 + k_2(s)^2} \tag{3.33}$$

Moreover, recalling the definition of the curvature binormal vector ($\boldsymbol{\kappa b}$) from eq. (3.17), it is easy to see that for an adapted moving frame the following relation holds :

$$\boldsymbol{\kappa b}(s) = k_1(s)\boldsymbol{e}_1(s) + k_2(s)\boldsymbol{e}_2(s) \tag{3.34}$$

Consequently, the angular velocity vector of an adapted moving frame can be written as :

$$\boldsymbol{\Omega}(s) = \boldsymbol{\kappa b}(s) + \tau(s)\boldsymbol{t}(s) \tag{3.35}$$

This last result is very interesting as it shows that any adapted moving frame will differ from each other only by their twisting speed as $\boldsymbol{\Omega}_\perp = \boldsymbol{\kappa b}$ only depends on the curve.

[17] Faire le lien avec l'énergie de flexion, qui ne dépend donc que de la géométrie de la courbe dans le cas d'une isotropic rod $\mathcal{E}_b = EI\kappa^2$.

3.5.3 Rotation-minimizing frame

Following [FGSS14, WJZL08] we introduce the *rotation-miniminzing frame* notion. A frame $\{\boldsymbol{e}_3, \boldsymbol{e}_1, \boldsymbol{e}_2\}$ is said to be *rotation-miniminzing* regrading a given direction $\boldsymbol{d}$ if :

$$\boldsymbol{\Omega}(s) \cdot \boldsymbol{d}(s) = 0 \tag{3.36}$$

3.5.4 Parallel transport

The notion of *parallel transport* is somehow a generalization of the classical notion of collinearity in flat euclidean spaces (e.g. $\mathbb{R}^2$ or $\mathbb{R}^3$), to spaces that exhibit some non vanishing curvature (e.g. spheric or hyperbolic spaces).[18]

Relatively parallel fields

Following [Bis75], we define what is a *(relatively) parallel field*. Let γ be a regular curve parametrized by arc length. Let $\boldsymbol{p}$ be a vector field along γ. The vector field $\boldsymbol{p}$ is said to be *parallel* if its derivative is purely tangential, that is :

$$\boldsymbol{p}'(s) \times \boldsymbol{t}(s) = 0 \tag{3.37}$$

Consequently, for an adapted moving frame, the *normal fields* $\boldsymbol{e}_1$ and $\boldsymbol{e}_2$ are both *relatively parallels* if and only if the frame angular velocity is itself a normal field, that is : [19]

$$\boldsymbol{\Omega}(s) = \boldsymbol{\Omega}_{\perp}(s) = \boldsymbol{\kappa b}(s) \Leftrightarrow \boldsymbol{\Omega}(s) \cdot \boldsymbol{t}(s) = 0 \Leftrightarrow \tau(s) = 0 \tag{3.38}$$

In other words, a *relatively parallel normal field* : "turns, only whatever amount is necessary for it to remain normal, so it is as close to being parallel as possible without losing normality" [Bis75].

Parallel transport of vectors along a curve

Reciprocally, it is possible to define the *parallel transport* of a vector along a curve γ as its propagation along γ at angular speed $\boldsymbol{\kappa b}$. An initial vector $\boldsymbol{p}_0 = \boldsymbol{p}(s_0)$ is parallel transported at arc length parameter s into the vector $\boldsymbol{p}(s)$ by integrating the following first-order differential equation along γ :

$$\boldsymbol{p}'(s) = \boldsymbol{\kappa b}(s) \times \boldsymbol{p}(s) \tag{3.39}$$

Consequently, the resulting vector field $\boldsymbol{p}$ is a parallel field. Note that a parallel field is not necessarily a normal field.

From the point of view of differential geometry, this means that the next vector $\boldsymbol{p}(s + ds)$ is obtained by rotating the previous one $\boldsymbol{p}(s)$ around the curve binormal $\boldsymbol{b}(s)$ by an

[18] https://www.youtube.com/watch?v=p1tfZD2Bm0w

[19] A vector field $\boldsymbol{p}$ is said to be *normal* along a curve γ if : $\forall s \in [0, L]$, $\boldsymbol{p} \cdot \boldsymbol{t} = 0$.

infinitesimal angle $d\theta(s) = \kappa(s)ds$. Note that $\boldsymbol{b}(s)$ has the same direction as $\boldsymbol{t}(s) \times \boldsymbol{t}(s+ds)$.

Parallel transport of frames along a curve

Identically, the *parallel transport* of an adapted frame is defined as the parallel transport of its components along γ.

3.5.5 Frenet frame

The Frenet frame is a well-known particular adapted moving frame. It is defined as the map that attach to any given point of γ the corresponding Frenet trihedron $\{\boldsymbol{t}(s), \boldsymbol{n}(s), \boldsymbol{b}(s)\}$ where :

$$\boldsymbol{t}(s) = \frac{\gamma^{'}(s)}{\|\gamma'(s)\|} \quad , \quad \boldsymbol{n}(s) = \frac{\boldsymbol{t'}(s)}{\kappa(s)} \quad , \quad \boldsymbol{b}(s) = \boldsymbol{t}(s) \times \boldsymbol{n}(s) \tag{3.40}$$

Governing equations

The Frenet frame satisfies the *Frenet-Serret formulas* (see §3.4.4), which govern the evolution of the frame along the curve γ :

$$\begin{bmatrix} \boldsymbol{t}^{'}(s) \\ \boldsymbol{n}^{'}(s) \\ \boldsymbol{b}^{'}(s) \end{bmatrix} = \begin{bmatrix} 0 & \kappa(s) & 0 \\ -\kappa(s) & 0 & \tau_f(s) \\ 0 & -\tau_f(s) & 0 \end{bmatrix} \begin{bmatrix} \boldsymbol{t}(s) \\ \boldsymbol{n}(s) \\ \boldsymbol{b}(s) \end{bmatrix} \tag{3.41}$$

Remember the generic system of differential equations of an adapted moving frame attached to a curve, established in eq. (3.29), where :

$$\boldsymbol{e_3}(s) = \boldsymbol{t}(s) \quad , \quad k_1(s) = 0 \quad , \quad k_2(s) = \kappa(s) \quad , \quad \tau(s) = \tau_f(s) \tag{3.42}$$

Angular velocity

Consequently, the angular velocity vector ($\boldsymbol{\Omega_f}$) of the Frenet frame, also known as the *Darboux vector* in this particular case, is given by :

$$\boldsymbol{\Omega_f}(s) = \begin{bmatrix} \tau_f(s) \\ 0 \\ \kappa(s) \end{bmatrix} = \boldsymbol{\kappa b}(s) + \tau_f(s)\boldsymbol{t}(s) \tag{3.43}$$

Remark that the Frenet frame satisfies $\boldsymbol{\Omega_f}(s) \cdot \boldsymbol{n}(s) = 0$ and is thus a *rotation-miniminzing* frame regarding the normal vector ($\boldsymbol{n}$). The motion of this frame through the curve is known as "pitch-free".

Note also that $\boldsymbol{t}^{'}(s)$ and $\boldsymbol{b}^{'}(s)$ are colinear to $\boldsymbol{n}(s)$. This means that the projection of $\boldsymbol{t}(s)$ and $\boldsymbol{b}(s)$ is conserved from one normal plane to another, that is $\boldsymbol{t}$ and $\boldsymbol{b}$ are parallel transported along the vector field $\boldsymbol{n}$.

Drawbacks and benefits

20,21,22

The Frenet frame is not continuously defined if γ is not $\mathcal{C}^2$. This is problematic for the study of slender beams as the centerline of a beam subject to punctual external forces and moments or to material discontinuities will not be $\mathcal{C}^2$ but only picewise $\mathcal{C}^2$. In that case, the centerline tangent will be continuously defined everywhere but the curvature will be subject to discontinuities, that is $\boldsymbol{t}'$ will not be continuously defined.

Moreover, even if γ is $\mathcal{C}^2$, the Frenet frame is not defined where the curvature vanishes, which obviously is an admissible configuration for a beam centerline. This issue can be partially addressed by parallel transporting the normal vector along the straight regions of the curve. Thus, the extended frame will still satisfy the governing equations exposed in eq. (3.41). However, if the osculating planes are not parallels on both sides of a region of null curvature, torsion will be subject to a discontinuity and so the Frenet frame (fig. 3.3).[23] Again, if the region of null curvature is not a point, that is the region is not an inflexion point but a locus where the curve is locally a straight line, the change in torsion on both sides of the region can be accommodated by a continuous rotation from one end to the other.

One benefit of the Frenet frame is that, when transported along a *closed curve*, the frame at the end of the curve will align back with the frame at the beginning of the curve, that is the frame will returns to its initial value after a complete turn. During its trip, the frame will make a total twist of $\int_0^L \tau_f(s)ds = 0[2\pi]$ around the tangent vector.

A second benefit is that any adapted frame can be obtained by a rotation of the Frenet frame around the unit tangent vector [Gug89, p.2].

3.5.6 Bishop frame

A *Bishop frame* denoted $\{\boldsymbol{t}, \boldsymbol{u}, \boldsymbol{v}\}$, also known as *zero-twisting* or *parallel-transported* frame, is an adapted moving frame that has no tangential angular velocity : [24]

$$\boldsymbol{\Omega} \cdot \boldsymbol{t} = \tau = \boldsymbol{u}' \cdot \boldsymbol{v} = -\boldsymbol{u} \cdot \boldsymbol{v}' = 0 \tag{3.44}$$

Because a Bishop frame is an adapted frame, it can be defined relatively to the Frenet frame by a rotation around the unit tangent vector. A Bishop frame is a frame that cancels out the rotational movement of the Frenet frame around the tangent vector. At arc length parameter s, the Frenet frame has continuously rotated around its tangent vector of a cumulative angle : $\int_0^s \tau_f(t)dt$. Thus, any Bishop frame will be obtained, within a constant

[20] une perturbation de la courbe dans le sens de la courbure engendre une variation de longueur de la courbe proportionnelle à l'inverse de la courbure (au premier ordre) + schéma.

[21] une perturbation de la courbe dans le sens de la binormale (en tout point) préserve la longueur de la courbe au 1er ordre : c'est un déplacement qui conserve l'hypothèse d'inextensibilité au premier ordre.

[22] Examiner la question de la fermeture sur une boucle fermée. Schéma.

[23] This is also highlighted in [Blo90, WJZL08].

[24] Bishop frames were Introduced as *relatively parallel adapted frames* in [Bis75].

rotation angle θ_0, through a rotation of the Frenet frame around the tangent vector by an angle :

$$\theta(s) = -\int_0^s \tau_f(t)dt + \theta_0(s) \tag{3.45}$$

Consequently, a Bishop frame can be expressed relatively to the Frenet frame as :

$$\begin{cases} \boldsymbol{u} = \cos\theta \boldsymbol{n} + \sin\theta \boldsymbol{b} \\ \boldsymbol{v} = -\sin\theta \boldsymbol{n} + \cos\theta \boldsymbol{b} \end{cases} \tag{3.46}$$

Governing equations

The Bishop frame satisfies the following system of differential equations, which govern the evolution of the frame along the curve γ :

$$\begin{bmatrix} \boldsymbol{t}'(s) \\ \boldsymbol{u}'(s) \\ \boldsymbol{v}'(s) \end{bmatrix} = \begin{bmatrix} 0 & \kappa(s)\sin\theta(s) & -\kappa(s)\cos\theta(s) \\ -\kappa(s)\sin\theta(s) & 0 & 0 \\ \kappa(s)\cos\theta(s) & 0 & 0 \end{bmatrix} \begin{bmatrix} \boldsymbol{t}(s) \\ \boldsymbol{u}(s) \\ \boldsymbol{v}(s) \end{bmatrix} \tag{3.47}$$

One can remember the generic differential equations of an adapted moving frame attached to a curve, where : [25]

$$k_1(s) = \kappa(s)\sin\theta(s) \quad , \quad k_2(s) = \kappa(s)\cos\theta(s) \quad , \quad \tau(s) = 0 \tag{3.48}$$

Angular velocity

Consequently, the angular velocity vector ($\boldsymbol{\Omega_b}$) of the Bishop frame is given by :

$$\boldsymbol{\Omega_b}(s) = \begin{bmatrix} 0 \\ \kappa(s)\sin\theta(s) \\ \kappa(s)\cos\theta(s) \end{bmatrix} = \boldsymbol{\kappa b}(s) \tag{3.49}$$

Remark that the Bishop frame satisfies $\boldsymbol{\Omega_b}(s) \cdot \boldsymbol{t}(s) = 0$ and is thus *rotation-miniminzing* regarding the tangent vector. The motion of this frame through the curve is known as "roll-free".

Because the motion of this frame is described by an angular velocity vector that is nothing but the curvature binormal vector ($\boldsymbol{\Omega_b} = \boldsymbol{\kappa b}$), it can be interpreted in terms of *parallel transport* as defined in §3.5.4. Thus, given an initial frame at arc length parameter $s = 0$, the Bishop frame at any arc length parameter (s) is obtained by parallel transporting the

[25]

$$\tau = \boldsymbol{u}' \cdot \boldsymbol{v} = (\boldsymbol{\Omega_f} \times \boldsymbol{u} + \theta' \boldsymbol{v}) \cdot \boldsymbol{v} = \tau_f - \tau_f = 0$$
$$k_1 = -\boldsymbol{t}' \cdot \boldsymbol{v} = -\kappa \boldsymbol{n} \cdot \boldsymbol{v} = \kappa \sin\theta$$
$$k_2 = \boldsymbol{t}' \cdot \boldsymbol{u} = \kappa \boldsymbol{n} \cdot \boldsymbol{u} = \kappa \cos\theta$$

initial frame $\{\boldsymbol{t}(0), \boldsymbol{u}(0), \boldsymbol{v}(0)\}$ along the curve from 0 to s.

Drawbacks and benefits

[26,27]

One of the main benefits of the Bishop frame is that its generative method : "is immune to degeneracies in the curvature vector" [Blo90]. Although we first expressed the construction of the Bishop frame relatively to the Frenet frame (which exists wherever γ is biregular), the existence of the Bishop frame, understood in terms of parallel transport, is guaranteed wherever the curvature binormal ($\boldsymbol{\kappa b} = \boldsymbol{t} \times \boldsymbol{t}'$) is defined. To be continuously defined over $[0, L]$, a Bishop frame only needs the curvature binormal vector to be picewise continuously defined over $[0, L]$, which only requires that γ' is $\mathcal{C}^0$ and that γ'' is picewise $\mathcal{C}^0$. Obviously, those weaker existence conditions are profitables to bypass the drawbacks of the Frenet frame regarding the modeling of slender beams listed in §3.5.5.

Strictly speaking, a Bishop frame is not a reference frame as it is defined within an initial condition. However, we will see later that strains in a beam are modeled as a rate of change in the Bishop frame, and consequently the initial condition will disappear in the equations.

Unlike the Frenet frame, when transported along a *closed curve*, the Bishop frame at the end of the curve will not necessarily align back with the frame at the beginning of the curve.[28] Even if the frame returns to its initial value after a complete turn, it may returns in its position after several complete turns ($2k\pi$) around the curve tangent. During its trip, the frame will make a total twist of $\int_0^L \tau_f(s)ds = \alpha[2\pi]$ around the tangent vector. This difference of angle is related to the concept of *holonomy*.

Remark also that Frenet and Bishop frames coincide for planar curves ($\tau_f = 0$), within a constant rotation around the unit tangent vector.

3.5.7 Comparison between Frenet and Bishop frames

Application A : circular helix

Let γ be a *circular helix* of parameter a and k. In a cartesian coordinate system, it is defined as :

$$\boldsymbol{r}(t) = \Big[a\cos t, a\sin t, kt\Big] = a\cos t\,\boldsymbol{e}_x + a\sin t\,\boldsymbol{e}_y + kt\,\boldsymbol{e}_z \tag{3.50}$$

[26] [Gug89, Klo86, Blo90, WJZL08, PFL95, Men13]

[27] "Regarder la méthode de la bi-reflexion pour le calcul du repère de bishop" [WJZL08, p.6]

[28] "it is possible for closed curves to have parallel transport frames that do not match up after one full circuit of the curve" [HM95]

The speed of this parametrization, the curvature and the geometric torsion are uniform and given by :

$$v(t) = \sqrt{a^2 + k^2} \quad , \quad \kappa(t) = \frac{a}{a^2 + k^2} \quad , \quad \tau_f(t) = \frac{k}{a^2 + k^2} \tag{3.51}$$

The Frenet frame components are given by (with $\alpha = v\kappa$ and $\beta = v\tau_f$) :

$$\begin{aligned} \boldsymbol{t}(t) &= \Big[-\alpha\cos t, \alpha\sin t, \beta t\Big] \\ \boldsymbol{n}(t) &= \Big[-\cos t, -\sin t, 0\Big] \\ \boldsymbol{b}(t) &= \Big[\beta\sin t, -\beta\cos t, \alpha\Big] \end{aligned} \tag{3.52}$$

And the Bishop frame components are given by :

$$\begin{aligned} \boldsymbol{u}(t) &= \Big[-\cos t\cos\beta t - \beta\sin t\sin\beta t, -\sin t\cos\beta t + \beta\cos t\sin\beta t, -\alpha\sin\beta t\Big] \\ \boldsymbol{v}(t) &= \Big[-\cos t\sin\beta t + \beta\sin t\cos\beta t, -\sin t\sin\beta t - \beta\cos t\cos\beta t, \alpha\cos\beta t\Big] \end{aligned} \tag{3.53}$$

soit pour une spirale dont on connait

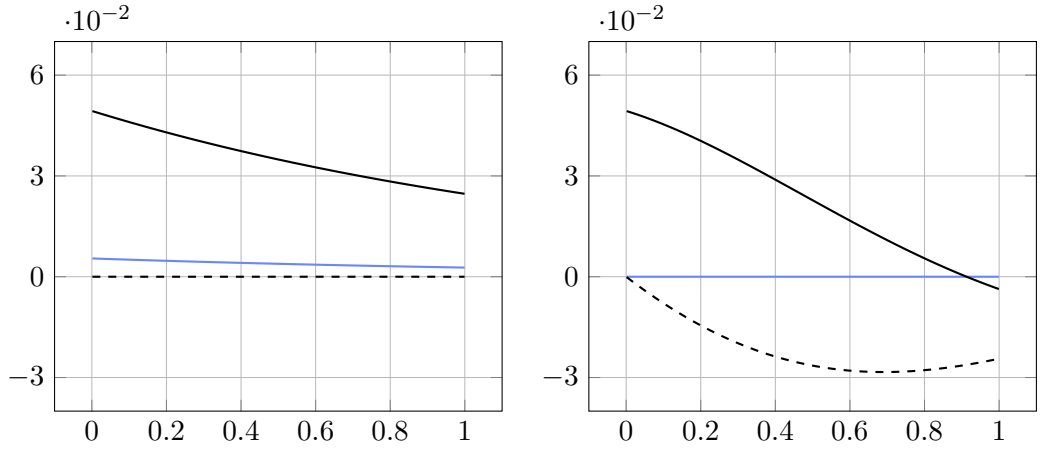

(a) Frenet frame (b) Bishop frame

Figure 3.6 – Comparison between Frenet and Bishop frame velocity for a spirale curve.

3.6 Discrete curves

The previous section has introduced the fundamental analytical tools to develop a solid understanding of the geometry of smooth space curves. These tools will be essentials for the construction of the beam model presented later in **??** and **??**. In this section, we look for equivalent notions in the case of discrete space curves, as the developed model will be implemented in a numerical program to solve real mechanical problems through a finite-difference method (see **??**).

The study of those discrete equivalent notions belong to the recent field of *Discrete*

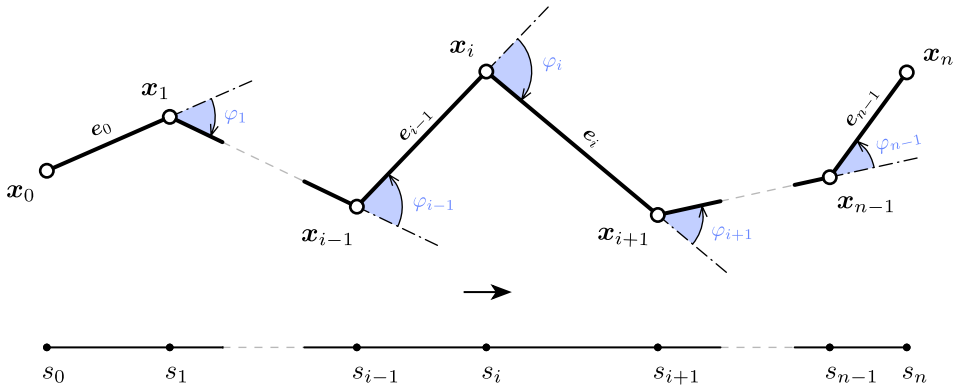

Figure 3.7 – Discrete curve representation and parametrization.

Differential Geometry : "In some sense discrete differential geometry can be considered more fundamental than differential geometry since the later can be obtained form the former as a limit" [Hof08, p.7]. In particular, we will see that they are several ways to define the discrete equivalents of the curvature and the unit tangent vector. Though these various ways are equivalent and match their smooth counterpart by passing to the limit, they exhibit different capabilities at the discrete level.

"There is no general theory or methodology in the literature, despite the ubiquitous use of discrete curves in mathematics and science. There are conflicting definitions of even basic concepts such as discrete curvature κ, discrete torsion τ, or discrete Frenet frame." [CHKS14, p.1].

3.6.1 Definition

Let Γ be a discrete (or polygonal) space curve. Γ is defined as an ordered sequence $\Gamma = (\boldsymbol{x}_0, \boldsymbol{x}_1, \dots, \boldsymbol{x}_n) \in \mathbb{R}^{3(n+1)}$ of $n+1$ pairwise disjoint *vertices* (see fig. 3.7). Consecutive pairs of vertices define n straight segments $(\boldsymbol{e}_0, \boldsymbol{e}_1, \dots, \boldsymbol{e}_{n-1})$ called *edges*, pointing from one vertex to the next one : $\boldsymbol{e}_i = \boldsymbol{x}_{i+1} - \boldsymbol{x}_i$. The midpoint of $\boldsymbol{e}_i$ is a vertex denoted : $\boldsymbol{x}_{i+1/2} = \boldsymbol{x}_i + \frac{1}{2}\boldsymbol{e}_i$. The length of $\boldsymbol{e}_i$ is denoted $l_i = \|\boldsymbol{e}_i\|$. The total length of Γ is denoted $L = \sum_{i=0}^{n-1} \|\boldsymbol{e}_i\|$. Additionally, we define the vertex-based mean length at vertex $\boldsymbol{x}_i$:

$$\begin{cases} \bar{l_0} = l_0 & i = 0 \\ \bar{l_i} = \dfrac{1}{2}(l_{i-1} + l_i) & i \in [\![1, n-1]\!] \\ \bar{l_n} = l_{n-1} & i = n \end{cases} \tag{3.54}$$

Discrete unit tangent vector

Edge vectors lead to a natural definition of the *discrete unit tangent vector* along each edge : $\boldsymbol{u}_i = \boldsymbol{e}_i / l_i$. However, this definition makes no sens at vertices where all the curvature is *condensed* and measured by the turning angle (φ_i). This is explained in terms of the Gauß

map as edges will map to points but vertices will map to curves on the unit sphere.

Discrete osculating plane

Consecutive pairs of edges lead to a natural definition of the *discrete osculating plane*, as the plane in which Γ locally lies on. This plane is well defined by its normal vector known as the *discrete unit binormal vector* ($\boldsymbol{b}_i = \frac{\boldsymbol{e}_{i-1} \times \boldsymbol{e}_i}{\|\boldsymbol{e}_{i-1} \times \boldsymbol{e}_i\|}$) only if $\boldsymbol{e}_{i-1}$ and $\boldsymbol{e}_i$ are non-collinear ; that is the curve is not locally a straight line, or equivalently the curvature does not vanish.

Discrete turning angle

The *turning angle* is defined as the oriented angle between to adjacent edges : $\varphi_i = \angle(\boldsymbol{e}_{i-1}, \boldsymbol{e}_i)$. It is defined only for all $i \in [\![1, n-1]\!]$. It corresponds to the angle of rotation, in the osculating plane, around the binormal vector ($\boldsymbol{b}_i$), to align $\boldsymbol{e}_{i-1}$ with $\boldsymbol{e}_i$. The sign of φ_i is taken in accordance to the right-hand rule regarding the orientation of $\boldsymbol{b}_i$. Thus, φ_i is necessarily bounded to $[0, \pi]$:

$$0 \leqslant \varphi_i \leqslant \pi \tag{3.55}$$

The next section will highlight the central role of the turning angle in the possible measurements of the discrete curvature.

Recall that for a planar curve, where φ denotes the angle between the tangent vector ($\boldsymbol{t} = \cos\varphi\, \boldsymbol{e}_x + \sin\varphi\, \boldsymbol{e}_y$) and the horizontal line of direction $\boldsymbol{e}_x$, the following relation holds : $\varphi(s_1) - \varphi(s_2) = \int_{s_1}^{s_2} \frac{d\varphi}{ds} ds = \int_{s_1}^{s_2} \kappa ds$.

3.6.2 Regularity

Let $\Gamma = (\boldsymbol{x}_0, \boldsymbol{x}_1, \ldots, \boldsymbol{x}_n)$ be a discrete curve of edges $\boldsymbol{e}_0, \boldsymbol{e}_1, \ldots, \boldsymbol{e}_{n-1}$. Γ is said to be :

- *regular* if it has no kinks : $\boldsymbol{e}_{i-1} + \boldsymbol{e}_i \neq 0 \Leftrightarrow \varphi_i \neq \pi \mid \forall i \in [\![1, n-1]\!]$

- *biregular* if no vertex is flat : $\boldsymbol{e}_{i-1} - \boldsymbol{e}_i \neq 0 \Leftrightarrow \varphi_i \neq 0 \mid \forall i \in [\![1, n-1]\!]$

3.6.3 Parametrization

In the literature, discrete curves are usually considered as maps defined on $I = [\![0, n]\!] \in \mathbb{N}^{n+1}$. As a consequence, the discrete derivative of Γ is an edge-based quantity defined as :

$$\Gamma'_i = \frac{\Gamma(t_{i+1}) - \Gamma(t_i)}{t_{i+1} - t_i} = \boldsymbol{e}_i \quad , \quad \boldsymbol{x}_i = \Gamma(t_i) \quad , \quad t_i = i \tag{3.56}$$

Thus, as in the smooth case, a discrete curve is said to be parametrized by arc length if $\|\Gamma'\| = 1$, that is every edges are of unit length ($\|\boldsymbol{e}_i\| = 1$).[29] This constraint is sometimes relaxed to curves of constant edge length ($\|\boldsymbol{e}_i\| = c$) that are said to be parametrized *proportional* to arc length.

In the present work, to stick closer to the smooth case, we instead consider discrete curves as maps defined on $I = [t_0, t_1, \dots, t_n] \in \mathbb{R}^{n+1}$ where t denotes the discrete parametrization of Γ. As in the smooth case, the way to parametrized a curve is not unique.

Arc length parameter

By analogy with the smooth case, we define the curve arc length at vertices (see fig. 3.7) as :

$$\begin{cases} s_0 = 0 & i = 0 \\ s_i = \sum_{k=1}^{i} \|\boldsymbol{e}_{k-1}\| & i \in [\![1, n-1]\!] \\ s_n = L & i = n \end{cases} \tag{3.57}$$

This definition naturally extends to the whole domain by piecewise linear interpolation. This is not different as considering the discrete curve as a continuous polygonal curve. Indeed, for any $s \in [s_i, s_{i+1}]$ there exist a normalized parameter $t = \frac{s - s_i}{s_{i+1} - s_i} \in [0, 1]$ so that :

$$\begin{cases} s(t) = (1-t)s_i + ts_{i+1} = s_i + tl_i \\ \boldsymbol{x}(t) = (1-t)\boldsymbol{x}_i + t\boldsymbol{x}_{i+1} = \boldsymbol{x}_i + t\boldsymbol{e}_i \end{cases} \tag{3.58}$$

Note that this parametrization satisfies $\|\Gamma'\| = 1$ on $\bigcup_{i=1}^{n}]s_{i-1}, s_i[$ but Γ' remains undefined at vertices. This issue is the reason why defining the tangent vector at vertices can not be done unequivocally for discrete curves.

3.7 Discrete curvature

Several approches. [Vou14] defines and compares three different definitions of the discrete curvature that does not suppose that $\|\boldsymbol{e}_i\| = cst$. By trying to mimic somme properties of the curvature in the smooth case. [Bob15]. [CHKS14] also defines and compares three different definitions of the discrete curvature from the osculating circle. One main drawback of all the said proposals is that the question of the curvature at start and end points is never treated. But this si of main importance when dealing worth beams as the nature of the boundary condition can make the curvature to be null or not at its ends, depending if somme moment has to be transfer or not. In this sens, the question of discrete curvature could not be treated separately with the question of the tangent vector.

[29] This assumption leads to the assertion that "A discrete curve is parameterized by arc length or it is not" [Hof08, p.10].

[Rom13]

3.7.1 Definition from osculating circles

Curvature is defined from the osculating circle, which is the best approximation of a curve by a circle.

Vertex-based osculating circle (circumscribed)

Let Γ be a discrete curve parametrized by arc length. The *vertex-based* (or circumscribed) osculating circle at vertex $\boldsymbol{x}_i$ is defined as the unique circle passing through the points $\boldsymbol{x}_{i-1}$, $\boldsymbol{x}_i$ and $\boldsymbol{x}_{i+1}$ (see fig. 3.8a). This circle leads to the following definition of the curvature : [30]

$$\boldsymbol{\kappa b}_i = \frac{2\,\boldsymbol{e}_{i-1} \times \boldsymbol{e}_i}{\|\boldsymbol{e}_{i-1}\|\|\boldsymbol{e}_i\|\|\boldsymbol{e}_{i-1} + \boldsymbol{e}_i\|} \quad , \quad \kappa_i = \|\boldsymbol{\kappa b}_i\| = \frac{2\,\sin(\varphi_i)}{\|\boldsymbol{e}_{i-1} + \boldsymbol{e}_i\|} \tag{3.59}$$

This definition shows a good locality as the curvature is attached to the vertex $\boldsymbol{x}_i$, right in the place where it occurs on the discret curve. In addition, this definition leads to a natural local spline interpolation by the circumscribed osculating circle itself. This interpolation has the advantage to pass exactly through three vertices, to lie on the osculating plane and to share the same curvature as Γ at $\boldsymbol{x}_i$. It also leads to a natural definition of the tangent vector at $\boldsymbol{x}_i$ (see §3.8).

Moreover, while this definition is valid only on the current portion of Γ ($i \in [1, n-1]$), it is straightforward extended to its endings ($i = 0, 1$), provided that a unit tangent vector $\boldsymbol{t}_0$ (respectively $\boldsymbol{t}_n$) is given at $\boldsymbol{x}_0$ (resp. $\boldsymbol{x}_n$), as the unique circle tangent to $\boldsymbol{t}_0$ (resp. $\boldsymbol{t}_n$) passing through $\boldsymbol{x}_0$ and $\boldsymbol{x}_1$ (resp. $\boldsymbol{x}_{n-1}$ and $\boldsymbol{x}_n$) :

$$\boldsymbol{\kappa b}_0 = \frac{2\,\boldsymbol{e}_0 \times \boldsymbol{t}_0}{\|\boldsymbol{e}_0\|^2} \quad , \quad \boldsymbol{\kappa b}_n = \frac{2\,\boldsymbol{t}_n \times \boldsymbol{e}_{n-1}}{\|\boldsymbol{e}_{n-1}\|^2} \tag{3.60}$$

This property will be very profitable in the discrete beam model developed later in the manuscript. It is examined more in details in section §3.8 about the definition of the tangent vector.

However, there are some important drawbacks as the curvature is bounded to $[0, 2]$ (see fig. 3.10). When the curve tends to kinks ($\varphi \mapsto \pi$), one would expect the curvature to diverge toward infinity, but instead it tends to a finite value equals to 0 ($l_{i-1} \neq l_i$) or 2 ($l_{i-1} = l_i$). This issue can be bypassed if the discretization is refined "enough". A criterion is given in the next section (**??**).

[30] This curvature is also known as the *Menger curvature*.

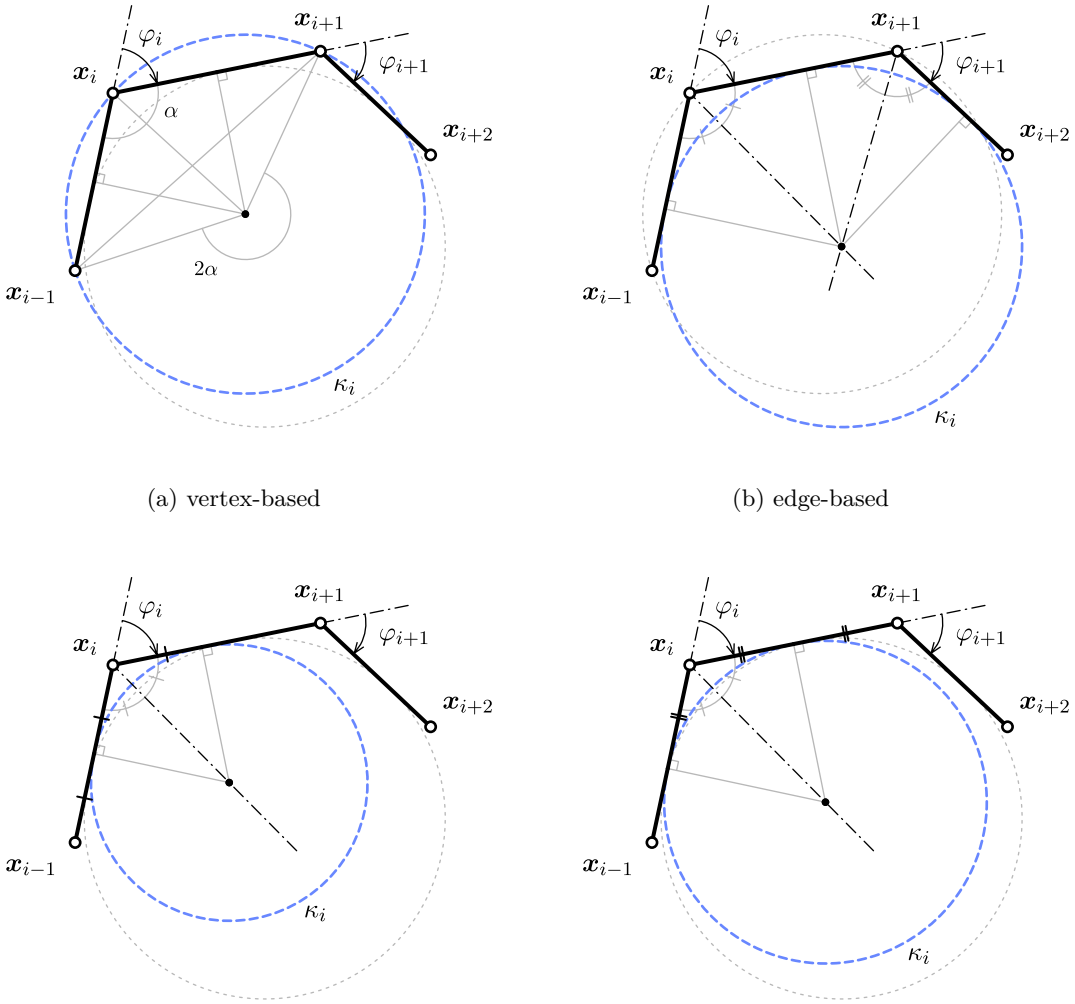

(a) vertex-based

(b) edge-based

(c) bitangent with $\|\boldsymbol{e}_{i-1}\|$

(d) bitangent with $\|\boldsymbol{e}_i\|$

Figure 3.8 – Several ways to define the osculating circle for discrete curves, leading to different notions of discrete curvature.

Curvature (κ_i)	Locality	$\varphi \mapsto 0$	$\varphi \mapsto \pi$	Ends	Dim	Fitting
$\kappa_1 = \frac{2\sin(\varphi_i)}{\|\boldsymbol{e}_{i-1}+\boldsymbol{e}_i\|}$	$\boldsymbol{x}_i$	0	$0, 2$	yes	space	clothoid
$\kappa_2 = \frac{\tan(\varphi_i/2)+\tan(\varphi_{i+1}/2)}{l_i}$	$\boldsymbol{e}_i$	0	∞	no	planar	circle
$\kappa_3 = \frac{2\tan(\varphi_i/2)}{l_i}$	$\boldsymbol{x}_i$	0	∞	no	space	circles
$\kappa_4 = \frac{2\sin(\varphi_i/2)}{l_i}$	$\boldsymbol{x}_i$	0	$0, 2$	no	space	clothoid
$\kappa_5 = \frac{\varphi_i}{l_i}$	$\boldsymbol{x}_i$	0	π/l_i	no	space	elastica

Table 3.1 – Review of several discrete curvature definitions mentioned in the literature.

Edge-based osculating circle (inscribed)

Let Γ be a discrete curve parametrized by arc length. The *edge-based* osculating circle at edge $\boldsymbol{e}_i$ is defined as the unique circle tangent to the edges $\boldsymbol{e}_{i-1}$, $\boldsymbol{e}_i$ and $\boldsymbol{e}_{i+1}$ (see fig. 3.8b).

$$\kappa_i = \frac{\tan(\varphi_i/2) + \tan(\varphi_{i+1}/2)}{\|\boldsymbol{e}_i\|} \tag{3.61}$$

This definition shows an appropriate behavior when the curve tends to kicks, as the radius of curvature tends to zero ($\tan\varphi/2 \mapsto \infty$), and when the curve tends to be a straight line, as the curvature tends to 0 ($\tan\varphi/2 \mapsto 0$).

However, it needs Γ to be planar which is by far to restrictive regarding our goal (the modeling of 3D slender beams). Finally, this way of defining the curvature is not as local as one would expect as it is defined relatively to the edge $\boldsymbol{e}_i$ but not where the turning occurs, at vertices.

Bitangent osculating circle (inscribed)

Let Γ be a discrete curve parametrized by arc length. Following [Vou14] we define the curvature regrading the mean length $\overline{l_i}$ attached to $\boldsymbol{x}_i$ as : [31]

$$\boldsymbol{\kappa b}_i = \frac{2}{\overline{l_i}}\left(\frac{\boldsymbol{e}_{i-1}\times\boldsymbol{e}_i}{\|\boldsymbol{e}_{i-1}\|\|\boldsymbol{e}_i\| + \boldsymbol{e}_{i-1}\cdot\boldsymbol{e}_i}\right) \quad , \quad \kappa_i = \|\boldsymbol{\kappa b}_i\| = \frac{2}{\overline{l_i}}\tan(\varphi_i/2) \tag{3.62}$$

This other definition combines the good locality of the vertex-based approach (see eq. (3.59)) and the proper behavior at bounds of the edge-based approach (see eq. (3.61)). Given two adjacent edges $\boldsymbol{e}_{i-1}$ and $\boldsymbol{e}_i$, there exist an infinite number of circles that are tangent to both edges (see fig. 3.8c and fig. 3.8d for two remarkable circles among them), which center points all lie on the $\varphi_i - \pi$ angle bisector line. The corresponding osculating circle, known as the *inscribed* circle, is constructed to touch both $\boldsymbol{e}_{i-1}$ and $\boldsymbol{e}_i$ at distance $\overline{l_i}$ from $\boldsymbol{x}_i$. In the case of a constant edge length discrete curve, this definition of the osculating circle merges to the circles proposed in fig. 3.8c and fig. 3.8d.

However, this definition still exhibits some drawbacks as there is no natural way to extend it to the end vertices $\boldsymbol{x}_0$ and $\boldsymbol{x}_{n-1}$. The lack of a natural interpolation spline that passes through vertices and that is in correlation to the osculating circle is also detrimental in the context of our application.

Other definitions of osculating circles

In the literature, one can find other definitions for the discrete curvature that also correspond to the definition of an osculating circle. All these definitions are summarized in table 3.1. For further informations, the reader should refer to [CHKS14, Vou14, Bob15, Rom13].

[31] This definition is also presented in [Bob15, CHKS14] but in the more restrictive case of constant edge length discrete curves ($l_i = cst$).

In particular, [Vou14] details which discrete curvature definitions parallel which property of the smooth curvature. It remarks that there is no "free-lunch" as none of the proposed definition satisfies every properties of the smooth curvature.

3.7.2 Benchmarking : sensitivity to non uniform discretization

In this section we compare the two main discrete curvature notions (circumscribed versus inscribed) regarding their sensibility to non uniform discretization.

This aspect is not treated in the actual literature, in which curves parametrized by arc length are usually treated as curves of constant edge length, though it is yet an important topic when it comes to the numerical modeling of true mechanical systems. Indeed, the presence of connexions between members will compromise the ability to enforce a constant discretization through all the elements of the structure. Additionally, vertices are obviously points of interest in a discrete model as they will be used to apply loads and enforce various constraints such as joints and support conditions. Finally, the accuracy of the discretized model is proportional to the sharpness of the discretization, whereas the computing time required to solve the model will grow as the sharpness increases. Consequently, one would distribute those points in the space as cleverly as possible and try to minimize their number as they increase the overall computation cost.

Introducing the coefficient $\alpha = \frac{\|\boldsymbol{e}_{i-1}\|}{\|\boldsymbol{e}_i\|}$, we rewrite the previous formulas for κ_1 and κ_3 as :

$$\begin{aligned} \kappa_1 &= \frac{2\,\sin(\varphi)}{\|\boldsymbol{e}_i\|(1+\alpha^2+2\alpha\,\cos(\varphi))^{1/2}} \\ \kappa_3 &= \frac{4\,\tan(\varphi/2)}{\|\boldsymbol{e}_i\|(1+\alpha)} \end{aligned} \tag{3.63}$$

These expressions lead to the following formula for the ratio κ_1/κ_3, which relies only on α and the turning angle φ between the edges $\boldsymbol{e}_{i-1}$ and $\boldsymbol{e}_i$:

$$\frac{\kappa_1}{\kappa_3}(\alpha) = \frac{\kappa_1}{\kappa_3}(1/\alpha) = \frac{(1+\alpha)\,cos^2(\varphi/2)}{((1-\alpha)^2+4\alpha\,cos^2(\varphi/2))^{1/2}} \tag{3.64}$$

Discrete curvatures are plotted in fig. 3.10 for three values of α. The thickest line is for the case of uniform discretization ($\alpha = 1$), whereas the thin lines mark the boundary cases ($\alpha = 0.5, 2$). The ratio κ_1/κ_3 is plotted in blue and leads to only one thin line (remind eq. (3.64)). The graph shows that κ_1 and κ_3 have a very close behavior for small turning angles. The variability regarding α is small when φ remains small and gets negligible as φ gets smaller.

Passing $\pi/4$ and increasing φ, κ_3 exhibits a good behavior : as the discrete curves tends to kink κ_3 diverges towards the infinity as the smooth curvature would for

However, for a given curvature, the turning angle decreases as the sharpness of the discretization increases ($\lim_{\|\boldsymbol{e}_i\|\mapsto 0}\varphi_i = 0$). Thus, it is possible to adapted the discretization

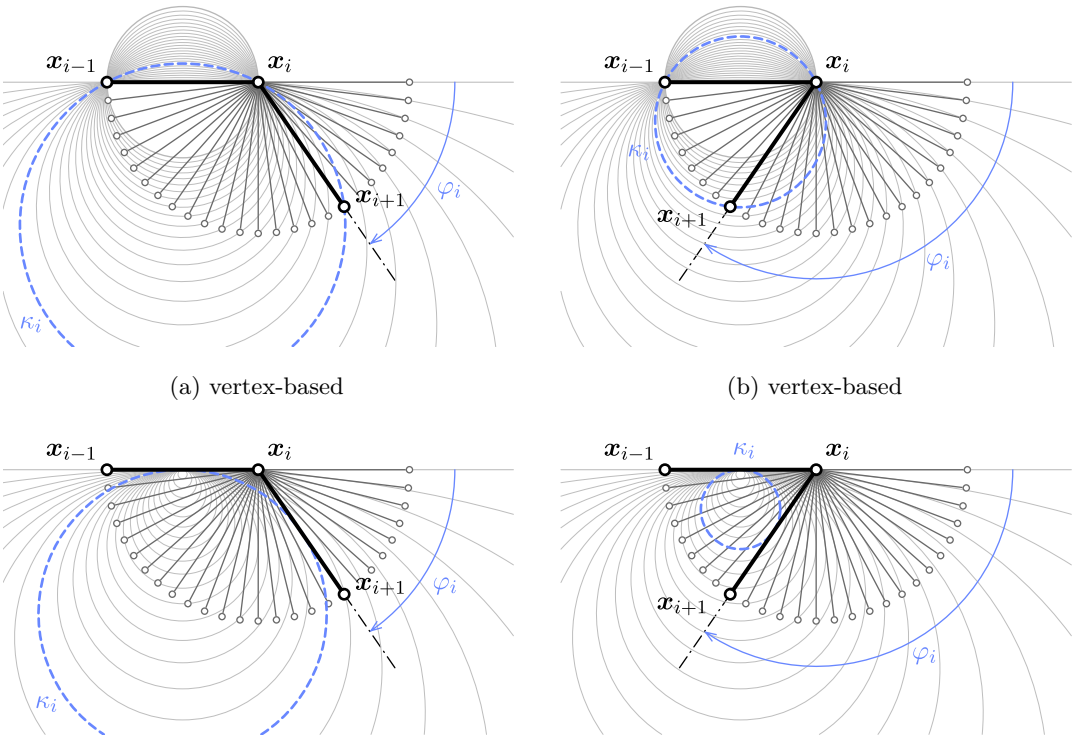

(a) vertex-based (b) vertex-based

(c) edge-based (d) edge-based

Figure 3.9 – Comparison of circumscribed (a-b) and inscribed (c-d) osculating circles for different values of the turning angle (φ).

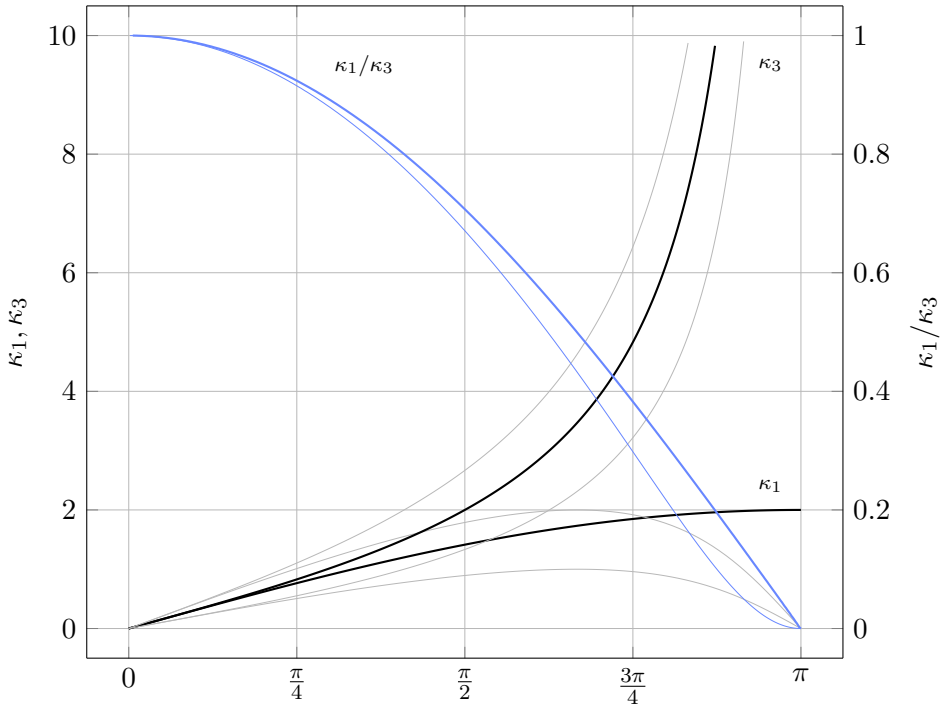

Figure 3.10 – Sensitivity of discrete curvatures to non uniform discretization ($\alpha \in [0.5, 2]$) over the whole domain of variation of the turning angle ($\varphi \in [0, \pi]$).

to make sure

3.7.3 Benchmarking : accuracy in bending energy representation

In this section we compare, for three remarkable types of curves (line, semicircle and elastica), the discrete bending energies $\mathcal{E}_1$ and $\mathcal{E}_3$ of the discrete curve, respectively based on definitions κ_1 and κ_3 (see table 3.1), to the bending energy $\mathcal{E}$ of the smooth curve. We study the convergence of these energies as the sharpness of the discretization increases. The energies are defined as :

$$\begin{aligned} \mathcal{E} &= \int_0^L \kappa^2 ds \\ \mathcal{E}_i &= \sum_i \bar{l}_i \kappa_i^2 \end{aligned} \tag{3.65}$$

Straight line

We consider any straight line. Its smooth curvature is null. So are the discrete curvatures κ_1 and κ_3 (see table 3.1). In this case, the discrete bending energies perfectly match the bending energy of the smooth curve :

$$\mathcal{E} = \mathcal{E}_1 = \mathcal{E}_3 = 0 \tag{3.66}$$

Semicircle

We consider a semicircle of curvature $\kappa = 1/r$ and length $L = \pi r$. This curve is discretized into n edges of equal length $|\boldsymbol{e}_n| = 2r\sin(\varphi/2)$ where $\varphi = \frac{\pi}{n}$ (see fig. 3.11). The total length of the discrete curve is given by : $L_n = n|\boldsymbol{e}_n| = L\frac{\sin(\varphi/2)}{\varphi/2}$. In this simple case, the bending energies can be expressed analytically :

$$\mathcal{E} = L\kappa^2 \tag{3.67a}$$

$$\mathcal{E}_1 = L_n\kappa_1^2 = \frac{\sin(\varphi/2)}{\varphi/2} \cdot \mathcal{E} \tag{3.67b}$$

$$\mathcal{E}_3 = L_n\kappa_3^2 = \frac{\sin(\varphi/2)}{(\varphi/2)\cos^2(\varphi/2)} \cdot \mathcal{E} \tag{3.67c}$$

Note that κ_1 equals the curvature of the smooth curve. Consequently, the estimation error is only due to the estimation of the curve length ($L_n \neq L$). The ratios $\mathcal{E}_1/\mathcal{E}$ and $\mathcal{E}_3/\mathcal{E}$ are plotted in fig. 3.12. Graphs show that $\mathcal{E}_1$ converges to the smooth case faster than $\mathcal{E}_3$.

Elastica

We consider a sequence of elastica curves of fixed length L and variable curvature κ (see fig. 3.13a). This curves correspond to a buckled shape of a straight pinned-pinned beam

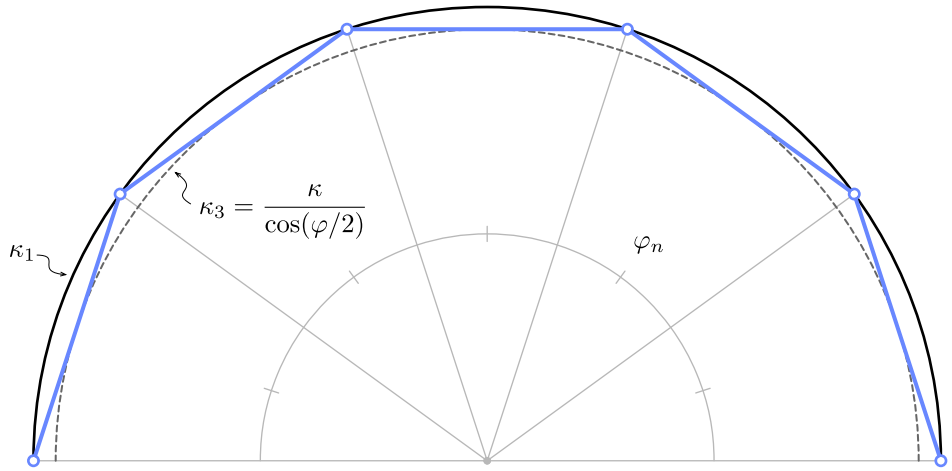

Figure 3.11 – Discretization of a semicircle for discrete bending energies evaluation.

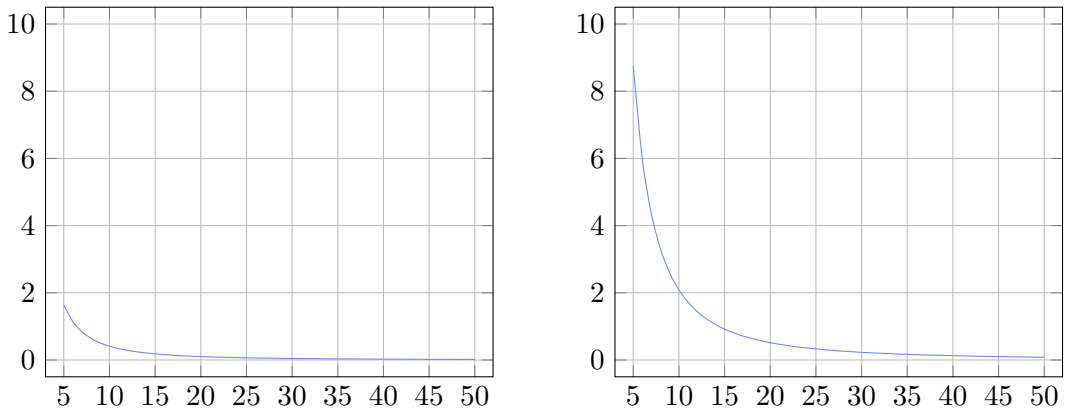

(a) $|1 - \frac{\mathcal{E}_1}{\mathcal{E}}(n)|$ in %

(b) $|1 - \frac{\mathcal{E}_3}{\mathcal{E}}(n)|$ in %

Figure 3.12 – Relative error in the estimation of the smooth bending energy ($\mathcal{E}$) by the discrete bending energies ($\mathcal{E}_1$ and $\mathcal{E}_3$) regarding the sharpness of the discretization, for a semicircle.

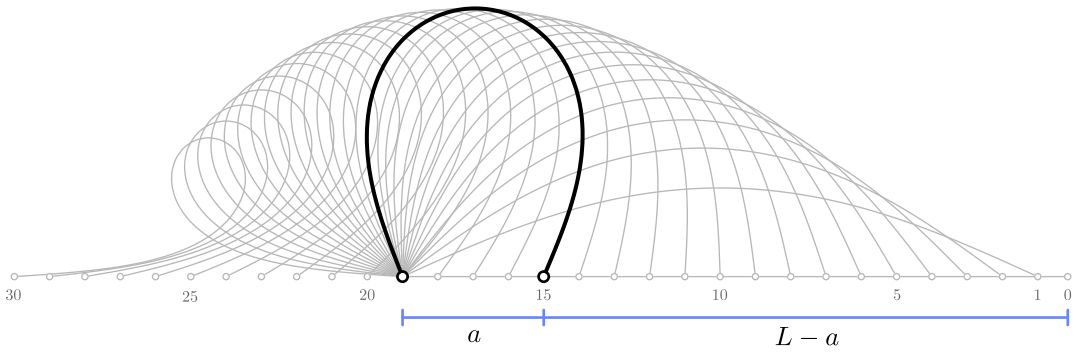

(a) sequence of elastica curves

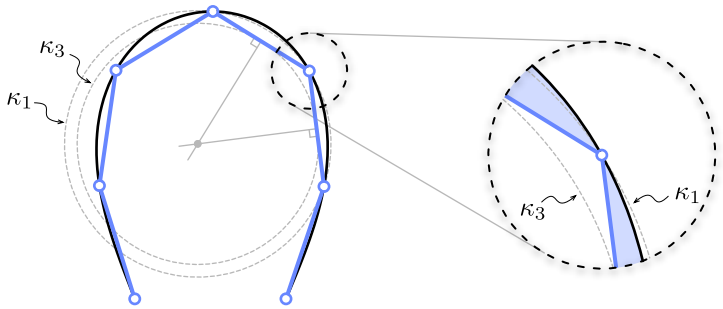

(b) zoom on the discretization

Figure 3.13 – Discretization (b) of a sequence of elastica curves (a) for discrete bending energies evaluation.

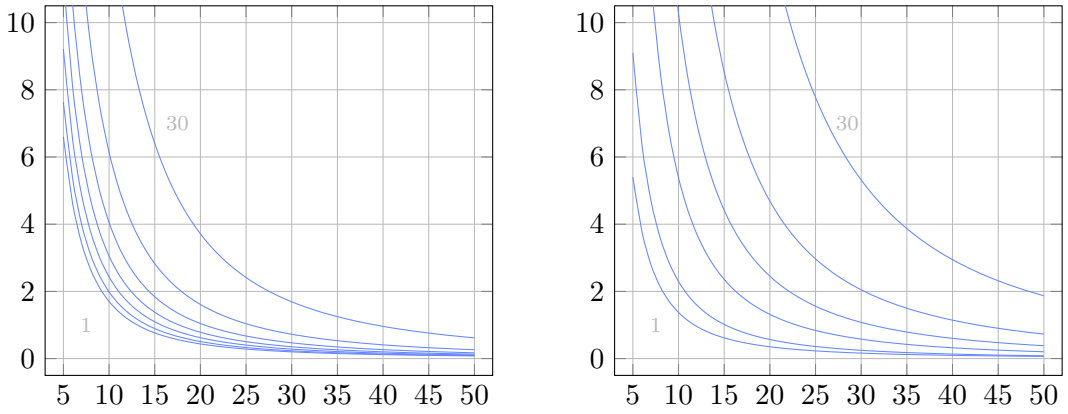

(a) $|1 - \frac{\mathcal{E}_1}{\mathcal{E}}(n)|$ in %

(b) $|1 - \frac{\mathcal{E}_3}{\mathcal{E}}(n)|$ in %

Figure 3.14 – Relative error in the estimation of the smooth bending energy ($\mathcal{E}$) by the discrete bending energies ($\mathcal{E}_1$ and $\mathcal{E}_3$) regarding the sharpness of the discretization, for several elastica curves. The curves are chosen from fig. 3.13a (1,5,10,15,20,25,30).

that would have been forced to retract its span. These curves are discretized into n edges of equal length (see fig. 3.13b). This time, there is no analytical expressions available for $\mathcal{E}$, $\mathcal{E}_1$ and $\mathcal{E}_3$. Results are obtained by numerical integration and plotted in fig. 3.14. Again, graphs show that $\mathcal{E}_1$ converges to the smooth case faster than $\mathcal{E}_3$ for most of the curves excepted the ones with low overall curvature (1 to 5).

3.8 Discrete tangent vector

In this section we study how to define the discrete unit tangent vector relative to a discrete curve. While a natural definition exists along the edges (see §3.6.1, there is no obvious choice at vertices were the curve kinks.

The ability to define a unique tangent vector is very important to define the normal to cross section, control beam endings, and relate it to curvature. You will controle the directiopn of the section (for a fixed/encastre support condition) or inversly, you would control the moment and seek the corresponding tangent direction (for a pin boundary condition, you know there is no end moments so the curvature is null and your looking for the tangent).

Problème de définition. Facile de définir une tangente sur un edge. Mais une infinité de tangentes possibles à chaque vertex. So in case of an arc length parameterized curve the vertex tangent vector points in the same direction as the averaged edge tangent vectors [Hof08, p.12]. Nous verrons que le cercle 3 points, en plus de mieux représenter l'énergie d'une courbe discrete dans les cas typiques, offre un choix de tangente non ambïgu.

3.8.1 Circumscribed case

We consider the case where the curvature is defined according to the circumscribed osculating circle (see fig. 3.15a).

Current portion

Let $\boldsymbol{x}_i$ be a vertex in the current portion of Γ. The circumscribed osculating circle gives a smooth approximation of Γ in the vicinity of $\boldsymbol{x}_i$ (see fig. 3.15a). It leads to a natural definition of a unit tangent vector for five remarkable vertices as the tangent to the osculating circle at those points (resp. $\boldsymbol{x}_{i-1}$, $\boldsymbol{x}_{i-1/2}$, $\boldsymbol{x}_i$, $\boldsymbol{x}_{i+1/2}$, $\boldsymbol{x}_{i+1}$) :

$$\boldsymbol{t}_i^- = 2(\boldsymbol{t}_i \cdot \boldsymbol{u}_{i-1})\boldsymbol{u}_{i-1} - \boldsymbol{t}_i \tag{3.68a}$$

$$\boldsymbol{t}_{i-1/2} = \boldsymbol{u}_{i-1} \tag{3.68b}$$

$$\boldsymbol{t}_i = \frac{\|\boldsymbol{e}_i\|}{\|\boldsymbol{e}_{i-1} + \boldsymbol{e}_i\|}\boldsymbol{u}_{i-1} + \frac{\|\boldsymbol{e}_{i-1}\|}{\|\boldsymbol{e}_{i-1} + \boldsymbol{e}_i\|}\boldsymbol{u}_i \tag{3.68c}$$

$$\boldsymbol{t}_{i+1/2} = \boldsymbol{u}_i \tag{3.68d}$$

$$\boldsymbol{t}_i^+ = 2(\boldsymbol{t}_i \cdot \boldsymbol{u}_i)\boldsymbol{u}_i - \boldsymbol{t}_i \tag{3.68e}$$

Note that $\boldsymbol{t}_i^-$ (resp. $\boldsymbol{t}_i^+$) is obtained by a reflection of $-\boldsymbol{t}_i$ across the bisecting plane of $\boldsymbol{e}_{i-1}$ (resp. $\boldsymbol{e}_i$). A very important property is that the curvature binormal vector at $\boldsymbol{x}_i$ can be computed by three different ways :

$$\boldsymbol{\kappa b}_i = \frac{2\,\boldsymbol{e}_{i-1}\times\boldsymbol{e}_i}{\|\boldsymbol{e}_{i-1}\|\|\boldsymbol{e}_i\|\|\boldsymbol{e}_{i-1}+\boldsymbol{e}_i\|} = \begin{cases} \dfrac{2\,\boldsymbol{u}_{i-1}\times\boldsymbol{t}_i}{\|\boldsymbol{e}_{i-1}\|} \\ \dfrac{2\,\boldsymbol{t}_i\times\boldsymbol{u}_i}{\|\boldsymbol{e}_i\|} \end{cases} \tag{3.69}$$

The first expression is interpreted as the unique circle passing through three points ($\boldsymbol{x}_{i-1}$, $\boldsymbol{x}_i$, $\boldsymbol{x}_{i+1}$) as explained in §3.7.1. Equivalently, there exist a unique circle defined by two points and a tangent vector. Precisely, the last two expressions in eq. (3.69) can be interpreted as the curvature binormal vector of the unique circle passing through $\boldsymbol{x}_{i-1}$, $\boldsymbol{x}_i$ (resp. $\boldsymbol{x}_i$, $\boldsymbol{x}_{i+1}$) and tangent to $\boldsymbol{t}_i$ at $\boldsymbol{x}_i$.

Discontinuity of curvature

Let $\boldsymbol{t}_i^*$ be an arbitrary tangent vector at $\boldsymbol{x}_i$. Following eq. (3.69) we define the *left-sided* (resp. *right-sided*) discrete curvatures at $\boldsymbol{x}_i$ in the circumscribed case as : as

$$\boldsymbol{\kappa b}_i^-(\boldsymbol{t}_i^*) = \frac{2\,\boldsymbol{u}_{i-1}\times\boldsymbol{t}_i^*}{\|\boldsymbol{e}_{i-1}\|} \tag{3.70a}$$

$$\boldsymbol{\kappa b}_i^+(\boldsymbol{t}_i^*) = \frac{2\,\boldsymbol{t}_i^*\times\boldsymbol{u}_i}{\|\boldsymbol{e}_i\|} \tag{3.70b}$$

The corresponding osculating circle will be called the *left-sided* (resp. *right-sided*) circumscribed osculating circle. When $\boldsymbol{t}_i^* = \boldsymbol{t}_i$, the limits agree one to each other ($\boldsymbol{\kappa b}_i^- = \boldsymbol{\kappa b}_i^+ = \boldsymbol{\kappa b}_i$) and the osculating circles coincide. These definitions perfectly mimic the smooth case where, at a regular ($\|\gamma'\| \neq 0$) but not biregular ($\|\gamma''\| = 0$) point, the curvature is discontinuous while the tangent vector reminds smoothly defined.

In mechanics, this situation is likely to arise as discontinuities in material properties or punctual applied moments will necessarily lead to discontinuities in curvature (recall that $M = EI\kappa$).

Curve endings

The definition of the left and right sided curvatures given for a vertex in the current portion of Γ are still valid for the end vertices $\boldsymbol{x}_0$ and $\boldsymbol{x}_n$. Provided that a unit tangent vector $\boldsymbol{t}_0^*$ (respectively $\boldsymbol{t}_n^*$) is given at $\boldsymbol{x}_0$ (resp. $\boldsymbol{x}_n$), the circumscribed osculating circle is defined as the unique circle passing through $\boldsymbol{x}_0$ and $\boldsymbol{x}_1$ (resp. $\boldsymbol{x}_{n-1}$ and $\boldsymbol{x}_n$) tangent to $\boldsymbol{t}_0^*$ (resp. $\boldsymbol{t}_n^*$) ;

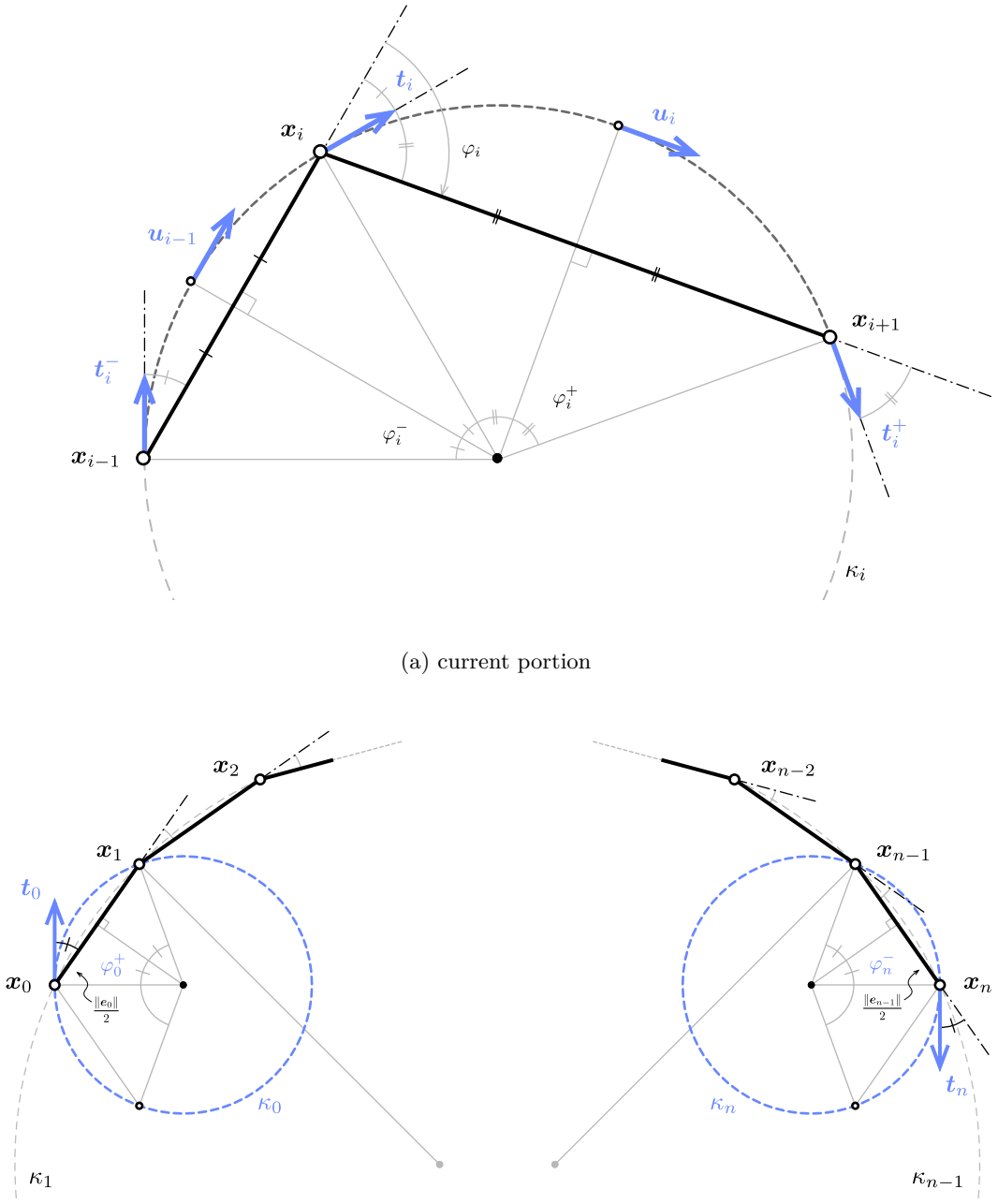

(a) current portion

(b) start

(c) end

Figure 3.15 – Definition of the tangent vector ($\boldsymbol{t}$) and related curvature binormal vector ($\boldsymbol{\kappa b}$) at vertices (circumscribed definition).

see fig. 3.15b and fig. 3.15c. It leads to the following curvature binormal vectors :

$$\boldsymbol{\kappa b}_0 = \boldsymbol{\kappa b}_0^+(\boldsymbol{t}_0^*) = \frac{2\,\boldsymbol{t}_0^* \times \boldsymbol{e}_0}{\|\boldsymbol{e}_0\|^2} \tag{3.71a}$$

$$\boldsymbol{\kappa b}_n = \boldsymbol{\kappa b}_n^-(\boldsymbol{t}_n^*) = \frac{2\,\boldsymbol{e}_{n-1} \times \boldsymbol{t}_n^*}{\|\boldsymbol{e}_{n-1}\|^2} \tag{3.71b}$$

Note that, contrary to the current portion, curvatures at endings are subjected to the definition of a unit tangent vector. This reflects the usual indetermination of boundary conditions. For a given beam whether the end is clamped, the tangent vector is known and one will seek the reacting moment due to the support ; whether the end is pinned, the reacting moment is null (so is the curvature) and one will seek the cross section orientation.

3.8.2 Inscribed case

We now consider the case where the curvature is defined according to the inscribed osculating circle (see fig. 3.16a). Remark that inscribed and circumscribed osculating circles are concentric when $l_{i-1} = l_i$.

Current portion

Let $\boldsymbol{x}_i$ be a vertex in the current portion of Γ. The inscribed osculating circle gives a smooth approximation of Γ in the vicinity of $\boldsymbol{x}_i$ (see fig. 3.16a) ; though this approximation does not pass through the vertices. It is again possible to construct some unit tangent vectors based on this circle, but the analytic expressions are less compact than in the circumscribed case (resp. at $\boldsymbol{x}_{i-1}$, $\boldsymbol{x}_i$, $\boldsymbol{x}_{i+1}$) :

$$\boldsymbol{t}_i^- = \cos(\frac{\varphi_i}{2} + \varphi_i^-)\frac{\boldsymbol{u}_{i-1} + \boldsymbol{u}_i}{\|\boldsymbol{u}_{i-1} + \boldsymbol{u}_i\|} + \sin(\frac{\varphi_i}{2} + \varphi_i^-)\frac{\boldsymbol{u}_{i-1} - \boldsymbol{u}_i}{\|\boldsymbol{u}_{i-1} - \boldsymbol{u}_i\|} \tag{3}$$

$$\boldsymbol{t}_i = \frac{\boldsymbol{u}_{i-1} + \boldsymbol{u}_i}{\|\boldsymbol{u}_{i-1} + \boldsymbol{u}_i\|} \tag{3}$$

$$\boldsymbol{t}_i^+ = \cos(\frac{\varphi_i}{2} + \varphi_i^+)\frac{\boldsymbol{u}_{i-1} + \boldsymbol{u}_i}{\|\boldsymbol{u}_{i-1} + \boldsymbol{u}_i\|} - \sin(\frac{\varphi_i}{2} + \varphi_i^+)\frac{\boldsymbol{u}_{i-1} - \boldsymbol{u}_i}{\|\boldsymbol{u}_{i-1} - \boldsymbol{u}_i\|} \tag{3}$$

In this form, the expressions of $\boldsymbol{t}_i^-$ and $\boldsymbol{t}_i^+$ exhibit lots of trigonometric computations. Consequently, they will be more costly to evaluate (numerically) than the ones given for the circumscribed case that exhibit only simple addition, product and division operations.

Though these points does not generally fall into mid-edge, the tangent vector can also be identified to $\boldsymbol{u}_{i-1}$ (resp. $\boldsymbol{u}_i$) at point $\tilde{\boldsymbol{x}}_i^- = \boldsymbol{x}_i - \frac{1}{2}\overline{l}_i\boldsymbol{u}_{i-1}$ (resp. $\tilde{\boldsymbol{x}}_i^+ = \boldsymbol{x}_i + \frac{1}{2}\overline{l}_i\boldsymbol{u}_i$) :

$$\tilde{\boldsymbol{t}}_i^- = \boldsymbol{u}_{i-1} \tag{3.73a}$$

$$\tilde{\boldsymbol{t}}_i^+ = \boldsymbol{u}_i \tag{3.73b}$$

Similarly to the circumscribed case, one can remark that the curvature binormal vector at

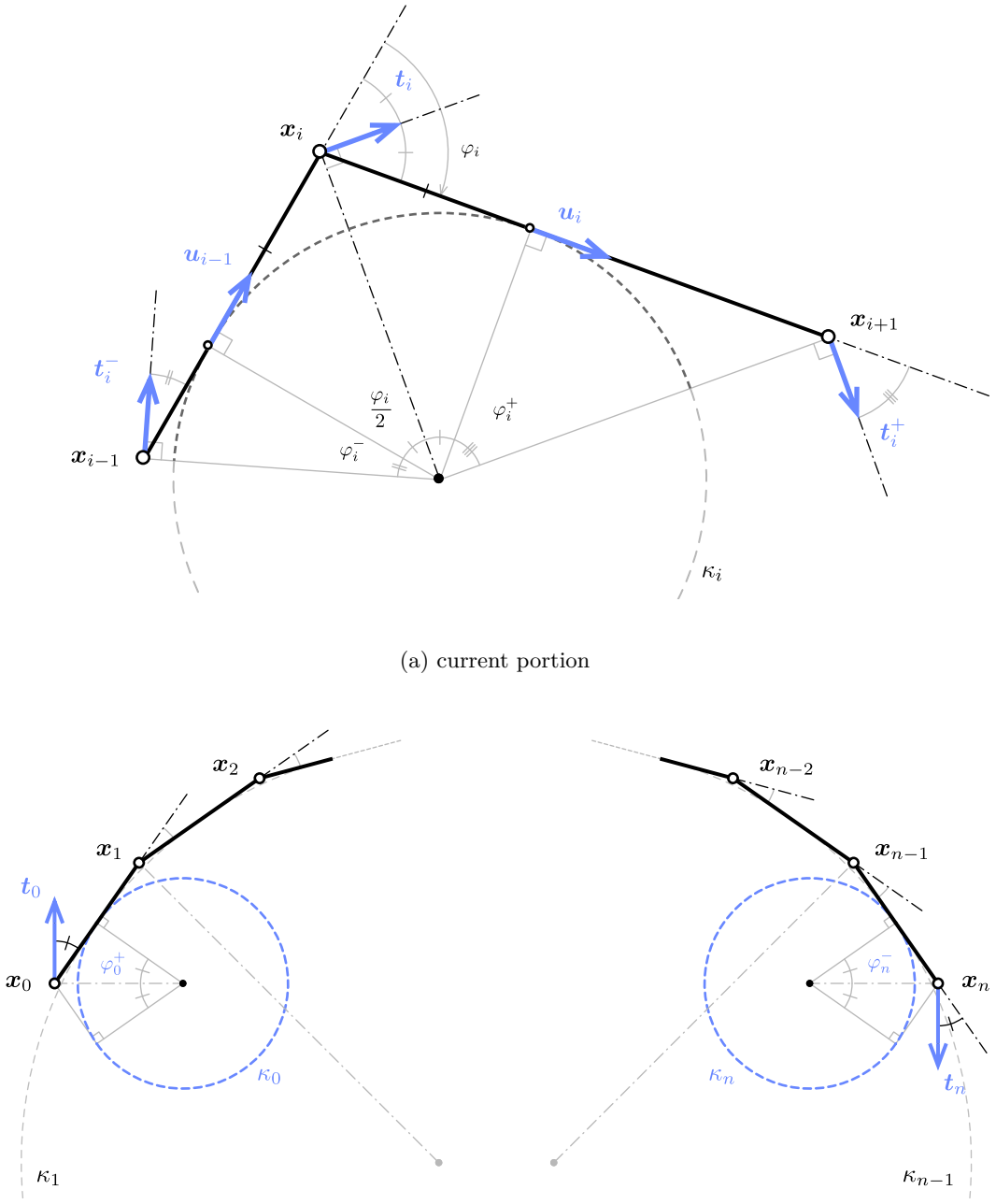

(a) current portion

(b) start

(c) end

Figure 3.16 – Definition of the tangent vector ($\boldsymbol{t}$) and related curvature binormal vector ($\boldsymbol{\kappa b}$) at vertices (inscribed definition).

$\boldsymbol{x}_i$ can be computed in three different manners :

$$\boldsymbol{\kappa b}_i = \frac{2}{\overline{\overline{l}}_i}\left(\frac{\boldsymbol{e}_{i-1}\times\boldsymbol{e}_i}{\|\boldsymbol{e}_{i-1}\|\|\boldsymbol{e}_i\| + \boldsymbol{e}_{i-1}\cdot\boldsymbol{e}_i}\right) = \begin{cases} \dfrac{2}{\overline{\overline{l}}_i}\left(\dfrac{\boldsymbol{e}_{i-1}\times\boldsymbol{t}_i}{\boldsymbol{e}_{i-1}\cdot\boldsymbol{t}_i}\right) \\ \dfrac{2}{\overline{\overline{l}}_i}\left(\dfrac{\boldsymbol{t}_i\times\boldsymbol{e}_i}{\boldsymbol{t}_i\cdot\boldsymbol{e}_i}\right) \end{cases} \tag{3.74}$$

The first expression is interpreted as the unique circle bitangent to $\boldsymbol{e}_{i-1}$ at $\tilde{\boldsymbol{x}}_i^-$ and $\boldsymbol{e}_i$ at $\tilde{\boldsymbol{x}}_i^+$, as explained in §3.7.1. Equivalently, the last two expressions in eq. (3.74) can be interpreted as the curvature binormal vector of the unique circle which center is on the line normal to $\boldsymbol{t}_i$ passing through $\boldsymbol{x}_i$, and that is tangent to $\boldsymbol{e}_{i-1}$ (resp. $\boldsymbol{e}_i$) at $\tilde{\boldsymbol{x}}_i^-$ (resp. $\tilde{\boldsymbol{x}}_i^+$).

Discontinuity of curvature

Let $\boldsymbol{t}_i^*$ be an arbitrary tangent vector at $\boldsymbol{x}_i$. Following eq. (3.74) we define the *left-sided* (resp. *right-sided*) discrete curvature at $\boldsymbol{x}_i$ in the inscribed case as :

$$\boldsymbol{\kappa b}_i^-(\boldsymbol{t}_i^*) = \frac{2}{\overline{\overline{l}}_i}\left(\frac{\boldsymbol{e}_{i-1}\times\boldsymbol{t}_i^*}{\boldsymbol{e}_{i-1}\cdot\boldsymbol{t}_i^*}\right) \tag{3.75a}$$

$$\boldsymbol{\kappa b}_i^+(\boldsymbol{t}_i^*) = \frac{2}{\overline{\overline{l}}_i}\left(\frac{\boldsymbol{t}_i^*\times\boldsymbol{e}_i}{\boldsymbol{t}_i^*\cdot\boldsymbol{e}_i}\right) \tag{3.75b}$$

The corresponding osculating circle will be called the *left-sided* (resp. *right-sided*) inscribed osculating circle. When $\boldsymbol{t}_i^* = \boldsymbol{t}_i$, the limits agree one to each other ($\boldsymbol{\kappa b}_i^- = \boldsymbol{\kappa b}_i^+ = \boldsymbol{\kappa b}_i$) and the osculating circles coincide. These definitions perfectly mimic the smooth case where, at a regular ($\|\gamma'\| \neq 0$) but not biregular ($\|\gamma''\| = 0$) point, the curvature is discontinuous while the tangent vector reminds smoothly defined.

Curve endings

The definition of the left and right sided curvatures given for a vertex in the current portion of Γ are still valid for the end vertices $\boldsymbol{x}_0$ and $\boldsymbol{x}_n$. Provided that a unit tangent vector $\boldsymbol{t}_0^*$ (respectively $\boldsymbol{t}_n^*$) is given at $\boldsymbol{x}_0$ (resp. $\boldsymbol{x}_n$), the circumscribed osculating circle is defined as the unique circle passing through $\boldsymbol{x}_0$ and $\boldsymbol{x}_1$ (resp. $\boldsymbol{x}_{n-1}$ and $\boldsymbol{x}_n$) tangent to $\boldsymbol{t}_0^*$ (resp. $\boldsymbol{t}_n^*$) ; see fig. 3.16b and fig. 3.16c. It leads to the following curvature binormal vectors :

$$\boldsymbol{\kappa b}_0 = \boldsymbol{\kappa b}_0^+(\boldsymbol{t}_0^*) = \frac{2}{\|\boldsymbol{e}_0\|}\left(\frac{\boldsymbol{t}_0^*\times\boldsymbol{e}_0}{\boldsymbol{t}_0^*\cdot\boldsymbol{e}_0}\right) \tag{3.76a}$$

$$\boldsymbol{\kappa b}_n = \boldsymbol{\kappa b}_n^-(\boldsymbol{t}_n^*) = \frac{2}{\|\boldsymbol{e}_{n-1}\|}\left(\frac{\boldsymbol{e}_{n-1}\times\boldsymbol{t}_n^*}{\boldsymbol{e}_{n-1}\cdot\boldsymbol{t}_n^*}\right) \tag{3.76b}$$

Note that, contrary to the current portion, curvatures at endings are subjected to the definition of a unit tangent vector. This reflects the usual indetermination of boundary conditions. For a given beam whether the end is clamped, the tangent vector is known and one will seek the reacting moment due to the support ; whether the end is pinned, the

reacting moment is null (so is the curvature) and one will seek the cross section orientation.

3.9 Discrete parallel transport

Discrete parallel transport can be computed by anaolgy to the smooth case as the rotation minimizing rotation around t : This methods is unstable when t1 an t2 gets almost colinear.

Note that while these definitions of parallel transport are illustrated to transport vectors in space from one location $\{\boldsymbol{x}, \boldsymbol{t}\}(s)$ to another $\{\boldsymbol{x}, \boldsymbol{t}\}(s + ds)$, it is identically transposed to parallel transport in time from one location $\{\boldsymbol{x}, \boldsymbol{t}\}(t)$ to another $\{\boldsymbol{x}, \boldsymbol{t}\}(t + dt)$ as suggested in [BAV+10].

3.9.1 The rotation method

The rotation method is given in [Blo90]. First, the frame at $\boldsymbol{x}_i$ is simply translated at vertex $\boldsymbol{x}_{i+1}$. Then, the translated frame is rotated so that $\boldsymbol{t}_i$ aligns with $\boldsymbol{t}_{i+1}$. The rotation axis is chosen to be $\boldsymbol{b} = \boldsymbol{t}_i \times \boldsymbol{t}_{i+1}$ and the angle of rotation is denoted α (see fig. 3.17a). This is analogous as the smooth case.

3.9.2 The double reflexion method

The double reflection method is given by [WJZL08]. It is supposed to be of order $o(h^4)$ whereas the rotation method is only $o(h^2)$, where $h = \sup_{i \in [\![0,1]\!]} \|\boldsymbol{e}_i\|$ is the sharpness of the discretization. Though their computation cost is quite similar, the double reflection method is not subjected to instability when $\boldsymbol{t}_i$ and $\boldsymbol{t}_{i+1}$ tend to be collinear, which is an obvious advantage.

We denote $\mathcal{R}^{\boldsymbol{n}}_{\boldsymbol{x}}$ the reflection across the plane passing through the point $\boldsymbol{x}$ and normal to the vector $\boldsymbol{n}$ of unit length ($\|\boldsymbol{n}\| = 1$). Thus, $\boldsymbol{v}$ is maped through $\mathcal{R}$ into $\boldsymbol{v}^* = \boldsymbol{v} - 2(\boldsymbol{v} \cdot \boldsymbol{n})\boldsymbol{n}$.

Let $\mathcal{R}_1 = \mathcal{R}^{\boldsymbol{n}_1}_{\boldsymbol{x}_{i+1/2}}$ be the reflection across the bisecting plane of $\boldsymbol{e}_i$ ($\boldsymbol{n}_1 = \boldsymbol{u}_i$). Let $\boldsymbol{t}^*_i = \mathcal{R}_1(\boldsymbol{t}_i)$ be the image of $\boldsymbol{t}_i$ by $\mathcal{R}_1$. Let $\mathcal{R}_2 = \mathcal{R}^{\boldsymbol{n}_2}_{\boldsymbol{x}_{i+1}}$ be the reflection across the bisecting plane of the points $\boldsymbol{x}_{i+1} + \boldsymbol{t}^*_i$ and $\boldsymbol{x}_{i+1} + \boldsymbol{t}_{i+1}$. Thus, $\boldsymbol{n}_2 = \frac{\boldsymbol{t}_{i+1} - \boldsymbol{t}^*_i}{\|\boldsymbol{t}_{i+1} - \boldsymbol{t}^*_i\|}$ (see fig. 3.17b).

The parallel transport is defined as the *double reflection* through $\mathcal{R}_1$ and $\mathcal{R}_2$:

$$\mathcal{P}^{\{\boldsymbol{x}_{i+1}, \boldsymbol{t}_{i+1}\}}_{\{\boldsymbol{x}_i, \boldsymbol{t}_i\}} = \mathcal{P}^{i+1}_i = \mathcal{R}_2 \circ \mathcal{R}_1 \tag{3.77}$$

Let $\mathcal{F}_i = \{\boldsymbol{t}_i, \boldsymbol{d}_1, \boldsymbol{d}_2\}$ be an orthonormal frame at $\boldsymbol{x}_i$. Let $\mathcal{F}^*_i = \mathcal{R}_1(\mathcal{F}_i) = \{\boldsymbol{t}^*_i, \boldsymbol{d}^*_1, \boldsymbol{d}^*_2\}$ be the image of $\mathcal{F}_i$ by $\mathcal{R}_1$. Then :

$$\boldsymbol{t}^*_i = \boldsymbol{t}_i - 2(\boldsymbol{t}_i \cdot \boldsymbol{n}_1)\boldsymbol{n}_1 \tag{3.78a}$$
$$\boldsymbol{d}^*_1 = \boldsymbol{d}_1 - 2(\boldsymbol{d}_1 \cdot \boldsymbol{n}_1)\boldsymbol{n}_1 \tag{3.78b}$$
$$\boldsymbol{d}^*_2 = \boldsymbol{d}^*_1 \times \boldsymbol{t}^*_i \tag{3.78c}$$

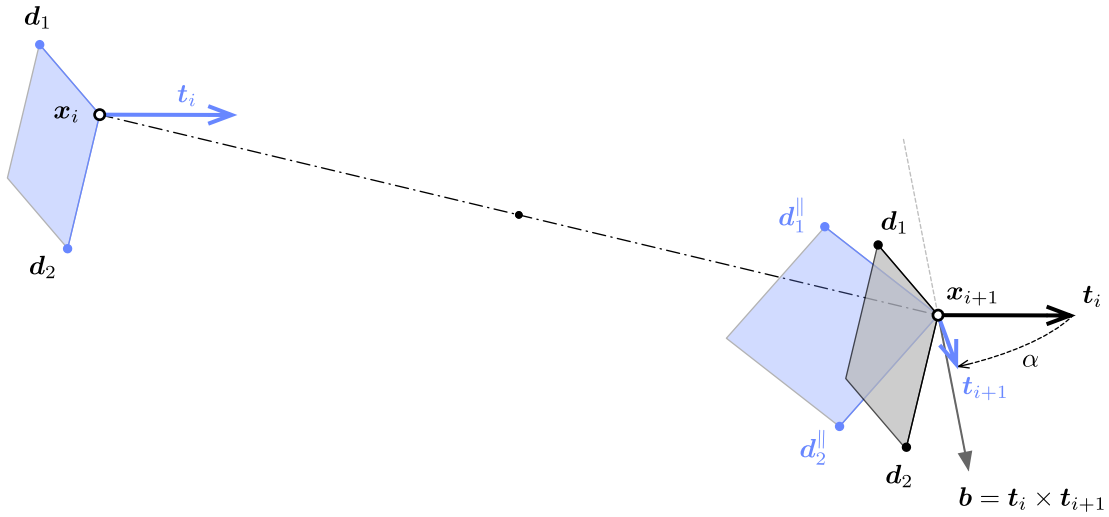

(a) rotation method

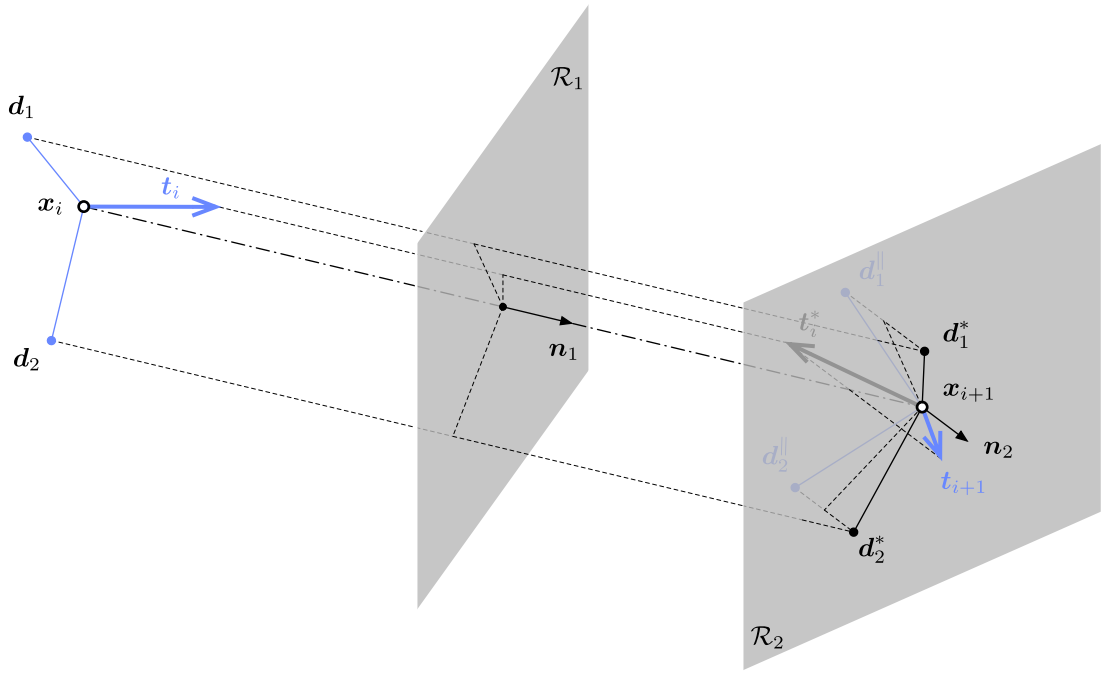

(b) double reflection method

Figure 3.17 – Parallel transport of vectors from $\{\boldsymbol{x}_i, \boldsymbol{t}_i\}$ to $\{\boldsymbol{x}_{i+1}, \boldsymbol{t}_{i+1}\}$.

Let $\mathcal{F}_i^{\parallel} = \mathcal{R}_2(\mathcal{F}_i^*) = \{\boldsymbol{t}_{i+1}, \boldsymbol{d}_1^{\parallel}, \boldsymbol{d}_2^{\parallel}\}$ be the image of $\mathcal{F}_i^*$ by $\mathcal{R}_2$. Then the parallel transported vectors are given by :

$$\boldsymbol{d}_1^{\parallel} = \boldsymbol{d}_1^* - 2(\boldsymbol{d}_1^* \cdot \boldsymbol{n}_2)\boldsymbol{n}_2 \tag{3.79a}$$

$$\boldsymbol{d}_2^{\parallel} = \boldsymbol{t}_{i+1} \times \boldsymbol{d}_1^{\parallel} \tag{3.79b}$$

The double reflection is equivalent to a rotation around the line $\mathcal{D}$ defined as the intersection of the two reflection planes, of direction $\boldsymbol{b} = \boldsymbol{n}_1 \times \boldsymbol{n}_2$, by an angle $\alpha = 2\angle(\boldsymbol{n}_1, \boldsymbol{n}_2) = 2\arcsin(\|\boldsymbol{b}\|)$.

Ici il faudrait calculer les coordonnées du centre de rotaion. Idem pour la méthode par rotation (translation + rotation = rotation ??) => trouver l'axe de rotation, l'angle et le centre la rotation équivalente. Comparer les méthodes.

Remark that for both the circumscribed (see fig. 3.15a) and inscribed (see fig. 3.16a) osculating circles :

$$\boldsymbol{t}_i = \mathcal{R}^{\boldsymbol{u}_{i-1}}_{\boldsymbol{x}_{i-1/2}} \circ \mathcal{R}^{\boldsymbol{t}_i}_{\boldsymbol{x}_i}(\boldsymbol{t}_i^-) \tag{3.80a}$$

$$\boldsymbol{t}_i = \mathcal{R}^{\boldsymbol{t}_i}_{\boldsymbol{x}_i} \circ \mathcal{R}^{\boldsymbol{u}_i}_{\boldsymbol{x}_{i+1/2}}(\boldsymbol{t}_i^+) \tag{3.80b}$$

3.10 Conclusion

Apres un rappel sur les courbes continues de l'espace, nous avons introduit, pour le cas continu, les notions de courbure, torsion géométrique, interinsèque à la courbe. Puis nous avons introduit les repères mobiles : adapté, de Frenet, de Bishop.

Nous avons fait le passage en discret et ca augmente en complexité. EN particulier, nous avons vu que la definition de la courbure n'est pas univoque. Nous avons identifé 2 approches, que nous avons comparé. Bien que la seconde est le comportement désiré pour pénaliser les courbures importantes, l'autre présente bcp d'avantages. Localité parfaite, interpolation par un arc, compatibilité des courbures droite/gauche et 3 points. Extension de la définiiton aux extrémitées. Meilleur représentativité" de l'énergie pour une discretization régulière sur des cas classiques.

Nous avons ensuite regardé la question de la definfition du vecteur tangent pour ces 2 définitions. Et sa corrélation avec la courbure.

En fin, nous avons exposé 2 méthodes pour le calcul du transport parallel sur une courbe discrete : la rotation et la double reflection, qui ne presente pas d'iunstabilité lorsque la courbure tend à s'annuler. (donc ti ti+1 colineaires).

[HM95, WJZL08]

Bibliography

[BAV+10] Miklós Bergou, Basile Audoly, Etienne Vouga, Max Wardetzky, and Eitan Grinspun. Discrete viscous threads. *ACM Transactions on ...*, pages 1–10, 2010.

[Ber28] Johannis Bernoulli. *Johannis Bernoulli... Opera omnia, tam antea sparsim edita, quam hactenus inedita.* Number IV. sumptibus Marci-Michaelis Bousquet, 1728.

[Bis75] Richard Bishop. There is more than one way to frame a curve. *Mathematical Association of America*, 1975.

[Blo90] Jules Bloomenthal. Calculation of reference frames along a space curve. In Andrew S Glassner, editor, *Graphics Gems*, volume 1, pages 567–571. Academic Press Professional, Inc., San Diego, CA, USA, 1990.

[Bob15] Alexander Bobenko. *Discrete differential geometry.* Second edition, 2015.

[BWR+08] Miklós Bergou, Max Wardetzky, Stephen Robinson, Basile Audoly, and Eitan Grinspun. Discrete elastic rods. *ACM SIGGRAPH*, pages 1–12, 2008.

[CHKS14] Daniel Carroll, Eleanor Hankins, Emek Kose, and Ivan Sterling. A survey of the differential geometry of discrete curves. *The Mathematical Intelligencer*, 36(4):28–35, 2014.

[Coo13] Julian Lowell Coolidge. *A history of geometrical methods.* Dover Books on Mathematics. Dover Publications, 2013.

[Del07] Jean Delcourt. *Analyse et géométrie : les courbes gauches de Clairaut à Serret.* PhD thesis, Université de Paris VI, 2007.

[Del11] Jean Delcourt. Analyse et géométrie, histoire des courbes gauches de Clairaut à Darboux. *Archive for History of Exact Sciences*, 65(3):229–293, 2011.

[Eul75] Leonhard Euler. Continens analysin, pro incuruatione fili in fingulis punctis inueniendia. *Novi Commentarii academiae scientiarum Petropolitanae*, 19:340–370, 1775.

[FGSS14] Rida T. Farouki, Carlotta Giannelli, Maria Lucia Sampoli, and Alessandra Sestini. Rotation-minimizing osculating frames. *Computer Aided Geometric Design*, 31(1):27–42, 2014.

[Fre52] Frédéric Frenet. Sur les courbes à double courbure. *Journal de Mathématiques Pures et Appliquées*, 17:437–447, 1852.

[GAS06] Alfred Gray, Elsa Abbena, and Simon Salamon. *Modern differential geometry of curves and surfaces with Mathematica.* CRC Press, third edition, 2006.

[Gug89] H. Guggenheimer. Computing frames along a trajectory. *Computer Aided Geometric Design*, 6(1):77–78, 1989.

[HM95] Andrew J Hanson and Hui Ma. Parallel Transport Approach to Curve Framing. Technical report, 1995.

[Hof08] Tim Hoffmann. Discrete Differential Geometry of Curves and Surfaces. 18, 2008.

[Klo86] Fopke Klok. Two moving coordinate frames for sweeping along a 3D trajectory. *Computer Aided Geometric Design*, 3(3):217–229, 1986.

[Men13] Toni Menninger. Frenet curves and successor curves : generic parametrizations of the helix and slant helix. Technical report, 2013.

[Mon09] Gaspard Monge. *Application de l'analyse à la géométrie*. 1809.

[PFL95] Tim Poston, Shiaofen Fang, and Wayne Lawton. Computing and approximating sweeping surfaces based on rotation minimizing frames. In *Proceedings of the 4th International Conference on CAD/CG*, pages 1–8, 1995.

[Pit26] Henri Pitot. Quadrature de la moitié d'une courbe des arcs appelée la compagne de la cycloïde. *Mémoires de l'Académie Royale des Sciences (1724)*, pages 107–113, 1726.

[Rom13] Pascal Romon. *Introduction à la géométrie différentielle discrète*. Références sciences. Ellipses, 2013.

[Vou14] Etienne Vouga. Plane Curves. In *Lectures in discrete differential geometry*, chapter 1, pages 1–11. 2014.

[WJZL08] Wenping Wang, Bert Jüttler, Dayue Zheng, and Yang Liu. Computation of rotation minimizing frames. *ACM Transactions on Graphics*, 27(1):1–18, 2008.

4 Elastic rod : variational approch

4.1 Introduction

4.1.1 Goals and contribution

In this section a novel element with 4 degrees of freedom accounting for torsion and bending behaviours is presented. The beam is considered in Kirchhoff's theory framework, so that it is supposed to be inextensible and its sections are supposed to remain orthogonal to the centreline during deformation. The reduction from the classic 6-DoF model to this 4-DoF model is achieved by an appropriate curve-angle representation based on a relevant curve framing. Energies are then formulated and leads to internal forces and moments acting on the beam. The static equilibrium is deduced from a damped fictitious dynamic with an adapted dynamic relaxation algorithm.

4.1.2 Related work

Basile [BAV+10] Basile [BWR+08] Basile [AAP10] Sina [**?**] [Ful78], [dV05], [Vau00], [Ber09]

Pou intro : [JLLO10]

Dynamic relaxation : [Lew03] En particulier,voir pour un comparatif avec une méthode implicite.

4.1.3 Overview

1. quaternion pour piloter les input / ouput ?
2. calcul de la hessienne au moins pour les θ comme Audoly. Ne serait-ce pas possible pour les x ? Avec ma technique du transport parallèle il me semble pourvoir avoir

accès au DL à l'ordre 2 ...

3. Formulation pour les efforts ponctuels / moments extérieurs en vue d'une résolution par minimisation. Voir F. Bertails

4. prise en compte des contraintes => méméthide des multiplicateurs de lagrange

4.2 Kirchhoff rod

The geometric configuration of the rod is described by its centerline $\boldsymbol{x}(s)$ and its cross sections. The centerline is parameterized by its arc-length. Cross sections orientations are followed along the centerline by their material frame $\{\boldsymbol{d}_3(s), \boldsymbol{d}_1(s), \boldsymbol{d}_2(s)\}$ which is an adapted orthonormal moving frame aligned to section's principal axes of inertia. Here, "adapted" means $\boldsymbol{d}_3(s) = \boldsymbol{x}'(s) = \boldsymbol{t}(s)$ is aligned to the centerline's tangent. In the literature, this description is also known as a *Cosserat Curve* [ST07].

4.2.1 Inextensibility

Note the previous description is only valid for inextensible rods in order to follow material points by their arc-length indifferently in their rest or deformed configuration. As explained in [AAP10], this hypothesis is usually relevant for slender beams. Indeed, in practice, if a slender member faces substantial axial strain the bending behaviour would become negligible due to the important difference between axial and bending stiffness. The length of the rod will be denoted L and the arc-length s will vary (with no loss of generality) in $[0, L]$.

4.2.2 Euler-Bernouilli

Strains are supposed to remain small so that material frame remains orthogonal to the centerline in the deformed configuration. Thus, differentiating the conditions of orthonormality leads to the following differential equations governing the evolution of $\{\boldsymbol{d}_3(s), \boldsymbol{d}_1(s), \boldsymbol{d}_2(s)\}$ along the centerline :

$$\begin{bmatrix} \mathbf{d_3}'(s) \\ \mathbf{d_1}'(s) \\ \mathbf{d_2}'(s) \end{bmatrix} = \begin{bmatrix} 0 & \kappa_2(s) & -\kappa_1(s) \\ -\kappa_2(s) & 0 & \tau(s) \\ \kappa_1(s) & -\tau(s) & 0 \end{bmatrix} \begin{bmatrix} \mathbf{d_3}(s) \\ \mathbf{d_1}(s) \\ \mathbf{d_2}(s) \end{bmatrix} \tag{4.1}$$

La théorie des poutres est une application de la théorie de l'élasticité isotrope. Pour mener les calculs de résistance des matériaux, on considère les hypothèses suivantes :

(1) hypothèse de Bernoulli : au cours de la déformation, les sections droites restent perpendiculaires à la courbe moyenne ;

(2) les sections droites restent planes selon Navier-Bernoulli (pas de gauchissement).

L'hypothèse de Bernoulli permet de négliger le cisaillement dans le cas de la flexion : le risque de rupture est alors due à l'extension des fibres situées à l'extérieur de la flexion, et la flèche est due au moment fléchissant. Cette hypothèse n'est pas valable pour les poutres courtes car ces dernières sont hors des limites de validité du modèle de poutre, à savoir que la dimension des sections doit être petite devant la longueur de la courbe moyenne. Le cisaillement est pris en compte dans le modèle de Timoshenko et Mindlin.

4.2.3 Darboux vector

Those equations can be formulated with the *Darboux vector* of the chosen material frame, which represents the rotational velocity of the frame along $\boldsymbol{x}(s)$:

$$\boldsymbol{d}_i'(s) = \boldsymbol{\Omega}_m(s) \times \boldsymbol{d}_i(s) \quad , \quad \boldsymbol{\Omega}_m(s) = \begin{bmatrix} \tau(s) \\ \kappa_1(s) \\ \kappa_2(s) \end{bmatrix} \tag{4.2}$$

Where $\kappa_1(s)$, $\kappa_2(s)$ and $\tau(s)$ represent respectively the rate of rotation of the material frame around the axis $\boldsymbol{d}_1(s)$, $\boldsymbol{d}_2(s)$ and $\boldsymbol{d}_3(s)$.

4.2.4 Curvatures and twist

The material curvatures are denoted $\kappa_1(s)$ and $\kappa_2(s)$ and represent the rod's flexion in the principal planes respectively normal to $\boldsymbol{d}_1(s)$ and $\boldsymbol{d}_2(s)$ .The material twist is denoted $\tau(s)$ and represents the section's rate of rotation around $\boldsymbol{d}_3(s)$. Those scalar functions measure directly the strain as defined in Kirchhoff's theory (Figure 4). Recall that the Frenet frame $\{\boldsymbol{t}(s), \boldsymbol{n}(s), \boldsymbol{b}(s)\}$ defines the osculating plane and the total curvature (κ) of a spatial curve :

$$\boldsymbol{t}'(s) = \kappa(s)\boldsymbol{n}(s) \quad , \quad \kappa(s) = \|\boldsymbol{t}'(s)\| \quad , \quad \boldsymbol{b}(s) = \boldsymbol{t}(s) \times \boldsymbol{n}(s) = \frac{\boldsymbol{t}(s) \times \boldsymbol{t}'(s)}{\kappa(s)} \tag{4.3}$$

To describe the osculating plane in which lies the bending part of the deformation, let's introduce the *curvature binormal* $\kappa\boldsymbol{b}(s) = \boldsymbol{t}(s) \times \boldsymbol{t}'(s)$, the vector of direction $\boldsymbol{b}(s)$ and norm $\kappa(s)$. At each point of arc-length s the osculating plane is normal to $\kappa\boldsymbol{b}(s)$.

4.2.5 Elastic energy

Kirrchhoff's theory assigns an elastic energy to beams according to their strain [AAP10]. In this theory, a beam is supposed to be inextensible. Thus the elastic energy ($\mathcal{E}_p$) only accounts for torsion and bending behaviors and is given by :

$$\mathcal{E}_p = \tfrac{1}{2}\int_0^L EI_1(\kappa_1 - \overline{\kappa}_1)^2 + EI_2(\kappa_2 - \overline{\kappa}_2)^2 ds + \tfrac{1}{2}\int_0^L \beta(\tau - \overline{\tau})^2 ds \tag{4.4}$$

Here, $\overline{\kappa}_1$, $\overline{\kappa}_2$ and $\overline{\tau}$ denote the natural curvature and twist of the rod in the rest position

(no stress).

4.3 Curve-angle representation

The previous paragraph has shown how the elastic potential energy of a rod can be computed following both its centerline and its cross sections orientations, which represents a model with 6-DoF : 3 for centerline positions and 3 for cross section orientations.

Following [BWR+08], let's introduce a reduced coordinate formulation of the rod that account for only 4-DoF. This reduction of DoF relies on the concept of zero-twisting frame which gives a reference frame with zero twist along a given centerline. Thus, cross section orientations $\{\boldsymbol{d}_3(s), \boldsymbol{d}_1(s), \boldsymbol{d}_2(s)\}$ can be tracked only by the measure of an angle θ from this reference frame denoted $\{\boldsymbol{d}_3(s), \boldsymbol{u}(s), \boldsymbol{v}(s)\}$ (Figure 5).

Note that an alternative solution could be to parameterize the global rotations of local material frame and to compute the rotation needed to align two successive frames along the curve's tangent.

Ici, expliquer la succession des dépendances : les vecteurs matériaux dépendent du repère de bishop par la seule variable theta. Le repère de bishop quand à lui est entièrement déterminé (au choix d'une constante de départ près) par la donnée de la centerline x.

Faire un schéma explicatif.

quid du transport parallèle en temps et non en espace ?

4.3.1 Zero-twisting frame

Zero-twisting frame, also known as Bishop frame, was introduced by Bishop in 1964. Bishop remarked that there was more than one way to frame a curve [Bis75]. Indeed, for a given curve, any orthonormal moving frame would satisfy the following differential equations, where $k_1(s)$, $k_2(s)$ and $\tau(s)$ are scalar functions that define completely the moving frame :

$$\begin{bmatrix} \mathbf{e_3}'(s) \\ \mathbf{e_1}'(s) \\ \mathbf{e_2}'(s) \end{bmatrix} = \begin{bmatrix} 0 & k_2(s) & -k_1(s) \\ -k_2(s) & 0 & \tau(s) \\ k_1(s) & -\tau(s) & 0 \end{bmatrix} \begin{bmatrix} \mathbf{e_3}(s) \\ \mathbf{e_1}(s) \\ \mathbf{e_2}(s) \end{bmatrix} \tag{4.5}$$

For instance, a Frenet frame $\{\boldsymbol{t}(s), \boldsymbol{n}(s), \boldsymbol{b}(s)\}$ is a frame which satisfies $k_1(s) = 0$. Note that this frame suffers from major disadvantages : it is undefined where the curvature vanishes and it flips at inflexion points. A Bishop frame $\{\boldsymbol{t}(s), \boldsymbol{u}(s), \boldsymbol{v}(s)\}$ is a frame which satisfies $\tau(s) = 0$. By construction, this frame has no angular velocity (i.e. no twist) around the curve's tangent ($\boldsymbol{u} \cdot \boldsymbol{v}' = \boldsymbol{u}' \cdot \boldsymbol{v} = 0$). Its evolution along the curve is described by the corresponding Darboux vector : $\boldsymbol{\Omega}_b(s) = \kappa \boldsymbol{b} = \boldsymbol{t} \times \boldsymbol{t}'$. Remark that $\boldsymbol{\Omega}_b(s)$ only depends on the centerline and is well defined even when the curvature vanishes.

Thus, by the help of $\boldsymbol{\Omega}_b(s)$, it's possible to transport a given vector $\boldsymbol{e}$ along the centerline

with no twist : $\boldsymbol{e'} = \kappa \boldsymbol{b} \times \boldsymbol{e}$. This is called *parallel transport*.

4.4 Strains

4.4.1 Axial strain

There is no axial strain to be considered as far as the rod is supposed to be unstretchable.

Remark that the inextensibility hypothesis implies that any admissible perturbation ($\lambda \boldsymbol{h}_x$) of the rod's centerline ($\boldsymbol{x}$) is locally orthogonal to the centerline itself. Indeed, at each arc-length s an inextensible rod must satisfies :

$$\|\boldsymbol{x}'\| = \|(\boldsymbol{x} + \lambda \boldsymbol{h}_x)'\| = 1 \Rightarrow \boldsymbol{d}_3 \cdot \boldsymbol{h}'_x = -\tfrac{\lambda^2}{2}\|\boldsymbol{h}'_x\|^2 = o(\lambda) \simeq 0 \tag{4.6}$$

In other words, this means that the same arc-length parametrization can be used to locate beam sections along the centerline along the deformation path. This would not be the case if the centerline would shorten or stretch out during its deformation. It is worth to mention here that this property ($\boldsymbol{d}_3 \cdot \boldsymbol{h}'_x = 0$) will be used several times in the following sections.

4.4.2 Bending strain

Let's compute the bending strains κ_1 and κ_2 regarding the geometric configuration of the rod. Remark that :

$$\kappa \boldsymbol{b} \cdot \boldsymbol{d}_1 = (\boldsymbol{d}_3 \times \boldsymbol{d}'_3) \cdot \boldsymbol{d}_1 = (\boldsymbol{d}_1 \times \boldsymbol{d}_3) \cdot \boldsymbol{d}'_3 = -\boldsymbol{d}_2 \cdot \boldsymbol{d}'_3 = \kappa_1 \tag{4.7a}$$

$$\kappa \boldsymbol{b} \cdot \boldsymbol{d}_2 = (\boldsymbol{d}_3 \times \boldsymbol{d}'_3) \cdot \boldsymbol{d}_2 = (\boldsymbol{d}_2 \times \boldsymbol{d}_3) \cdot \boldsymbol{d}'_3 = \boldsymbol{d}_1 \cdot \boldsymbol{d}'_3 = \kappa_2 \tag{4.7b}$$

That is to say $\kappa \boldsymbol{b}$ is orthogonal to $\boldsymbol{d}_3$:

$$\kappa \boldsymbol{b} = \kappa_1 \boldsymbol{d}_1 + \kappa_2 \boldsymbol{d}_2 \tag{4.8}$$

Thus, the vector of material curvatures ($\boldsymbol{\omega}$) expressed on material frame axes $\{\boldsymbol{d}_1(s), \boldsymbol{d}_2(s)\}$ is defined as :

$$\boldsymbol{\omega} = \begin{bmatrix} \kappa_1 \\ \kappa_2 \end{bmatrix} = \begin{bmatrix} \kappa \boldsymbol{b} \cdot \boldsymbol{d}_1 \\ \kappa \boldsymbol{b} \cdot \boldsymbol{d}_2 \end{bmatrix} = \begin{bmatrix} -\boldsymbol{x}'' \cdot \boldsymbol{d}_2 \\ \boldsymbol{x}'' \cdot \boldsymbol{d}_1 \end{bmatrix} \tag{4.9}$$

4.4.3 Torsional strain

Let's compute the twist or torsional strain τ regarding the geometric configuration of the rod. Decomposing the material frame on the bishop frame gives :

$$\begin{bmatrix} \boldsymbol{d}_1 \\ \boldsymbol{d}_2 \end{bmatrix} = \begin{bmatrix} \cos\theta & \sin\theta \\ -\sin\theta & \cos\theta \end{bmatrix} \begin{bmatrix} \boldsymbol{u} \\ \boldsymbol{v} \end{bmatrix} \tag{4.10}$$

Thus, the twist can be identified directly as the variation of θ along the curve :

$$\tau = \boldsymbol{d}_1' \cdot \boldsymbol{d}_2 = (\theta' \boldsymbol{d}_2 + \kappa \boldsymbol{b} \times \boldsymbol{d}_1) \cdot \boldsymbol{d}_2 = \theta' + \boldsymbol{d}_3 \cdot \kappa \boldsymbol{b} = \theta' \tag{4.11}$$

Note that the Frenet frame does not lead to a correct evaluation of the twist.

4.5 Elastic energy

Introducing $\boldsymbol{\omega}$ and θ, the elastic energy can be rewritten as follow :

$$\mathcal{E}_p = \mathcal{E}_b + \mathcal{E}_t = \tfrac{1}{2} \int_0^L (\boldsymbol{\omega} - \bar{\boldsymbol{\omega}})^T B (\boldsymbol{\omega} - \bar{\boldsymbol{\omega}}) ds + \tfrac{1}{2} \int_0^L \beta (\theta' - \bar{\theta}')^2 ds \tag{4.12}$$

Where B is the bending stiffness matrix along the principal axes of inertia and β is the torsional stiffness :

$$B = \begin{bmatrix} EI_1 & 0 \\ 0 & EI_2 \end{bmatrix} \quad , \quad \beta = GJ \tag{4.13}$$

Recall that the rod is supposed to be inextensible in Kirchhoff's theory. Thus, there is no stretching energy associated with an axial strain. However, this constraint may be enforced via a penalty energy, which in practice is somehow very similar as considering an axial stiffness into the beam's

Remark that the twisting energy ($\mathcal{E}_t$) only depends on θ and is independent regarding $\boldsymbol{x}$ while the bending energy ($\mathcal{E}_b$) depends on both θ and $\boldsymbol{x}$ variables (remind that κ_1 and κ_2 are the projections of $\kappa \boldsymbol{b}$ over $\boldsymbol{d}_1$ over $\boldsymbol{d}_2$). Thus, a coupling between bending and twisting appears as the minimum of the whole elastic energy is not necessarily reached for concomitant minimums of bending and twisting energies.

From this energy formulation, an interesting an well-known result on elastic rods could be highlighted : "torsion is uniform in an isotropic rod that is straight in its rest configuration" [ABW99].

Indeed, let's take an isotropic rod ($EI_1 = EI_2 = EI$) that is straight in its rest configuration ($\bar{\kappa}_1 = \bar{\kappa}_2 = 0$). Then, the bending energy becomes : $\mathcal{E}_b = EI_1 \kappa_1^2 + EI_2 \kappa_2^2 = EI\kappa^2$, and consequently doesn't depends on θ anymore. The curvature of the rod only depends on the geometry of its centerline ($\kappa = ||\kappa \boldsymbol{b}|| = ||\boldsymbol{x}' \times \boldsymbol{x}''||$). Thus, there is no more coupling between bending and twisting and the global minimum of elastic energy is reached while minimizing separately bending an twisting energies. That is to say the geometry of the rod ($\boldsymbol{x}$) is the one that minimized $\mathcal{E}_b$. The minimum of $\mathcal{E}_t$ is zero and is achieved for a uniform twist along the centerline, only prescribed by the boundary conditions.

4.6 Quasistatic assumption

Following [BWR+08], it is relevant to assume that the propagation of twist waves is instantaneous compared to the one of bending waves. Thus, internal forces $\boldsymbol{f}^{int}$ and moment of torsion $\boldsymbol{m}^{int}$ acts on two different timescales in the rod dynamic. Thus on the timescale of action of the force $\boldsymbol{f}^{int}$ on the center line, driving the bending waves, the twist waves propagate instantaneously, so that $\forall s \in [0, L]$, $\delta\mathcal{E}_p/\delta\theta = 0$ for the computation of $\boldsymbol{f}^{int}$. This assumption may not be enforced, as in [**?**], but leads to simpler and faster computations.

4.7 Energy gradient with respect to θ : moment of torsion

Internal moment of torsion and forces acting on the rod are classically obtained by differentiating the potential energy of the system with respect to θ and $\boldsymbol{x}$. Here, the calculus is a bit tricky as far as the differentiation takes place in function spaces. After a brief reminder on functional derivative, the main results of the calculations of the energy derivatives are given.

4.7.1 Derivative of material directors with respect to θ

Recalling that θ and $\boldsymbol{x}$ are independant variables and that Bishop frame $\{\boldsymbol{u}, \boldsymbol{v}\}$ only depends on $\boldsymbol{x}$, the decomposition of material frame directors $\{\boldsymbol{d}_1, \boldsymbol{d}_2\}$ on Bishop frame leads directly to the following expression for the derivative of the material directors :

$$\boldsymbol{D}_\theta \boldsymbol{d}_1(s) \cdot h_\theta = \frac{d}{d\lambda}\boldsymbol{d}_1[\theta + \lambda h_\theta]\Big|_{\lambda=0} = (-\sin\theta\, \boldsymbol{u} + \cos\theta\, \boldsymbol{v}) \cdot h_\theta = \boldsymbol{d}_2 \cdot h_\theta \tag{4.14a}$$

$$\boldsymbol{D}_\theta \boldsymbol{d}_2(s) \cdot h_\theta = \frac{d}{d\lambda}\boldsymbol{d}_2[\theta + \lambda h_\theta]\Big|_{\lambda=0} = (-\cos\theta\, \boldsymbol{u} - \sin\theta\, \boldsymbol{v}) \cdot h_\theta = -\boldsymbol{d}_1 \cdot h_\theta \tag{4.14b}$$

4.7.2 Derivative of the material curvatures vector with respect to θ

Regarding the definition of the material curvatures vector and the derivative of material directors with respect to θ, it follows immediately that :

$$\boldsymbol{D}_\theta \boldsymbol{\omega}(s) \cdot h_\theta = \frac{d}{d\lambda}\boldsymbol{\omega}[\theta + \lambda h_\theta]\Big|_{\lambda=0} = \begin{bmatrix} \kappa\boldsymbol{b} \cdot \boldsymbol{d}_2 \\ -\kappa\boldsymbol{b} \cdot \boldsymbol{d}_1 \end{bmatrix} \cdot h_\theta = -\boldsymbol{J}\boldsymbol{\omega} \cdot h_\theta \tag{4.15}$$

Where $\boldsymbol{J}$ is the matrix that acts on two dimensional vectors by counter-clockwise rotation of angle $\frac{\pi}{2}$:

$$\boldsymbol{J} = \begin{bmatrix} 0 & -1 \\ 1 & 0 \end{bmatrix} \tag{4.16}$$

4.7.3 Computation of the moment of torsion

The moment of torsion is given by the functional derivative of the potential elastic energy with respect to θ which can be decomposed according to the chaine rule :

$$\begin{aligned}\langle -m(s)\,, h_\theta \rangle = \boldsymbol{D}_\theta \mathcal{E}_p(s) \cdot h_\theta &= \boldsymbol{D}_\theta \mathcal{E}_b(s) \cdot h_\theta + \boldsymbol{D}_\theta \mathcal{E}_t(s) \cdot h_\theta \\ &= \boldsymbol{D}_\theta \mathcal{E}_b[\boldsymbol{\omega}[\theta]](s) \cdot h_\theta + \boldsymbol{D}_\theta \mathcal{E}_t[\theta](s) \cdot h_\theta\end{aligned} \tag{4.17}$$

Derivative of the torsion energy with respect to θ

Decomposing the previous calculus gives:

$$\begin{aligned}\boldsymbol{D}_\theta \mathcal{E}_t[\theta](s) \cdot h_\theta &= \frac{d}{d\lambda} \mathcal{E}_t[\theta + \lambda h_\theta]\Big|_{\lambda=0} \\ &= \frac{d}{d\lambda} \left(\tfrac{1}{2} \int_0^L \beta \left((\theta + \lambda h_\theta)' - \overline{\theta}' \right)^2 \, dt \right)\Big|_{\lambda=0} \\ &= \int_0^L \beta(\theta' - \overline{\theta}') \cdot h_\theta' \, dt \\ &= \left[\beta(\theta' - \overline{\theta}') \cdot h_\theta\right]_0^L - \int_0^L \left(\beta(\theta' - \overline{\theta}')\right)' \cdot h_\theta \, dt \\ &= \int_0^L \Big(\beta(\theta' - \overline{\theta}')(\delta_L - \delta_0) - \left(\beta(\theta' - \overline{\theta}')\right)' \Big) \cdot h_\theta \, dt\end{aligned} \tag{4.18}$$

Derivative of the bending energy with respect to θ

The derivative of $\mathcal{E}_b$ is obtained with the chaine rule :

$$\begin{aligned}\boldsymbol{D}_\omega \mathcal{E}_b[\boldsymbol{\omega}](s) \cdot \boldsymbol{h}_\omega &= \frac{d}{d\lambda} \mathcal{E}_b[\boldsymbol{\omega} + \lambda \boldsymbol{h}_\omega]\Big|_{\lambda=0} \\ &= \frac{d}{d\lambda} \left(\tfrac{1}{2} \int_0^L \left((\boldsymbol{\omega} + \lambda \boldsymbol{h}_\omega) - \bar{\boldsymbol{\omega}} \right)^T \boldsymbol{B} \left((\boldsymbol{\omega} + \lambda \boldsymbol{h}_\omega) - \bar{\boldsymbol{\omega}} \right) \, dt \right)\Big|_{\lambda=0} \\ &= \int_0^L (\boldsymbol{\omega} - \bar{\boldsymbol{\omega}})^T \boldsymbol{B} \cdot \boldsymbol{h}_\omega \, dt\end{aligned} \tag{4.19}$$

Finally, reminding eq 4.14 :

$$\begin{aligned}\boldsymbol{D}_\theta \mathcal{E}_b[\boldsymbol{\omega}[\theta]](s) \cdot h_\theta &= \boldsymbol{D}_\omega \mathcal{E}_b[\boldsymbol{\omega}](s) \cdot (\boldsymbol{D}_\theta \boldsymbol{\omega}[\theta](s) \cdot h_\theta) \\ &= -\int_0^L (\boldsymbol{\omega} - \bar{\boldsymbol{\omega}})^T \boldsymbol{B} \boldsymbol{J} \boldsymbol{\omega} \cdot h_\theta \, dt\end{aligned} \tag{4.20}$$

Moment of torsion

Thus, the

$$\begin{aligned}\langle -m(s)\,, h_\theta \rangle &= \boldsymbol{D}_\theta \mathcal{E}_b[\boldsymbol{\omega}[\theta]](s) \cdot h_\theta + \boldsymbol{D}_\theta \mathcal{E}_t[\theta](s) \cdot h_\theta \\ &= \int_0^L \Big(\Big(\beta(\theta' - \overline{\theta}')(\delta_L - \delta_0) - (\beta(\theta' - \overline{\theta}'))' \Big) - (\boldsymbol{\omega} - \bar{\boldsymbol{\omega}})^T \boldsymbol{B}\boldsymbol{J}\boldsymbol{\omega} \Big) \cdot h_\theta \, dt \end{aligned} \tag{4.21}$$

Finally, we can conclude on the expression of the internal moment of torsion :

$$m(s) = -\Big(\beta(\theta' - \overline{\theta}')(\delta_L - \delta_0) - (\beta(\theta' - \overline{\theta}'))' \Big) + (\boldsymbol{\omega} - \bar{\boldsymbol{\omega}})^T \boldsymbol{B}\boldsymbol{J}\boldsymbol{\omega} \tag{4.22}$$

Quasistatic hypothesis

$$(\beta(\theta' - \overline{\theta}'))' + (\boldsymbol{\omega} - \bar{\boldsymbol{\omega}})^T \boldsymbol{B}\boldsymbol{J}\boldsymbol{\omega} = 0 \tag{4.23}$$

4.8 Energy gradient with respect to x : internal forces

Internal torsional moments and forces acting on the rod are classically obtained by differentiating the potential energy of the system with respect to θ and $\boldsymbol{x}$. Here, the calculus is a bit tricky as far as the differentiation takes place in function spaces. After a brief reminder on functional derivative, the main results of the calculations of the energy derivatives are given.

paragraphe entièrment à revoir. Expliquer le cheminement. x fixe bishop et theta fixe d1,d2 par rapport à bishop. x est indépendant de theta. Seul des CL peuvent créer des couplages entre x et theta

Donc les vrais degrés de liberté du problème sont en fait les vecteurs matériels et les positions x. Se reporter à une modélisation du pb dans SO3 comme Spillmann par exemple.

Le calcul des gradients se résume donc à calculer les gradients des vecteurs matériels par rapport à des perturbations infinitésimales en x et theta. Pour theta, c'est facile. Pour kb, c'est facile. Reste la variation par rapport à x, qui est en fait la variation de bishop qu'on explique avec le writhe (défaut de fermeture de bishop sur une boucle fermée) et le transport parallèle. Le calcul se fait aisément en écrivant la double rotation et en effectuant le DL au premier ordre.

Le reste est quasiment immédiat. Reste la question des CL et des termes aux bords.

Il faut aussi se positionner par rapport à l'article de Basile. Regarder la question applied displacement vs settlement pour imposer une CL.

4.8.1 Derivative of material directors with respect to x

ici expliquer le fonctionnement de la figure

A variation of the centerline $\boldsymbol{x}$ by $\boldsymbol{\epsilon} = \lambda \boldsymbol{h}_x$ would cause a variation in the Bishop frame because parallel transport depends on the centerline itself. As far as $\boldsymbol{x}$ and θ are independent variables, this leads necessarily to a variation of the material frame. Let us denote :

- $F = \{\boldsymbol{t}, \boldsymbol{u}, \boldsymbol{v}\}$: the Bishop frame in the reference configuration ;
- $F_\epsilon = \{\boldsymbol{t}_\epsilon, \boldsymbol{u}_\epsilon, \boldsymbol{v}_\epsilon\}$: the Bishop frame in the deformed configuration ;
- $\tilde{F}_\epsilon = \{\boldsymbol{t}, \tilde{\boldsymbol{u}}_\epsilon, \tilde{\boldsymbol{v}}_\epsilon\}$: the frame obtained by parallel transporting F_ϵ back on F.

What we want to achive is to write at arc-length s the Bishop frame in the deformed configuration $\{\boldsymbol{t}_\epsilon, \boldsymbol{u}_\epsilon, \boldsymbol{v}_\epsilon\}$ on the Bishop frame in the reference configuration $\{\boldsymbol{t}, \boldsymbol{u}, \boldsymbol{v}\}$ for a small perturbation ϵ of the centerline. This transformation can be decomposed in two rotations :

- $F_\epsilon \to \tilde{F}_\epsilon$: parallel transporting F_ϵ from $\boldsymbol{t}_\epsilon$ to $\boldsymbol{t}$. This is equivalent to a rotation around $\boldsymbol{t}_\epsilon \times \boldsymbol{t}$ by an angle α_ϵ.
- $\tilde{F}_\epsilon \to F$: aligning $\tilde{F}_\epsilon$ over F. This is equivalent to a rotation around $\boldsymbol{t}$ of an angle Ψ_ϵ.

Firstly, let's decompose $\{\boldsymbol{t}_\epsilon, \boldsymbol{u}_\epsilon, \boldsymbol{v}_\epsilon\}$ on the basis $\{\boldsymbol{t}, \tilde{\boldsymbol{u}}_\epsilon, \tilde{\boldsymbol{v}}_\epsilon\}$. Note that $\tilde{F}_\epsilon$ is expressed by rotating $\tilde{F}_\epsilon$ by an angle $\Psi_\epsilon[\boldsymbol{x}](s)$ around $\boldsymbol{t}$ because $\tilde{F}_\epsilon$ is obtained by parallel transporting F_ϵ from $\boldsymbol{t}_\epsilon$ to $\boldsymbol{t}$.

Calculation of Ψ_ϵ

This variation is closely related to the writhe of closed curves. As explained in [Ful78] when parallel transporting an adapted frame around a closed curve it might not realigned with itself after one complete loop. This "lack of alignement" is directly measured by the change of writhe which can be computed with Fuller's Formula [Ful78].

Note that the derivative of θ with respect to $\boldsymbol{x}$ can be evaluated by the change of writhe in the curve as suggested in [dV05]. This approach is completly equivalent.

One can also see this lack of alignement in terms of rotation. Parallel transport being a propagation of frame from $s = 0$, the cumulated rotation of Bishop frame from the deformed configuration around the initial configuration at arc-length s is the cumulated angle of rotation of $\boldsymbol{u}[\boldsymbol{x} + \lambda \boldsymbol{h}_x]$ around $\boldsymbol{d}_3[\boldsymbol{x}]$. Recalling the rotation rate of $\boldsymbol{u}[\boldsymbol{x} + \lambda \boldsymbol{h}_x]$ is $\kappa \boldsymbol{b}[\boldsymbol{x} + \lambda \boldsymbol{h}_x]$ by definition of zero-twisting frame, one can write :

$$\Psi_\epsilon[\boldsymbol{x}](s) = -\int_0^s \kappa \boldsymbol{b}[\boldsymbol{x} + \lambda \boldsymbol{h}_x] \cdot \boldsymbol{d}_3[\boldsymbol{x}]\, dt \tag{4.24}$$

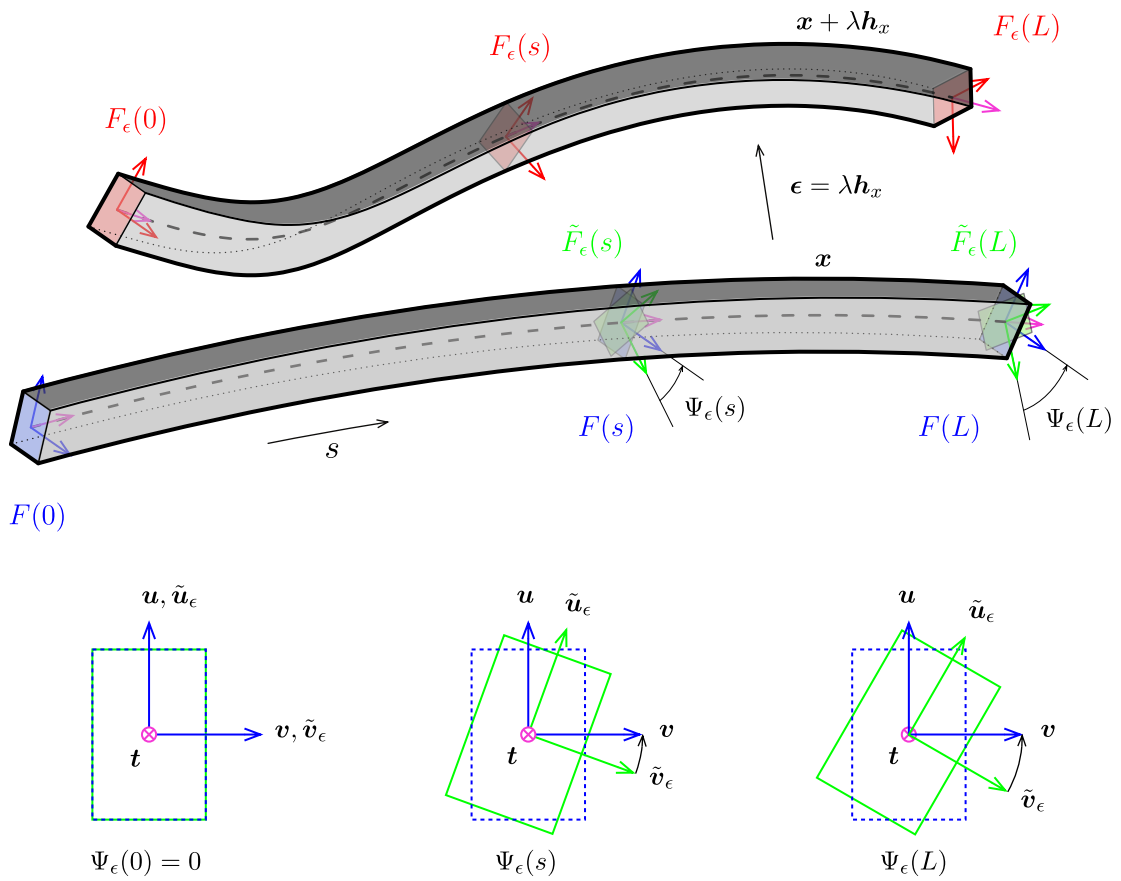

Figure 4.1 – Repères de Frenet attachés à γ.

The calculation of $\kappa\boldsymbol{b}[\boldsymbol{x}+\lambda\boldsymbol{h}_x]$ is straight forward from the curvature binormal definition :

$$\begin{aligned}\kappa\boldsymbol{b}[\boldsymbol{x}+\lambda\boldsymbol{h}_x] &= (\boldsymbol{x}+\lambda\boldsymbol{h}_x)'\times(\boldsymbol{x}+\lambda\boldsymbol{h}_x)''\\ &= \kappa\boldsymbol{b}[\boldsymbol{x}]+\lambda(\boldsymbol{x}'\times\boldsymbol{h}_x''+\boldsymbol{h}_x'\times\boldsymbol{x}'')+\lambda^2(\boldsymbol{h}_x'\times\boldsymbol{h}_x'')\\ &= \kappa\boldsymbol{b}[\boldsymbol{x}]+\lambda(\boldsymbol{x}'\times\boldsymbol{h}_x''+\boldsymbol{h}_x'\times\boldsymbol{x}'')+o(\lambda)\end{aligned} \tag{4.25}$$

Thus, reminding that $\boldsymbol{d}_3[\boldsymbol{x}]=\boldsymbol{x}'$ and $\kappa\boldsymbol{b}[\boldsymbol{x}]\cdot\boldsymbol{d}_3[\boldsymbol{x}]=0$, and using the invariance of circular product by cyclic permutation, one can express :

$$\begin{aligned}\Psi_\epsilon[\boldsymbol{x}](s) &= -\int_0^s \kappa\boldsymbol{b}[\boldsymbol{x}+\lambda\boldsymbol{h}_x]\cdot\boldsymbol{d}_3[\boldsymbol{x}]\,dt\\ &= -\lambda\int_0^s(\boldsymbol{x}'\times\boldsymbol{h}_x''+\boldsymbol{h}_x'\times\boldsymbol{x}'')\cdot\boldsymbol{x}'\,dt+o(\lambda)\\ &= -\lambda\int_0^s\kappa\boldsymbol{b}[\boldsymbol{x}]\cdot\boldsymbol{h}_x'\,dt+o(\lambda)\end{aligned} \tag{4.26}$$

By integration by parts, dropping the implicit reference to $\boldsymbol{x}$ in the notation, and denoting by δ_s and H_s the Dirac function and the Heaviside step function centered at s, $\Psi_\epsilon(s)$ could

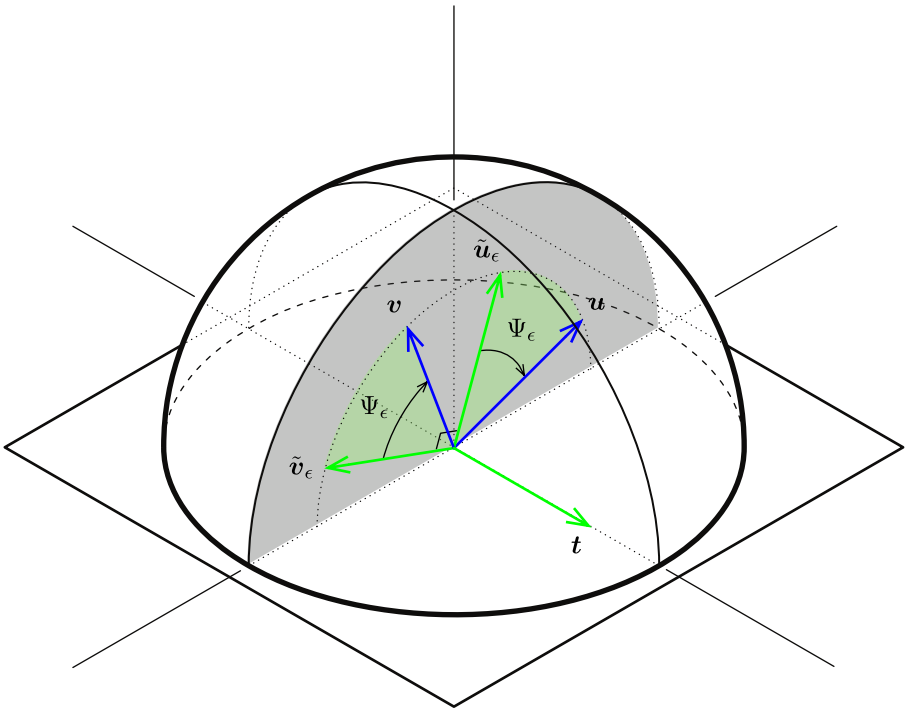

Figure 4.2 – F is obtained by rotating $\tilde{F}_\epsilon$ around $\boldsymbol{t}$ of an angle Ψ_ϵ.

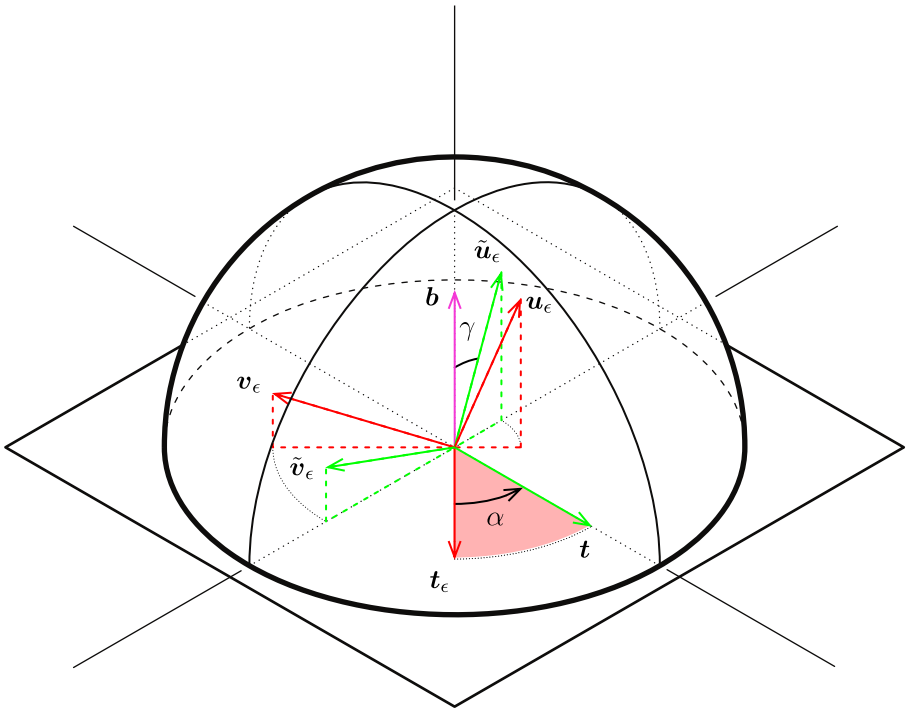

Figure 4.3 – $\tilde{F}_\epsilon$ is obtained by parallel tranpsporting F_ϵ from $\boldsymbol{t}_\epsilon$ to $\boldsymbol{t}$. This operation could be seen as a rotation around $\boldsymbol{t}_\epsilon \times \boldsymbol{t}$ of an angle α_ϵ.

be rewritten as :

$$\begin{aligned}\Psi_\epsilon(s) &= -\lambda \int_0^s \kappa \boldsymbol{b} \cdot \boldsymbol{h}'_x \, dt + o(\lambda) \\ &= -\lambda \left(\Big[\kappa \boldsymbol{b} \cdot \boldsymbol{h}_x \Big]_0^s - \int_0^s \kappa \boldsymbol{b}' \cdot \boldsymbol{h}_x \, dt \right) + o(\lambda) \\ &= -\lambda \left(\int_0^s \left((\delta_s - \delta_0) \, \kappa \boldsymbol{b} - \kappa \boldsymbol{b}' \right) \cdot \boldsymbol{h}_x \, dt \right) + o(\lambda) \\ &= -\lambda \left(\int_0^L \left((\delta_s - \delta_0) \, \kappa \boldsymbol{b} - (1 - H_s) \kappa \boldsymbol{b}' \right) \cdot \boldsymbol{h}_x \, dt \right) + o(\lambda)\end{aligned} \tag{4.27}$$

Note that, as expected, $\Psi_\epsilon(s)$ is in first order of λ and thus gets negligible when λ tends to zero, that is to say when the perturbation of $\boldsymbol{x}$ is infinitesimal :

$$\lim_{\lambda \to 0} \Psi_\epsilon(s) = 0 \tag{4.28}$$

$H_s : t \mapsto \begin{cases} 0, & t < s \\ 1, & t \geqslant s \end{cases}$ est la fonction de Heaviside.

$\delta_s : t \mapsto \delta(t - s)$ est la distribution de dirac centrée en s.

Calculation of α_ϵ

Recall that $\tilde{F}_\epsilon$ is obtained by parallel tranpsporting F_ϵ from $\boldsymbol{t}_\epsilon$ to $\boldsymbol{t}$. $\tilde{F}_\epsilon$ results from the rotation of F_ϵ around $\boldsymbol{b} = \boldsymbol{t}_\epsilon \times \boldsymbol{t}$ by an angle α_ϵ.

Recall from (4.6) that because the rod is supposed to be unstretchable, $\boldsymbol{t}_\epsilon$ stays collinear to $\boldsymbol{t}$ for an infinitesimal perturbation of the centerline :

$$\|\boldsymbol{t}\| = \|\boldsymbol{t}_\epsilon\| = 1 \Rightarrow (\boldsymbol{x} + \boldsymbol{\epsilon})' \cdot (\boldsymbol{x} + \boldsymbol{\epsilon})' = 1 \Leftrightarrow \boldsymbol{x}' \cdot \boldsymbol{\epsilon}' = -\tfrac{\lambda^2}{2} \|\boldsymbol{h}'_x\|^2 \tag{4.29}$$

Which leeds to :

$$\cos \alpha_\epsilon(s) = \boldsymbol{t} \cdot \boldsymbol{t}_\epsilon = \boldsymbol{x}' \cdot (\boldsymbol{x} + \boldsymbol{\epsilon})' = 1 + \boldsymbol{x}' \cdot \boldsymbol{\epsilon}' = 1 - \tfrac{\lambda^2}{2} \|\boldsymbol{h}'_x\|^2 \tag{4.30}$$

Thus, at second order in λ :

$$\cos \alpha_\epsilon = 1 - \tfrac{\lambda^2}{2} \|\boldsymbol{h}'_x\|^2 \tag{4.31a}$$

$$\sin \alpha_\epsilon = \sqrt{1 - \cos^2 \alpha_\epsilon} = \lambda \|\boldsymbol{h}'_x\| + o(\lambda^2) \tag{4.31b}$$

$$\sin^2 \alpha_\epsilon / 2 = \tfrac{\lambda^2}{4} \|\boldsymbol{h}'_x\|^2 \tag{4.31c}$$

Finally, it's possible to conclude that $\alpha_\epsilon(s)$ is in first order of λ and thus gets negligible when λ tends to zero :

$$\lim_{\lambda \to 0} \alpha_\epsilon(s) = 0 \tag{4.32}$$

Aligning $\tilde{F}_\epsilon$ towards F_ϵ

Recall that aligning $\tilde{F}_\epsilon$ over F is nothing but a rotation around $\boldsymbol{t}$ by an angle Ψ_ϵ. This leads to :

$$\tilde{\boldsymbol{u}}_\epsilon = \cos\Psi_\epsilon\, \boldsymbol{u} + \sin\Psi_\epsilon\, \boldsymbol{v} \tag{4.33a}$$

$$\tilde{\boldsymbol{v}}_\epsilon = -\sin\Psi_\epsilon\, \boldsymbol{u} + \cos\Psi_\epsilon\, \boldsymbol{v} \tag{4.33b}$$

Aligning F_ϵ towards t

Recall that $\tilde{F}_\epsilon$ is obtained by parallel tranpsporting F_ϵ from $\boldsymbol{t}_\epsilon$ to $\boldsymbol{t}$. This operation could be seen as a rotation around $\boldsymbol{t}_\epsilon \times \boldsymbol{t}$ of an angle α_ϵ. Where :

$$\boldsymbol{b} = \boldsymbol{t}_\epsilon \times \boldsymbol{t} = \cos\gamma\, \tilde{\boldsymbol{u}}_\epsilon + \sin\gamma\, \tilde{\boldsymbol{v}}_\epsilon = \cos\gamma\, \boldsymbol{u}_\epsilon + \sin\gamma\, \boldsymbol{v}_\epsilon \tag{4.34}$$

Expressing F_ϵ on the basis $\tilde{F}_\epsilon$ gives for $\boldsymbol{u}_\epsilon$ and $\boldsymbol{v}_\epsilon$:

$$\boldsymbol{u}_\epsilon = \sin\gamma\, \boldsymbol{b} + \cos\gamma\, \Big(\sin\alpha_\epsilon\, \tilde{\boldsymbol{t}} + \cos\alpha_\epsilon\, (\cos\gamma\, \tilde{\boldsymbol{u}}_{\boldsymbol{\epsilon}} - \sin\gamma\, \tilde{\boldsymbol{v}}_{\boldsymbol{\epsilon}})\Big) \tag{4.35a}$$

$$\boldsymbol{v}_\epsilon = \cos\gamma\, \boldsymbol{b} + \sin\gamma\, \Big(-\sin\alpha_\epsilon\, \tilde{\boldsymbol{t}} + \cos\alpha_\epsilon\, (\sin\gamma\, \tilde{\boldsymbol{u}}_{\boldsymbol{\epsilon}} - \cos\gamma\, \tilde{\boldsymbol{v}}_{\boldsymbol{\epsilon}})\Big) \tag{4.35b}$$

Which can be rearranged in :

$$\boldsymbol{u}_\epsilon = \cos\gamma \sin\alpha_\epsilon\, \boldsymbol{t} + (\cos\alpha_\epsilon \cos^2\gamma + \cos^2\gamma)\tilde{\boldsymbol{u}}_{\boldsymbol{\epsilon}} + \sin\gamma\cos\gamma\, (1-\cos\alpha_\epsilon)\tilde{\boldsymbol{v}}_{\boldsymbol{\epsilon}} \tag{4.36a}$$

$$\boldsymbol{v}_\epsilon = -\sin\gamma \sin\alpha_\epsilon\, \boldsymbol{t} + \cos\gamma\sin\gamma\, (1-\cos\alpha_\epsilon)\tilde{\boldsymbol{u}}_{\boldsymbol{\epsilon}} + (\cos^2\gamma + \cos\alpha_\epsilon \sin^2\gamma)\tilde{\boldsymbol{v}}_{\boldsymbol{\epsilon}} \tag{4.36b}$$

Variation of Bishop frame with respect to x

Finally, one can express F_ϵ on the basis F as the composition of two rotations :

$$\boldsymbol{u}_\epsilon = \begin{bmatrix} 1 & 0 & 0 \\ 0 & \cos\Psi_\epsilon & -\sin\Psi_\epsilon \\ 0 & \sin\Psi_\epsilon & \cos\Psi_\epsilon \end{bmatrix} \begin{bmatrix} \cos\gamma\sin\alpha_\epsilon \\ 1 - 2\cos^2\gamma\sin^2\alpha_\epsilon/2 \\ 2\sin\gamma\cos\gamma\sin^2\alpha_\epsilon/2 \end{bmatrix} = \begin{bmatrix} \alpha_\epsilon\cos\gamma \\ 1 \\ \Psi_\epsilon \end{bmatrix} + o(\lambda) \tag{4.37a}$$

$$\boldsymbol{v}_\epsilon = \begin{bmatrix} 1 & 0 & 0 \\ 0 & \cos\Psi_\epsilon & -\sin\Psi_\epsilon \\ 0 & \sin\Psi_\epsilon & \cos\Psi_\epsilon \end{bmatrix} \begin{bmatrix} -\sin\gamma\sin\alpha_\epsilon \\ 2\sin\gamma\cos\gamma\sin^2\alpha_\epsilon/2 \\ 1 - 2\sin\gamma^2\sin^2\alpha_\epsilon/2 \end{bmatrix} = \begin{bmatrix} -\alpha_\epsilon\sin\gamma \\ -\Psi_\epsilon \\ 1 \end{bmatrix} + o(\lambda) \tag{4.37b}$$

Here, the expressions have been developed in first order of λ as far as α_ϵ and Ψ_ϵ it's been proofed in eq [] that those quantities tends two zero when the perturbation of the centerline is infinitesimal.

Finally, one can express the variation of material directors with respect to an infinitesimal

variation of rod's centerline :

$$\boldsymbol{u}_\epsilon = \alpha_\epsilon \cos\gamma\ \boldsymbol{t} + \boldsymbol{u} + \Psi_\epsilon \boldsymbol{v} + o(\lambda) \tag{4.38a}$$
$$\boldsymbol{v}_\epsilon = -\alpha_\epsilon \sin\gamma\ \boldsymbol{t} + \boldsymbol{v} - \Psi_\epsilon \boldsymbol{u} + o(\lambda) \tag{4.38b}$$

Variation of material frame with respect to $\boldsymbol{x}$

Recalling the expression of the material frame expressed in the reference Bishop frame, it's now easy to deduce the variation of material frame with respect to a variation of the rod's centerline :

$$\boldsymbol{d}_1[\boldsymbol{x} + \lambda \boldsymbol{h}_x] = \cos\theta\ \boldsymbol{u}_\epsilon + \sin\theta\ \boldsymbol{v}_\epsilon \tag{4.39a}$$
$$\boldsymbol{d}_2[\boldsymbol{x} + \lambda \boldsymbol{h}_x] = -\sin\theta\ \boldsymbol{u}_\epsilon + \cos\theta\ \boldsymbol{v}_\epsilon \tag{4.39b}$$

Which leads according to the previous equation to :

$$\boldsymbol{d}_1[\boldsymbol{x} + \lambda \boldsymbol{h}_x] = \boldsymbol{d}_1[\boldsymbol{x}] + \Psi_\epsilon \boldsymbol{d}_2[\boldsymbol{x}] + \alpha_\epsilon \cos(\theta - \gamma)\ \boldsymbol{t}[\boldsymbol{x}] + o(\lambda) \tag{4.40a}$$
$$\boldsymbol{d}_2[\boldsymbol{x} + \lambda \boldsymbol{h}_x] = \boldsymbol{d}_2[\boldsymbol{x}] - \Psi_\epsilon \boldsymbol{d}_1[\boldsymbol{x}] - \alpha_\epsilon \sin(\theta + \gamma)\ \boldsymbol{t}[\boldsymbol{x}] + o(\lambda) \tag{4.40b}$$

4.8.2 Derivative of the material curvatures vector with respect to x

It's know straightforward from the previous section to express the variation of the material curvatures with respect to a variation $\boldsymbol{\epsilon} = \lambda \boldsymbol{h}_x$ of $\boldsymbol{x}$ while θ remains unchanged.

$$(\boldsymbol{x} + \lambda \boldsymbol{h}_x)'' \cdot \boldsymbol{d}_1[\boldsymbol{x} + \lambda \boldsymbol{h}_x] = (\boldsymbol{x}'' + \lambda \boldsymbol{h}_x'') \cdot \Big(\boldsymbol{d}_1 + \Psi_\epsilon \boldsymbol{d}_2 + \alpha_\epsilon \cos(\theta - \gamma)\ \boldsymbol{t} + o(\lambda)\Big) \tag{4.41a}$$
$$(\boldsymbol{x} + \lambda \boldsymbol{h}_x)'' \cdot \boldsymbol{d}_2[\boldsymbol{x} + \lambda \boldsymbol{h}_x] = (\boldsymbol{x}'' + \lambda \boldsymbol{h}_x'') \cdot \Big(\boldsymbol{d}_2 - \Psi_\epsilon \boldsymbol{d}_1 - \alpha_\epsilon \sin(\theta + \gamma)\ \boldsymbol{t} + o(\lambda)\Big) \tag{4.41b}$$

Thus, recalling that $\boldsymbol{x}'' \cdot \boldsymbol{d}_3 = 0$ and that α_ϵ and Ψ_ϵ are first order quantities in λ :

$$(\boldsymbol{x} + \lambda \boldsymbol{h}_x)'' \cdot \boldsymbol{d}_1[\boldsymbol{x} + \lambda \boldsymbol{h}_x] = \boldsymbol{x}'' \cdot \boldsymbol{d}_1 + \Psi_\epsilon \boldsymbol{x}'' \cdot \boldsymbol{d}_2 + \lambda \boldsymbol{h}_x'' \cdot \boldsymbol{d}_1 + o(\lambda) \tag{4.42a}$$
$$(\boldsymbol{x} + \lambda \boldsymbol{h}_x)'' \cdot \boldsymbol{d}_2[\boldsymbol{x} + \lambda \boldsymbol{h}_x] = \boldsymbol{x}'' \cdot \boldsymbol{d}_2 - \Psi_\epsilon \boldsymbol{x}'' \cdot \boldsymbol{d}_1 + \lambda \boldsymbol{h}_x'' \cdot \boldsymbol{d}_2 + o(\lambda) \tag{4.42b}$$

Which finally leads to :

$$\boldsymbol{\omega}[\boldsymbol{x} + \lambda \boldsymbol{h}_x] = \boldsymbol{\omega}[\boldsymbol{x}] - \Psi_\epsilon \boldsymbol{J}\boldsymbol{\omega}[\boldsymbol{x}] + \lambda \begin{bmatrix} -\boldsymbol{h}_x'' \cdot \boldsymbol{d}_2 \\ \boldsymbol{h}_x'' \cdot \boldsymbol{d}_1 \end{bmatrix} + o(\lambda) \tag{4.43}$$

Reminding the expression of Ψ_ϵ computed in paragraphe[], one can express the derivative of the material curvatures vector with respect to $\boldsymbol{x}$:

$$\boldsymbol{D}_x\boldsymbol{\omega}(s) \cdot \boldsymbol{h}_x = \left(\int_0^L \left((\delta_s - \delta_0)\, \kappa \boldsymbol{b} - (1 - H_s) \kappa \boldsymbol{b}' \right) \cdot \boldsymbol{h}_x\, dt \right) \boldsymbol{J}\boldsymbol{\omega} + \begin{bmatrix} -\boldsymbol{d}_2{}^T \\ \boldsymbol{d}_1{}^T \end{bmatrix} \cdot \boldsymbol{h}_x'' \tag{4.44}$$

4.8.3 Computation of the forces acting on the centerline

The forces acting on the centerline are given by the functional derivative of the potential elastic energy with respect to x which can be decomposed according to the chaine rule :

$$\begin{aligned}\langle -f(s)\,, \boldsymbol{h}_x \rangle = \boldsymbol{D}_x \mathcal{E}_p(s) \cdot \boldsymbol{h}_x &= \boldsymbol{D}_x \mathcal{E}_b(s) \cdot \boldsymbol{h}_x + \boldsymbol{D}_x \mathcal{E}_t(s) \cdot \boldsymbol{h}_x \\ &= \boldsymbol{D}_x \mathcal{E}_b[\boldsymbol{\omega}[\boldsymbol{x}]](s) \cdot \boldsymbol{h}_x + \boldsymbol{D}_x \mathcal{E}_t[\boldsymbol{x}](s) \cdot \boldsymbol{h}_x\end{aligned} \tag{4.45}$$

Derivative of the torsion energy with respect to x

Recall that the torsion energy only depends on θ which is independent of x. Thus, $\mathcal{E}_t$ is independent of x :

$$\boldsymbol{D}_x \mathcal{E}_t[\boldsymbol{x}](s) \cdot \boldsymbol{h}_x = \frac{d}{d\lambda} \mathcal{E}_t[\boldsymbol{x} + \lambda \boldsymbol{h}_x]\Big|_{\lambda=0} = 0 \tag{4.46}$$

Derivative of the bending energy with respect to x

The derivative of $\mathcal{E}_b$ is obtained with the chaine rule :

$$\boldsymbol{D}_\omega \mathcal{E}_b[\boldsymbol{\omega}](s) \cdot \boldsymbol{h}_\omega = \frac{d}{d\lambda} \mathcal{E}_b[\boldsymbol{\omega} + \lambda \boldsymbol{h}_\omega]\Big|_{\lambda=0} = \int_0^L (\boldsymbol{\omega} - \bar{\boldsymbol{\omega}})^T \boldsymbol{B} \cdot \boldsymbol{h}_\omega \, dt \tag{4.47}$$

Finally, reminding eq 4.14 :

$$\boldsymbol{D}_x \mathcal{E}_b[\boldsymbol{\omega}[\boldsymbol{x}]](s) \cdot \boldsymbol{h}_x = \boldsymbol{D}_\omega \mathcal{E}_b[\boldsymbol{\omega}](s) \cdot (\boldsymbol{D}_x \boldsymbol{\omega}[\boldsymbol{x}](s) \cdot \boldsymbol{h}_x) = \mathcal{A} + \mathcal{B} + \mathcal{C} \tag{4.48}$$

Where :

$$\mathcal{A} = \int_0^L (\boldsymbol{\omega} - \bar{\boldsymbol{\omega}})^T \boldsymbol{B} \begin{bmatrix} -\boldsymbol{d}_2{}^T \\ \boldsymbol{d}_1{}^T \end{bmatrix} \cdot \boldsymbol{h}_x'' \, dt \tag{4.49a}$$

$$\mathcal{B} = \int_{t=0}^L (\boldsymbol{\omega} - \bar{\boldsymbol{\omega}})^T \boldsymbol{B} \boldsymbol{J} \boldsymbol{\omega} \left(\int_{u=0}^L (\delta_t - \delta_0) \, \kappa \boldsymbol{b} \cdot \boldsymbol{h}_x \, du \right) \, dt \tag{4.49b}$$

$$\mathcal{C} = \int_{t=0}^L -(\boldsymbol{\omega} - \bar{\boldsymbol{\omega}})^T \boldsymbol{B} \boldsymbol{J} \boldsymbol{\omega} \left(\int_{u=0}^L (1 - H_t) \, \kappa \boldsymbol{b}' \cdot \boldsymbol{h}_x \, du \right) \, dt \tag{4.49c}$$

Calculus of $\mathcal{A}$:

$$\mathcal{A} = \int_0^L (\boldsymbol{\omega} - \bar{\boldsymbol{\omega}})^T \boldsymbol{B} \begin{bmatrix} -\boldsymbol{d}_2{}^T \\ \boldsymbol{d}_1{}^T \end{bmatrix} \cdot \boldsymbol{h}_x'' \, dt \tag{4.50}$$

Recalling the bending moment is given by :

$$\boldsymbol{M} = (\kappa_1 - \bar{\kappa}_1) E I_1 \boldsymbol{d}_1 + (\kappa_2 - \bar{\kappa}_2) E I_2 \boldsymbol{d}_2 = M_1 \boldsymbol{d}_1 + M_2 \boldsymbol{d}_2 \tag{4.51}$$

One can remark that :

$$(\boldsymbol{\omega} - \bar{\boldsymbol{\omega}})^T \boldsymbol{B} \begin{bmatrix} -\boldsymbol{d}_2{}^T \\ \boldsymbol{d}_1{}^T \end{bmatrix} = M_2 \boldsymbol{d}_1{}^T - M_1 \boldsymbol{d}_2{}^T = -(\boldsymbol{d}_3 \times \boldsymbol{M})^T \tag{4.52}$$

Rq : on mixe abusivement 2 formes d'écritures, matricielle et vectorielle, à cause du produit scalaire que l'on écrit tantôt sous sa forme vectorielle et parfois matricielle (à l'aide de la transposée).

Thus, $\mathcal{A}$ could be rewritten in it's vectoriel form :

$$\begin{aligned} \mathcal{A} &= -\int_0^L (\boldsymbol{d}_3 \times \boldsymbol{M}) \cdot \boldsymbol{h}_x'' \, dt \\ &= -\left[(\boldsymbol{d}_3 \times \boldsymbol{M}) \cdot \boldsymbol{h}_x'\right]_0^L + \int_0^L (\boldsymbol{d}_3 \times \boldsymbol{M})' \cdot \boldsymbol{h}_x' \, dt \\ &= -\left[(\boldsymbol{d}_3 \times \boldsymbol{M}) \cdot \boldsymbol{h}_x'\right]_0^L + \int_0^L \left((\boldsymbol{d}_3 \times \boldsymbol{M}') \cdot \boldsymbol{h}_x' + (\boldsymbol{h}_x' \times \boldsymbol{d}_3') \cdot \boldsymbol{M}\right) \, dt \end{aligned} \tag{4.53}$$

Recall that from (4.6) that $\boldsymbol{h}_x' \cdot \boldsymbol{d}_3 = 0$ and from (4.1) that $\boldsymbol{d}_3' \cdot \boldsymbol{d}_3 = 0$. Hence, $\boldsymbol{h}_x' \times \boldsymbol{d}_3'$ is colinear to $\boldsymbol{d}_3$. Or by definition $\boldsymbol{M}$ is orthogonal to $\boldsymbol{d}_3$. Thus, $(\boldsymbol{h}_x' \times \boldsymbol{d}_3') \cdot \boldsymbol{M} = 0$. Finally, after a second integration by parts :

$$\begin{aligned} \mathcal{A} &= -\left[(\boldsymbol{d}_3 \times \boldsymbol{M}) \cdot \boldsymbol{h}_x'\right]_0^L + \int_0^L (\boldsymbol{d}_3 \times \boldsymbol{M}') \cdot \boldsymbol{h}_x' \, dt \\ &= \left[(\boldsymbol{d}_3 \times \boldsymbol{M}') \cdot \boldsymbol{h}_x'' \; - (\boldsymbol{d}_3 \times \boldsymbol{M}) \cdot \boldsymbol{h}_x'\right]_0^L - \int_0^L (\boldsymbol{d}_3 \times \boldsymbol{M}')' \cdot \boldsymbol{h}_x \, dt \end{aligned} \tag{4.54}$$

Calculus of $\mathcal{B}$:

$$\begin{aligned} \mathcal{B} &= \int_{t=0}^L (\boldsymbol{\omega} - \bar{\boldsymbol{\omega}})^T \boldsymbol{B}\boldsymbol{J}\boldsymbol{\omega} \left(\int_{u=0}^L (\delta_t - \delta_0) \, \kappa \boldsymbol{b} \cdot \boldsymbol{h}_x \, du \right) \, dt \\ &= -(\kappa \boldsymbol{b} \cdot \boldsymbol{h}_x)(0) \int_{t=0}^L (\boldsymbol{\omega} - \bar{\boldsymbol{\omega}})^T \boldsymbol{B}\boldsymbol{J}\boldsymbol{\omega} \, dt + \int_{t=0}^L (\boldsymbol{\omega} - \bar{\boldsymbol{\omega}})^T \boldsymbol{B}\boldsymbol{J}\boldsymbol{\omega}\kappa \boldsymbol{b} \cdot \boldsymbol{h}_x \, dt \end{aligned} \tag{4.55}$$

Calculus of $\mathcal{C}$:

$$\begin{aligned} \mathcal{C} &= \int_{t=0}^L -(\boldsymbol{\omega} - \bar{\boldsymbol{\omega}})^T \boldsymbol{B}\boldsymbol{J}\boldsymbol{\omega} \left(\int_{u=0}^L (1 - H_t) \, \kappa \boldsymbol{b}' \cdot \boldsymbol{h}_x \, du \right) \, dt \\ &= \int_{u=0}^L \int_{t=u}^L - \left((\boldsymbol{\omega} - \bar{\boldsymbol{\omega}})^T \boldsymbol{B}\boldsymbol{J}\boldsymbol{\omega} \right)(t) \, (\kappa \boldsymbol{b}' \cdot \boldsymbol{h}_x)(u) \, dt \, du \\ &= \int_{u=0}^L - \left(\int_{t=u}^L (\boldsymbol{\omega} - \bar{\boldsymbol{\omega}})^T \boldsymbol{B}\boldsymbol{J}\boldsymbol{\omega} \, dt \right) (\kappa \boldsymbol{b}' \cdot \boldsymbol{h}_x) \, du \end{aligned} \tag{4.56}$$

By several integration by parts, using Fubini's theorem once and supposing that the terms

vanishes at $s = 0$ and $s = L$:

$$\begin{aligned}
\mathcal{B} + \mathcal{C} &= \int_{t=0}^{L} \left((\boldsymbol{\omega} - \bar{\boldsymbol{\omega}})^T \boldsymbol{B}\boldsymbol{J}\boldsymbol{\omega}\kappa\boldsymbol{b} - \left(\int_{u=t}^{L} (\boldsymbol{\omega} - \bar{\boldsymbol{\omega}})^T \boldsymbol{B}\boldsymbol{J}\boldsymbol{\omega}\, du \right) \kappa\boldsymbol{b}' \right) \cdot \boldsymbol{h}_x\, dt \\
&= \int_{t=0}^{L} \left(- \left(\int_{u=t}^{L} (\boldsymbol{\omega} - \bar{\boldsymbol{\omega}})^T \boldsymbol{B}\boldsymbol{J}\boldsymbol{\omega}\, du \right)' \kappa\boldsymbol{b} - \left(\int_{u=t}^{L} (\boldsymbol{\omega} - \bar{\boldsymbol{\omega}})^T \boldsymbol{B}\boldsymbol{J}\boldsymbol{\omega}\, du \right) \kappa\boldsymbol{b}' \right) \cdot \boldsymbol{h}_x\, dt \\
&= \int_{t=0}^{L} \left(- \left(\int_{u=t}^{L} (\boldsymbol{\omega} - \bar{\boldsymbol{\omega}})^T \boldsymbol{B}\boldsymbol{J}\boldsymbol{\omega}\, du \right) \kappa\boldsymbol{b} \right)' \cdot \boldsymbol{h}_x\, dt
\end{aligned} \tag{4.57}$$

Which can be rewritted using the quasi-static hypothesis :

$$\begin{aligned}
\mathcal{B} + \mathcal{C} &= \int_{t=0}^{L} \left(- \left(\int_{u=t}^{L} (\boldsymbol{\omega} - \bar{\boldsymbol{\omega}})^T \boldsymbol{B}\boldsymbol{J}\boldsymbol{\omega}\, du \right) \kappa\boldsymbol{b} \right)' \cdot \boldsymbol{h}_x\, dt \\
&= \int_{t=0}^{L} \left(- \left(\int_{u=t}^{L} \beta(\theta' - \overline{\theta}')(\delta_L - \delta_0) - (\beta(\theta' - \overline{\theta}'))'\, du \right) \kappa\boldsymbol{b} \right)' \cdot \boldsymbol{h}_x\, dt \\
&= \int_{t=0}^{L} \left(- \left(\beta(\theta' - \overline{\theta}')(L) - \left[\beta(\theta' - \overline{\theta}')\right]_t^L \right) \kappa\boldsymbol{b} \right)' \cdot \boldsymbol{h}_x\, dt \\
&= \int_{t=0}^{L} - \left(\beta(\theta' - \overline{\theta}')\kappa\boldsymbol{b}\right)' \cdot \boldsymbol{h}_x\, dt
\end{aligned} \tag{4.58}$$

Finally :

$$\boldsymbol{D}_x \mathcal{E}_b[\boldsymbol{\omega}[\boldsymbol{x}]](s) \cdot \boldsymbol{h}_x = \int_0^L \left(- \left(\boldsymbol{d}_3 \times \boldsymbol{M}'\right)' - \left(\beta(\theta' - \overline{\theta}')\kappa\boldsymbol{b}\right)' \right) \cdot \boldsymbol{h}_x\, dt \tag{4.59}$$

Internal forces

Thus, the internal forces are related to the variation of internal elastic energy as :

$$\left\langle -\boldsymbol{f}(s)\,, \boldsymbol{h}_x \right\rangle = \boldsymbol{D}_x \mathcal{E}_p(s) \cdot \boldsymbol{h}_x = - \int_0^L \left(\left(\boldsymbol{d}_3 \times \boldsymbol{M}'\right)' + \left(\beta(\theta' - \overline{\theta}')\kappa\boldsymbol{b}\right)' \right) \cdot \boldsymbol{h}_x\, dt \tag{4.60}$$

Finally, we can conclude on the expression of the internal forces :

$$\boldsymbol{f}(s) = \left(\boldsymbol{d}_3 \times \boldsymbol{M}'\right)' + \left(\beta(\theta' - \overline{\theta}')\kappa\boldsymbol{b}\right)' \tag{4.61}$$

Remarquer ici que l'expression est purement locale. Elle ne dépend pas du sens de parcours de la poutre, contrairement au raisonnement suivi. Cette différence est notable avec la démarche de B. Audoly. Faire le bilan des bénéfices de l'hypothèse quasi-statique : - expressions rigoureusement vraies à l'équilibre statique - simplification ds le calcul des efforts - rapidité dans le calcul avec des expressions plus simples - il n'est pas forcément intéressant en terme d'algorithmie d'imposer l'hypothèse quasistatique au cours du calcul. Il faudrait faire un bench pour savoir.

On retombe sur les équations de Kirchhoff à un terme manquant pret. Qui exprime la contribution de la variation moment de flexion à cause de la torsion $\tau \boldsymbol{M}$‘. Peut-être que ce terme est finalement d’un ordre supérieur, si l’on suppose une variation lente de la torsion ? Comment comprendre la disparition de ce terme qui semble nécessaire à l’équilibre statique d’un élément de poutre si l’on en croit les équations de Kirchhoff ?

4.9 Conclusion

On retrouve les équations de kirchhoff dynamique où l’on a négligé les forces inertielles de rotation d’un élément de poutre autour de $\boldsymbol{d}_1$ et $\boldsymbol{d}_2$ pour ne garder que la dynamique de rotation de la section autour de la fibre neutre $\boldsymbol{d}_3$.

The shear force acting on the right side of a section is nothing but $\boldsymbol{T} = \int \boldsymbol{f}$:

$$\boldsymbol{T}(s) = \boldsymbol{d}_3 \times \boldsymbol{M}' + Q\kappa\boldsymbol{b} \tag{4.62}$$

The linear momentum acting on the centerline is given by :

$$m(s) = Q' - \kappa\boldsymbol{b} \cdot (\boldsymbol{d}_3 \times \boldsymbol{M}) \tag{4.63}$$

The main hypothesis are :

- Bernoulli : $\boldsymbol{d}_i \cdot \boldsymbol{d}_j = \delta_{ij}$
- Inextensibility : $\|\boldsymbol{d}_3'\| = 1$
- Quasistatic : at each timestep regarding bending motion $m(s) = 0$

Bibliography

[AAP10] Basile Audoly, M Amar, and Yves Pomeau. *Elasticity and geometry*. 2010.

[ABW99] Sigrid Adriaenssens, Michael Barnes, and Christopher Williams. A new analytic and numerical basis for the form-finding and analysis of spline and gridshell structures. In B Kumar and B H V Topping, editors, *Computing Developments in Civil and Structural Engineering*, pages 83–91. Civil-Comp Press, Edinburgh, 1999.

[BAV+10] Miklós Bergou, Basile Audoly, Etienne Vouga, Max Wardetzky, and Eitan Grinspun. Discrete viscous threads. *ACM Transactions on ...*, pages 1–10, 2010.

[Ber09] Mitchell Berger. Topological Quantities: Calculating Winding, Writhing, Linking, and Higher order Invariants. *Lecture Notes in Mathematics*, 1973:75–97, 2009.

[Bis75] Richard Bishop. There is more than one way to frame a curve. *Mathematical Association of America*, 1975.

[BWR+08] Miklós Bergou, Max Wardetzky, Stephen Robinson, Basile Audoly, and Eitan Grinspun. Discrete elastic rods. *ACM SIGGRAPH*, pages 1–12, 2008.

[dV05] Renko de Vries. Evaluating changes of writhe in computer simulations of supercoiled DNA. *The Journal of Chemical Physics*, 122(6), 2005.

[Ful78] F Brock Fuller. Decomposition of the linking number of a closed ribbon : A problem from molecular biology. 75(8):3557–3561, 1978.

[JLLO10] Pascal Jung, Sigrid Leyendecker, Joachim Linn, and Michael Ortiz. A discrete mechanics approach to the Cosserat rod theory—Part 1: static equilibria. *International journal for numerical methods in engineering*, 85(1):31–60, 2010.

[Lew03] Wanda Lewis. *Tension structures: form and behaviour*. Telford, Thomas, 2003.

[ST07] Jonas Spillmann and Matthias Teschner. CORDE : Cosserat Rod Elements for the Dynamic Simulation of One-Dimensional Elastic Objects. *Eurographics/ ACM SIGGRAPH Symposium on Computer Animation*, pages 1–10, 2007.

[Vau00] Rue Vauquelin. Writhing Geometry at Finite Temperature : Random Walks and Geometric phases for Stiff Polymers. (1), 2000.

5 Elastic rod : equilibrium approach

5.1 Introduction

Ici on explique que l'approche par les équations d'équilibre est beaucoup plus directe que l'approche énergétique.

5.1.1 Goals and contribution

Dans ce chapitre, après un bref rappel sur le cadre mathématique d'étude des courbes paramétrique de l'espace, on présente les notions de courbures et de torsion géométrique associées au repère de fraient. On montre ensuite le cas plus général d'un repère mobile quelconque attaché à une courbe gamma. On définit enfin la particularité d'un repère mobile adapté à un courbe, et on présente, en sus du repère de Frenet, une approche différente pour accrocher des repères le long d'une courbe (Bishop / RMF / Zéro-twisting frame)

Ici il faudrait préciser la terminologie des auteurs / équations / hypothèses : Euler-Bernoulli, Navier-Bernoulli, Kirchhoff, Love, Clebesh, Cosserat, Vlassov

5.1.2 Related work

On peu s'instruire dans la publi de Dill [Dil92]. Regarder en particulier le premier chapitre de l'HDR de Neukirch [Neu09]. Regarder également la chronologie des modèles proposée dans la thèse de Theetten [The07]. Pourquoi pas proposer une frise chronologique + un tableau de synthèse des hyptohèses.

[Dil92] **(author?)** [Neu09] [ABW99] [Hoo06] [LL09] [Spi08] [Ant05]

[Neu09] : p69 - [Dil92] : p16

Dans les tentatives dans notre domaine, citer :

Kirchhoff : [Kir50, Kir76]
Clebsch : [Cle83]
Love : [Lov92]
Timoshenko : [Tim21, Tim22, TG51]

"Note that γ having unit speed corresponds to the rod being inextensible; this is not always assumed in the theory, nor is the material frame necessarily assumed to be orthonormal as it is here" [LS96, p. 607]

"Natural frames and the curve angle representation of rod" [LS96, p. 607]

Départ : [Day65] : already includes a rotational DOF !! [Wak80] [Bar99] : revue intéressante de la DR.

3 pts classique : [ABW99] [DBC06]

2 x 3pts : [BAK13]

6 Dofs : [DKZ14]

4Dofs : [dPTL+15] [DZK16]

Dans le champ de l'animation avec élément finis [DLP13] [MPW14]

5.1.3 Overview

Résumé du chapitre

1 2 3

"The battle between weight and rigidity constitutes, in itself, the single aesthetic theme of art in architecture : and to bring out this conflict in the most varied and clearest way is its office." [Ben91b, p. xvii]

> The theory of elastic structures is, by definition, the collection of all reasonable models, proposed during almost three centuries, concerned with simplifying the solutions of problems involving elastic bodies. The equations describing the motion and equilibrium of a three-dimensional elastic body were formulated in full generality during the first half of the nineteenth century, but their solutions are known only in a few cases. [Vil97, p. xvii]

[1] For a shearable rod, the condition that $\boldsymbol{d}_3$ and $\boldsymbol{t}$ coincide is relaxed.
[2] in the directions of the principal axes of inertia of its cross-section
[3] The parameter $\overline{s}$, usually chosen as the arc length parameter for the undeformed rod, is no longer the arc length parameter for the deformed rod, since there are deformations of shear and extension. The current arc length of the deformed rod is a function of $\overline{s}$, which is often denoted by $s(\overline{s})$.

> In a deformed state, the center line has no particular reason to remain straight and, in general, $\boldsymbol{d}_1$ and $\boldsymbol{d}_2$ will twist along the center line. However, in the case of small strain that we consider, the triad $(\boldsymbol{d}_1, \boldsymbol{d}_2, \boldsymbol{d}_3)$ remains approximately orthonormal, provided it has been chosen orthonormal in the reference configuration. This is known as the Euler-Bernoulli or Navier-Bernoulli kinematical hypothesis, or sometimes the assumption of unshearable rods. [AAP10, p. 68]

Extension to the case of thin-walled sections by [DA15, Vet14] in the case of ribbons. From the Vlasov

> For thin beams having a slender cross-section, $h \ll w$, the classical rod theory of Kirchhoff is known to be inapplicable. Such beams are usually modeled using Vlasov's theory for thin-walled beams. Vlasov's models can be justified from 3D elasticity but only in the case of moderate deformations, when the cross-sections bend by a small amount. In the present work, however, we have considered large deformations of thin strips. The strip has been modeled as an inextensible plate, and the geometric constraint of inextensibility has been treated exactly : the cross-sections are allowed to bend by a significant amount. Our model extends the classical strip model of Sadowsky, and reformulate it in a way that fits into the classical theory of rods. [DA14, p.]

5.2 Introduction to the special Cosserat theory of rods

This paragraph gives a very brief overview of the *special Cosserat theory of rods*, as presented in [Ant05], that accounts for bending, torsion, extension and shear behaviors of slender beams.[4] This theory – which is a *director theory* of rods – was first introduced by [Ant74]. It gives a larger scope to the basements of the present work – which relies on the *Kirchhoff theory of rods* – as the last is a special case of this larger theoretical framework. Thus, what is presented in this paragraph could be considered as a reasonable starting point to extend the present work, for instance to take account for shear or large extension, which might be relevant for some engineering problems or form-finding processes.

It has been largely employed in various fields [SBH95, BAV+10].

5.2.1 Description of the motion

The special Cosserat theory of rods consider dynamics of rods. It relies on a precise geometric description (see fig. 5.1) of rods build upon three vector-valued functions that are time dependent :

- $\boldsymbol{x}$, a position vector describing the geometry in space of a specific *fiber* called the rod *axis* or *centerline*. This function describes the rod in its longitudinal dimension. This dimension is of prime importance in the case of slender bodies such as rods as what is intend is to build a reduced theory, namely a 1-dimensional theory. This curve will often be understood as the curve passing through the cross-section centroids along the rod, although this is not mandatory in the theory.
- $\boldsymbol{d}_1$, $\boldsymbol{d}_2$, two unit vector fields describing the lateral spatiality of the rod and called material *directors*. These vectors will often be understood as the principal axis of the cross-section, although this is not mandatory in the theory.

Modeling the geometry of the rod in any configuration is not sufficient to build a mechanical model. Indeed, one must know a *reference* state for the solid as strains measure relative change in geometry and stresses are related to strains through the constitutive relation of the rod material. Thus, the special Cosserat theory of rods consider two configurations :

- The *actual* configuration, that is the configuration of the rod at time t during the motion.
- The *reference* configuration, that is the configuration of the rod in a specific state where its geometry (possibly curved and twisted) is known and its mechanical state (strains, stresses) under possible loads (dead weight, temperature, wind, snow , pre-stress, ...) and possible boundary conditions is known. In practice, this configuration

[4] "[we formulate] a general dynamical theory of rods that can undergo large deformations in space by suffering flexure, torsion, extension, and shear. We call the resulting geometrically exact theory the *special Cosserat theory of rods*." [Ant05, p. 270]

will often be chosen as a *stress-free* configuration when the beam is not subject to any loads nor restrains of any kind, although this is not mandatory in the theory.

Thus, the equations governing the motion of a *special Cosserat rod* will be based on the description of a fully known reference configuration and the description of the actual or deformed configuration of the rod at time t during its motion (see fig. 5.1). Usually, what is intended is to predict the motion of a particular rod given its reference configuration, material properties, boundary conditions, and loading. In this thesis, the equations of the motion will be integrated to converged as fast as possible to the quasi-static response of the system, as this work only deals with statics of structures. However, it is still possible to use a more convenient and accurate time integrator to compute the motion, if one wants to study the (true) dynamic of a rod and go beyond the knowledge of its static equilibrium.

Hereafter, when ambiguity is possible, symbols referring to the reference configuration will be marked with an overline while symbols referring to the actual configuration will be marked with a subscript in the variable t. Generally, scalar quantities are marked with the subscript t and vector quantities with an overline in order to avoid double subscripts when one will refer to vector components.

Actual configuration

At time t, the *actual* or *deformed* configuration of the rod $\{\boldsymbol{x}, \boldsymbol{d}_1, \boldsymbol{d}_2\}$ is described by its *centerline* $\gamma_t \in \mathcal{C}^1([0, L] \times \mathbb{R}^3)$, a regular space curve :

$$\begin{array}{rccc} \gamma_t(t,\cdot): & [0,L] & \longrightarrow & \mathbb{R}^3 \\ & s & \longmapsto & \boldsymbol{x}(t,s) \end{array} \tag{5.1}$$

and two perpendicular unit vector fields : [5]

$$\begin{array}{rccc} (\boldsymbol{d}_1,\boldsymbol{d}_2)(t,\cdot): & [0,L] & \longrightarrow & \mathbb{R}^3 \times \mathbb{R}^3 \\ & s & \longmapsto & (\boldsymbol{d}_1(t,s), \boldsymbol{d}_2(t,s)) \;/\; \boldsymbol{d}_1(t,s) \cdot \boldsymbol{d}_2(t,s) = 0 \end{array} \tag{5.2}$$

In addition, we define a third unit vector field as :

$$\boldsymbol{d}_3 = \boldsymbol{d}_1 \times \boldsymbol{d}_2 \tag{5.3}$$

Thus, the centerline is framed with the orthonormal moving frame $\{\boldsymbol{d}_1, \boldsymbol{d}_2, \boldsymbol{d}_3\}$. The unit vectors $\boldsymbol{d}_i(t,s)$ are called *material directors*.

Note that the centerline is parametrized by s chosen to be the arc length parameter of the *reference* configuration. It may not coincide with the arc length parameter of the *actual* configuration denoted by $s_t = \Psi(t,s) = \Psi_t(s)$ as the rod may suffer elongation. L denotes the length of the centerline in the reference configuration. The actual length of γ_t is denoted by L_t so that $s_t \in [0, L_t]$.

[5] Requiring that $\boldsymbol{d}_1 \perp \boldsymbol{d}_2$ implies that the description of the motion is conveninent only for small in-plane stretching and shearing of the cross-section. This constrain can be relaxed to lead to an even more general theory, called the *2-director Cosserat theory*.

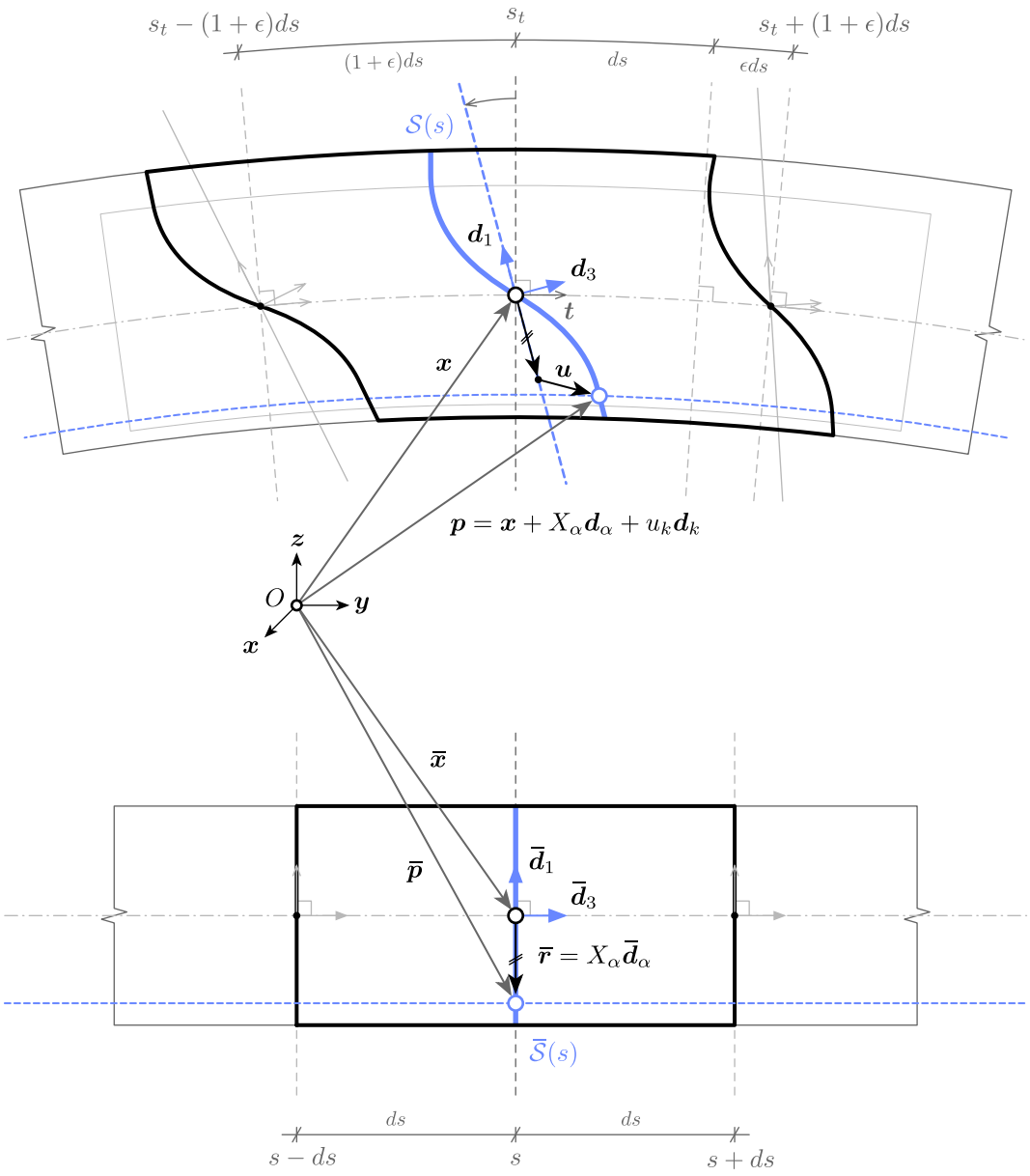

Figure 5.1 – Description of the motion for a Cosserat rod. This is a typical longitudinal section of a rectangular beam deformed from a reference configuration (bottom) to an actual configuration (top) at time t. Cross-sections are defined in the reference configuration to be planar surfaces perpendicular to the beam axis ($\overline{\mathcal{S}}$). A material point $\overline{\boldsymbol{p}} \in \overline{\mathcal{S}}(s)$ is located relatively to the cross-section centroid ($\overline{\boldsymbol{x}}(s)$) thanks to its material coordinates (X_1, X_2, s). During the motion, this material point reaches a new position $\boldsymbol{p} \in \mathcal{S}(s)$. The deformed cross-section $\mathcal{S}(s)$ is no more planar. The material frame is no more aligned with the beam axis ($\boldsymbol{d}_3$ and $\boldsymbol{t}$ are not parallel any more). The actual position is measured from the centroid of the deformed cross-section ($\boldsymbol{x}(s)$) plus an in-plane component ($X_\alpha \boldsymbol{d}_\alpha$) and a deformation vector ($\boldsymbol{u}$). If the cross-sections deform in a rigid-body manner, then $\boldsymbol{u}$ is null everywhere.

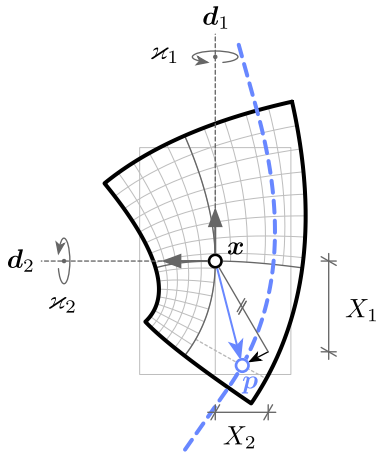

(a) Deformed cross-section $\mathcal{S}(s)$.

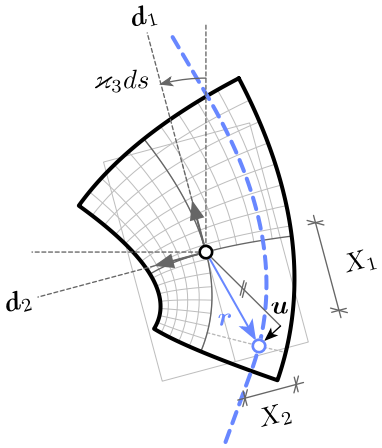

(b) Deformed cross-section $\mathcal{S}(s+ds)$.

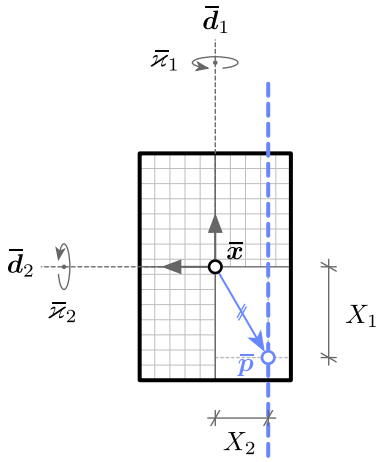

(c) Reference cross-section $\overline{\mathcal{S}}(s)$.

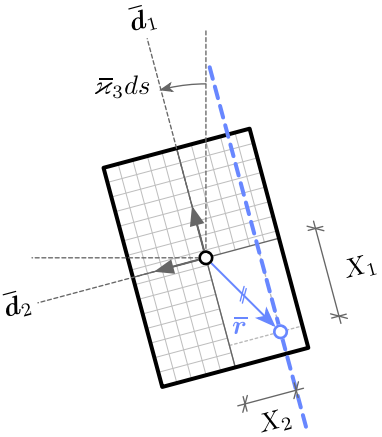

(d) Reference cross-section $\overline{\mathcal{S}}(s+ds)$.

Figure 5.2 – Description of the motion for a Cosserat rod. These are the transverse sections from fig. 5.1 (however note that fig. 5.1 is drawn with $\varkappa_2 < 0$ while $\varkappa_2 > 0$ in fig. 5.2). The section curve is drawn in a dashed blue fashion. Remark how the deformed material point is located through $\boldsymbol{x}$ and $\boldsymbol{r} = X_\alpha \boldsymbol{d}_\alpha + u_k \boldsymbol{d}_k$. Cross-sections are rotating around $\boldsymbol{d}_3$ at speed $\varkappa_3$. The beam is subjected to flexion ($\varkappa_1 > 0$, $\varkappa_2 > 0$), torsion ($\varkappa_3 > 0$) and extension ($\epsilon > 0$). Fibers that are compressed – both directly by axial compression or indirectly by flexion – are subjected to transverse expansion due to the Poisson effect (see up-right of figures 5.2a and 5.2b). Reciprocally, fibers in tension – both directly by axial tension or indirectly by flexion – are subjected to transverse contraction (see bottom-left of figures 5.2a and 5.2b).

Finally, a material point $\boldsymbol{p}$ of the body is located relatively to the centerline with the help of the local position vector $\boldsymbol{r}$ such that (see figures 5.2a and 5.2b) :

$$\boldsymbol{p}(\overline{\boldsymbol{r}}, t) = \boldsymbol{x}(s,t) + \boldsymbol{r}\Big(\boldsymbol{x}(s,t), \boldsymbol{d}_1(s,t), \boldsymbol{d}_2(s,t), \overline{\boldsymbol{r}}, t\Big) \tag{5.4}$$

Note that in the above expression a material point is uniquely identified – in a very generic manner – by its local position in the reference configuration ($\overline{\boldsymbol{r}} = \overline{\boldsymbol{p}} - \overline{\boldsymbol{x}}$).

Reference configuration

We now identify a *reference* configuration of the rod $\{\overline{\boldsymbol{x}}, \overline{\boldsymbol{d}}_1, \overline{\boldsymbol{d}}_2\}$ with centerline $\overline{\gamma} \in \mathcal{C}^1([0, L] \times \mathbb{R}^3)$, a regular space curve. This time, s is the arc length parameter of $\overline{\gamma}$, which leads to the important relation between $\overline{\boldsymbol{x}}$ and the unit tangent vector $\overline{\boldsymbol{t}}$ of $\overline{\gamma}$:

$$\frac{d\overline{\boldsymbol{x}}}{ds} = \overline{\boldsymbol{t}} \quad , \quad \|\overline{\boldsymbol{t}}\| = 1 \tag{5.5}$$

In this configuration, we define a cross-section $\mathcal{S}(s)$ as the set of material points lying in a plane perpendicular to $\overline{\gamma}$ at position $\overline{\boldsymbol{x}}(s)$. By definition, it is a planar surface in the reference configuration. However, there is no evidence that this surface will remain planar in any other configuration. Moreover, and only for this configuration, it makes sens to choose the centerline as the curve passing through the cross-section centroids.

Finally, we call *material coordinates* of point $\overline{\boldsymbol{p}} \in \mathcal{S}(s)$ the triple $(X_1, X_2, s = X_3)$ such that (see figures 5.2c and 5.2d) :

$$\overline{\boldsymbol{p}}(\overline{\boldsymbol{r}}) = \overline{\boldsymbol{x}}(s) + \overline{\boldsymbol{r}}\Big(\overline{\boldsymbol{x}}(s), \overline{\boldsymbol{d}}_1(s), \overline{\boldsymbol{d}}_2(s), X_1, X_2\Big) \tag{5.6a}$$

$$\overline{\boldsymbol{r}}(X_1, X_2, s) = X_1\overline{\boldsymbol{d}}_1(s) + X_2\overline{\boldsymbol{d}}_2(s) \tag{5.6b}$$

We also identify a *fiber* as the set of material points that share the same cross-section coordinates (X_1, X_2) all along the rod in the reference configuration.

5.2.2 Time evolution

The evolution in time of the rod is simply given by the velocity of its centerline ($\dot{\boldsymbol{x}}$) and the angular velocity or *spin vector* ($\boldsymbol{\omega}$) of its material directors :

$$\frac{\partial \boldsymbol{x}}{\partial t}(s,t) = \dot{\boldsymbol{x}} \tag{5.7a}$$

$$\frac{\partial \boldsymbol{d}_k}{\partial t}(s,t) = \dot{\boldsymbol{d}}_k = \boldsymbol{\omega}(s,t) \times \boldsymbol{d}_k(s,t) \tag{5.7b}$$

From now on, the derivative with respect to time is denoted with an overdot symbol.

5.2.3 Strains

Strains are described with the help of the strains vectors $\boldsymbol{\eta}$ and $\boldsymbol{\varkappa}$ – respectively the force strains vector and moment strains vector [Rei73] :

$$\frac{\partial \boldsymbol{x}}{\partial s}(s,t) = \boldsymbol{x}' = \boldsymbol{\eta}(s,t) \tag{5.8a}$$

$$\frac{\partial \boldsymbol{d}_k}{\partial s}(s,t) = \boldsymbol{d}_k' = \boldsymbol{\varkappa}(s,t) \times \boldsymbol{d}_k(s,t) \tag{5.8b}$$

where the derivative with respect to s is denoted with a prime symbol.[6] The components of $\boldsymbol{\eta} = \eta_k \boldsymbol{d}_k$ and $\boldsymbol{\varkappa} = \varkappa_k \boldsymbol{d}_k$ expressed in the material frame basis $\{\boldsymbol{d}_1, \boldsymbol{d}_2, \boldsymbol{d}_3\}$ can be interpreted as the classical engineering strains that lead to the engineering stresses.[7,8] In particular $\eta_1 = \boldsymbol{x}' \cdot (\boldsymbol{d}_1 \times \boldsymbol{d}_2)$ characterizes the change in volume of the body while η_2 and η_3 characterize the shear deformations ; $\varkappa_3$ is the material twist of the rod while $\varkappa_1$ and $\varkappa_2$ are the material curvatures of the rod.[9]

Observe the symmetry of eq. (5.7a) and (5.7b) and eq. (5.8a) and (5.8b) regarding the parameters s and t :

- $(\dot{\boldsymbol{x}}, \boldsymbol{\omega})$ governs the time evolution of the material frame.
- $(\boldsymbol{x}', \boldsymbol{\varkappa})$ governs the spatial evolution of the material frame along the centerline.

5.2.4 Parametrization of the centerline

Recall that because the centerline of the reference configuration is parametrized by arc length, the unit tangent vector in this configuration is given by :

$$\overline{\boldsymbol{t}}(s) = \frac{d\overline{\boldsymbol{x}}}{ds}(\overline{s}) = \overline{\boldsymbol{x}}'(s) \quad , \quad \|\overline{\boldsymbol{x}}'\| = 1 \tag{5.9}$$

In the deformed configuration, the centerline is still parametrized by s which is no more an arc length parameter because the centerline has suffered stretch. Thus, the unit tangent vector in this configuration is given by : [10]

$$\boldsymbol{t}(s,t) = \frac{\boldsymbol{x}'(s,t)}{\|\boldsymbol{x}'(s,t)\|} \quad , \quad \|\boldsymbol{x}'\| = \|\boldsymbol{\eta}'\| \neq 1 \tag{5.10}$$

[6] For an extensible rod, the derivative with respect to s and s_t are not equivalent. The prime notation stands only for the derivation with respect to s, the arc length parameter of the rod in the reference configuration.

[7] For a complete interpretation, see [Ant05, p. 285] or [AAP10, ch. 3].

[8] Einstein's notation is employed here. For instance : $\boldsymbol{\eta} = \eta_k \boldsymbol{d}_k = \eta_1 \boldsymbol{d}_1 + \eta_2 \boldsymbol{d}_2 + \eta_3 \boldsymbol{d}_3$.

[9] Here, the term "material" is necessary as the material curvatures don't coincide with the geometric curvatures, although they are related one to each other. Precisely, the distinction originates in the fact that s is not a unit-speed parametrization of the centerline in the actual configuration.

[10] However, because s_t is an arc length parameter of γ_t : $\boldsymbol{t}(s,t) = \frac{\partial \boldsymbol{x}}{\partial s_t}(s,t)$.

We introduce ϵ, the extension of the rod which characterizes the local change in length of the rod centerline, defined as :

$$\|\boldsymbol{\eta}'(s,t)\| = \frac{\partial s_t}{\partial s}(s,t) = \Psi'(s,t) = 1 + \epsilon(s,t) \tag{5.11}$$

Inextensibility

The rod is said to be inextensible if $\epsilon = 0$ everywhere and at all time. In this case, s is a valid arc length parameter for the centerline in every configurations. Later, we will restrict to the case of rods subjected to small extension, that is $\epsilon(t,s) \ll 1$.

Reparametrization

Although either s and s_t can be chosen as the third material coordinate to describe a rod, the definition of the material strains are given with respect to s and not s_t. This is a matter of concern as the constitutive relations – classically of the form $M = EI\kappa$, $N = ES\epsilon$, $Q = GJ\tau$ – relies upon material strains. Thus, in theses equations, what takes place is a derivation with respect to s and not to s_t, which matters if the rod is not required to be inextensible.

5.2.5 To go further

The reader is invited to refer to [Ant05] to get a deeper understanding of the *Cosserat theory for rods*, in particular to see how the governing equations are derived. Here, only the geometric description of a Cosserat rod has been presented in a very generic but still concise manner. This description will be used in the next sections in the narrower scope of the (first order) *Kirchhoff theory for rods* but could be usefully employed for richer theories.

	reference configuration	actual configuration
arc length	$s = \Psi_t^{-1}(s_t)$	$s_t = \Psi_t(s)$
length	L	L_t
centerline	$\overline{\gamma}$	γ_t
position vector	$\overline{\boldsymbol{x}}$	$\boldsymbol{x}$
material frame	$\{\overline{\boldsymbol{d}}_1, \overline{\boldsymbol{d}}_2, \overline{\boldsymbol{d}}_3\}$	$\{\boldsymbol{d}_1, \boldsymbol{d}_2, \boldsymbol{d}_3\}$
material coordinates	(X_1, X_2, s)	(X_1, X_2, s)
force strains	$\overline{\boldsymbol{\eta}}$	$\boldsymbol{\eta}$
moment strains	$\overline{\boldsymbol{\varkappa}}$	$\boldsymbol{\varkappa}$
spin vector	$\overline{\boldsymbol{\omega}}$	$\boldsymbol{\omega}$
axial extension	$\overline{\epsilon} = 0$	$\|\eta\| = \Psi_t'(s) = 1 + \epsilon$
arc length derivative	$\frac{\partial}{\partial s}\cdot = (\cdot)'$	$\frac{\partial}{\partial s_t}\cdot = (1+\epsilon)^{-1}(\cdot)'$
time derivative	$\frac{\partial}{\partial t}\cdot = \dot{(\cdot)}$	$\frac{\partial}{\partial t}\cdot = \dot{(\cdot)}$

Table 5.1 – Summary of the notations employed throughout this section.

5.3 Kirchhoff theory of rods

The theory for the finite displacement of thin rods has been developed by Kirchhoff, Clebsch and Love.

force and moment strains (Reissnner) : ↗ S'inspirer de l'intro de Reissner 1973

In this section we follow [Dil92] to introduce *Kirchhoff's theory of rods*, where Dill "examine the classical theory of finite displacements of thin rods as developped by Kirchhoff and Clebesch, and presented by Love". "The classical elastic rod theory of Kirchhoff (1859), called the kinetic analogue, is is a special case of our rod theory [...]" [Ant05, p. 238]

Dans un même genre, le papier de Reissner (1973) vaut le détour [Rei73]

We assume that material and section properties are slowly varying along the centerline. Note that symbols referring to this configuration will carry an overbar.

référence importante pour la rod [MLG13] , [Vil97, p. 109]. modeling of DNA molecules, pipes or hosing, plant, hair, surgery,

[11] [12] [13] A thorough order-of-magnitude analysis is exposed in [Dil92, CDL+93] [14] [15]

Pour la rod extensible : [CH02]

ces équations sont valables à l'ordre 2 en α [CDL+93] où :

Kirchhoff's theory is a first order theory regarding the parameter α, valid when α is small. This means that terms of order $O(\alpha^2)$ will be considered negligible :

$$\alpha = \sup_{s\in[0,L]} \{h/L, h\|\boldsymbol{\omega}\|, h\|\bar{\boldsymbol{\omega}}\|, \epsilon\} \tag{5.12}$$

The model is valid for uniform torsion. No restrained warping. For more and warping, see : The correction for shear in Kirchhoff's theory, introduce by Timoshenko in [Tim21] The

[11] "The principal normal, binormal, and torsion of the axis, viewed as an element of a space curve, have no special significance in the theory of rods. Use of those special directions as base vectors does not simplify the theory and can mislead the reader into attributing significance to them when none exists. In particular, the curvature of the rod should not be confused with the curvature of the space curve which the axis forms." [Dil92, p. 5]

[12] "Kirchhoff's theory can only apply to that class of problems for three dimensional bodies such that the loads on the sides are relatively small and slowly varying. The dominate mode of deformation must be a global bending and twisting with small axial extension. If there are substantial local variations in curvatures or substantial transverse shears, his theory of bending of rods will not provide a satisfactory first approximation." [Dil92, p. 18]

[13] "There are no constitutive relations for F_1 or F_2. They are determined by the balance of momentum as in the elementary linear theory of bending of rods." [Dil92, p. 15]

[14] "We discuss here the dynamical equations of a theory of elastic rods that is due to Kirchhoff and Clebsch. This properly invariant theory is applicable to motions in which the strains relative to an undistorted configuration remain small, although rotations may be large. It is constructed to be a first-order theory, i.e., a theory that is complete to within an error of order two in an appropriate dimensionless measure of thickness, curvature, twist, and extension." [CDL+93, p. 1]

[15] "In a first-order theory of thin rods, one can treat the rod as inextensible [...]" [CDL+93, p. 1]

Timoshenko theory of beams : [Tim45a, Tim45b, Tim45c] Include non uniform torsion

> The problem becomes more complicated if cross sections are not free to warp or if the torque varies along the length of the bar. Warping in such cases varies along the bar and tor- sion is accompanied by tension or compression of longitudinal fibers. The rate of change of the angle of twist along the axis of the bar also varies, and we call this the case of non-uniform torsion. [Tim45b]

Linear theory for non uniform torsion [Vla61] Formula for shear center [Elt84] A geometrically exact Kirchhoff beam model including torsion warping : [MG16]

Pioneer works on non lieanr dynamics of rods [Wei02] More recent works : [MG16]

For an historical review : [Ben91a] Short review of the history of 1D beam models :[Ant05, p. 243]

See [Rei73] for an extension of Kirchhoff's theory, as mentioned also in [Rei81]

going further with non uniform torsion [Alv14]

> In the traditional theory of non-uniform torsion the axial displacement field is expressed as the product of the unit twist angle and the warping function. The first one, variable along the beam axis, is obtained by a global congruence condition; the second one, instead, defined over the cross-section, is determined by solving a Neumann problem associated to the Laplace equation, as well as for the uniform torsion problem. So, as in the classical theory the warping function doesn't punctually satisfy the first indefinite equilibrium equation, the principal aim of this work is to develop a new theory for non-uniform torsion of beams with axial symmetric cross-section, fully restrained on both ends and loaded by a constant torque, that permits to punctually satisfy the previous equation, by means of a trigonometric expansion of the axial displacement and unit twist angle functions. Furthermore, as the classical theory is generally applied with good results to the global and local analysis of ship structures, two beams having the first one an open profile, the second one a closed section, have been analyzed, in order to compare the two theories. [CMPP09]

Hypothesis

- the rod is slender
- cross-section deformations remain small, although rotations may be large
- cross-section shear-center and centroid are at the same location
- material and cross-section properties vary slowly along the rod

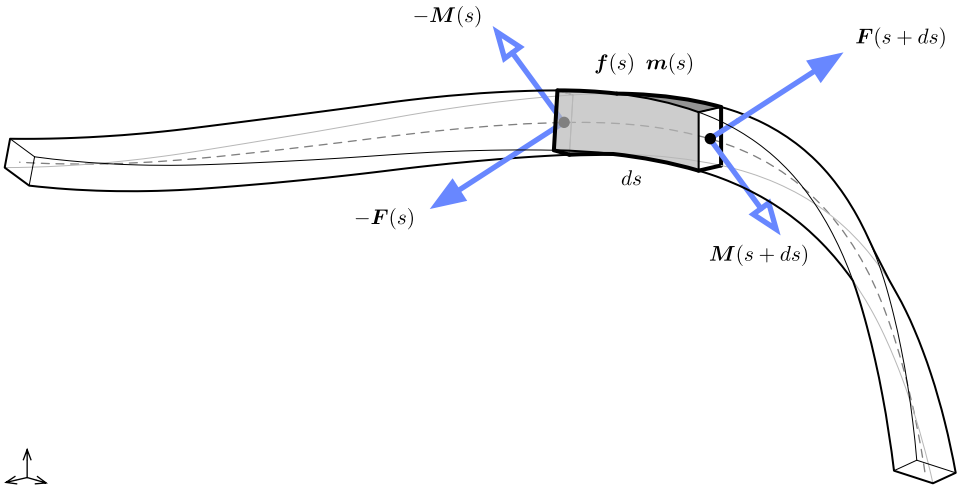

Figure 5.3 – Internal forces ($\boldsymbol{F}$) and moments ($\boldsymbol{M}$) acting on an infinitesimal beam slice of length ds. The beam is also subject to distributed external forces ($\boldsymbol{f}$) and moments ($\boldsymbol{m}$). By convention, internal forces and moments are forces and moments applied by the right part to the left part of the beam.

5.3.1 Description of the motion

To describe the motion of a Kirchhoff rod, we use the framework presented in §5.2.1 for Cosserat rods.[16] However, we restrict its scope by requiring that transverse shear strains are negligible quantities, which is one of the fundamental assumptions made by Kirchhoff in his theory :

$$\eta_1 \simeq 0 \tag{5.13a}$$
$$\eta_2 \simeq 0 \tag{5.13b}$$

As a consequence, the material frame remains adapted to the centerline. The rod is not supposed to be strictly inextensible. However, as strains are assumed to be small, the axial strain is supposed to be small itself ($\epsilon \ll 1$), which translates to :

$$\eta_3(s,t) = 1 + \epsilon(s,t) \tag{5.14a}$$
$$\boldsymbol{d}_3(s,t) = \boldsymbol{t}(s,t) \tag{5.14b}$$
$$\boldsymbol{x}'(s,t) = (1+\epsilon)\boldsymbol{t}(s,t) \tag{5.14c}$$

[16] We use the notation employed by Antman in his *special Cosserat theory of rods* : "The motion of a special Cosserat rod is defined by three vector-valued functions : $[s_1, s_2]\times\mathbb{R} \ni (s,t) \mapsto \boldsymbol{r}(s,t),\ \boldsymbol{d}_1(s,t),\ \boldsymbol{d}_2(s,t) \in \mathbb{E}^3$" [Ant05, p. 270]. However, somme specific assumptions will be made over the directors in the context of Kirchhoff's theory.

Stress-free configuration

We now consider a *stress-free* configuration of the rod as the *reference* configuration.[17] The rod is described by its centerline $\overline{\gamma}$ and its material frame $\{\overline{\boldsymbol{d}}_1, \overline{\boldsymbol{d}}_2, \overline{\boldsymbol{d}}_3\}$. Again, a planar cross-section is defined as the set of material points lying in the plane perpendicular to $\overline{\gamma}$ and passing through $\overline{\boldsymbol{x}}(s)$. The material directors $\overline{\boldsymbol{d}}_1$ and $\overline{\boldsymbol{d}}_2$ are now chosen to be aligned with the principal axes of inertia of the cross-section.[18] Thus, $\overline{\boldsymbol{d}}_3 = \overline{\boldsymbol{d}}_1 \times \overline{\boldsymbol{d}}_2$ is normal to the plane of the cross-section and adapted to the centerline ($\overline{\boldsymbol{d}}_3 = \overline{\boldsymbol{t}}$). Moreover, the centerline is chosen to be the curve passing through the cross-section centroids and is required to be at least a regular space curve, which means that its tangent is continuously defined.

For a sufficiently slender rod, the position of material point $\overline{\boldsymbol{p}}$ that belongs to cross-section $\mathcal{S}(s)$ is expressed through its material coordinates (X_1, X_2, s) as (see figures 5.1, 5.2a and 5.2b) : [19]

$$\overline{\boldsymbol{p}}(X_1, X_2, s) = \overline{\boldsymbol{x}}(s) + \overline{\boldsymbol{r}}(X_1, X_2, s) \tag{5.15a}$$

$$\overline{\boldsymbol{r}}(X_1, X_2, s) = X_1 \overline{\boldsymbol{d}}_1(s) + X_2 \overline{\boldsymbol{d}}_2(s) \tag{5.15b}$$

Consequently, for each s in the reference configuration, (X_1, X_2) is a cartesian coordinate system for the plane $\mathcal{S}(s)$. In this system the local coordinates of the cross-section centroid are $(0, 0)$.

Finally, the cross-section is assumed to be bounded and the planar boundary curve is defined by the implicit equation : $f_s(X_1, X_2) = 0$. It is also required that the shear center and the centroid of the cross-section are at the same location, otherwise one would require a more complex kinematic description of the rod.[20]

Deformed configuration

We now examine the motion of the rod and we call *deformed* configuration its actual configuration at time t. In this configuration the rod undergoes internal stresses under body loads, external loads and constrains.

The deformed configuration of the rod at time t is described by its centerline γ_t, its material frame $\{\boldsymbol{d}_1, \boldsymbol{d}_2, \boldsymbol{d}_3\}$ and a local displacement field $\boldsymbol{u}$. The centerline of the rod is deformed into the space curve γ_t with position vector $\boldsymbol{x}$:

$$\begin{array}{rccc} \gamma_t : & [0, L] & \longrightarrow & \mathbb{R}^3 \\ & s & \longmapsto & \boldsymbol{x}(s, t) \end{array} \tag{5.16}$$

A material point $\overline{\boldsymbol{p}}$ in the *reference* configuration is transported to position $\boldsymbol{p}$ in the *actual*

[17] See [AAP10, p. 20] for precisions when such a configuration may not exist.

[18] In case of an axisymmetric section, any pair of perpendicular unit vectors lying in the cross-section plane will be valid.

[19] The lateral dimension of the rod must be smaller than its radius of curvature. Otherwise, this description would lead to self intersecting cross-sections.

[20] Some details are given in the conclusion.

configuration so that (see figures 5.1, 5.2c and 5.2d) :

$$\boldsymbol{p}(X_1, X_2, s, t) = \boldsymbol{x}(s, t) + \boldsymbol{r}(X_1, X_2, s, t) \tag{5.17a}$$
$$\boldsymbol{r}(X_1, X_2, s, t) = X_1 \boldsymbol{d}_1(s, t) + X_2 \boldsymbol{d}_2(s, t) + \boldsymbol{u}(X_1, X_2, s, t) \tag{5.17b}$$
$$\boldsymbol{u}(X_1, X_2, s, t) = u_k(X_1, X_2, s, t) \boldsymbol{d}_k(s, t) \tag{5.17c}$$

Although the cross-section $\mathcal{S}(s)$ is a planar surface in the *reference* configuration, it deforms to a non-planar surface in the *actual* configuration since $\boldsymbol{u} \neq \boldsymbol{0}$.[21] The components $(u_1, u_2, u_3)^T$ of the local displacement field expressed in the material frame basis are required to be small in Kirchhoff's theory of rods.[22] In practice, as explained by [Dil92] this means that the considered motions must satisfy :

$$\frac{u_k}{h} = O(\alpha) \quad , \quad \frac{\partial u_k}{\partial X_1} = O(\alpha) \quad , \quad \frac{\partial u_k}{\partial X_2} = O(\alpha) \quad , \quad \frac{\partial u_k}{\partial s} = O(\alpha^2) \tag{5.18}$$

In this theory, the material frame in the reference configuration deforms in a rigid-body manner so that it remains orthonormal and aligned to the principal axes of the cross-section – within an error $O(\alpha^2)$.[23] Remark that this is different than assuming that cross-sections deform in a rigid-body manner, which is known as the *Euler-Bernoulli* hypothesis and is equivalent to the special case $\boldsymbol{u} = \boldsymbol{0}$.

5.3.2 Reparametrization

This subsection highlights the role played by the change in length of the rod during its motion. It was found that this aspect is often treated partially or with confusion in the literature, although it is of prime importance to understand correctly the influence of axial stretch in the computation of moment strains. Indeed, for an inextensible rod, the notions of geometric curvatures and (flexural) material curvatures are somehow the same notions. But this is not the case for extensible rods as explained in §5.3.3.

The rod is parametrized by s, the arc length parameter of the *reference* configuration, as the constitutive laws will be expressed relatively to this configuration. But recall once again that s is no more the arc length parameter of the *deformed* centerline as the rod may have suffer axial extension.[24] Kirchhoff's theory assumes that the material frame remains

[21] $\mathcal{S}(s)$ refers to the same set of material points in any configurations. Sometimes a distinction is made between $\bar{\mathcal{S}}(s)$ and $\mathcal{S}(s)$ to highlight that the planarity of cross-sections is lost during the motion.

[22] Note that this hypothesis is the one made by Kirchhoff and does not correspond to the well-known *Euler-Bernoulli* or *Navier-Bernoulli* assumption where the sections remain planar, undeformed and normal to the centerline during the rod deformation. In particular, torsion is responsible for the warping of cross-sections – that is cross-sections don't remain planar during the motion – and leads to a distinct value of the twist modulus. This is clearly stipulated in [Dil92, AAP10] but is often treated with confusion in the literature.

[23] "[...] upon deformation, the principal axes of $\mathcal{S}(s)$ do remain normal to each other and to the rod axis, at least to within the approximations of the present theory, i.e., to within an error $O(\alpha^2)$." [CDL+93, p. 344].

[24] In Kirchhoff's theory, rods are not supposed to be strictly inextensible but extension has to remain small. Thus, the internal axial force is given by a constitutive law and not considered as a geometric constrained. However, some authors have remarked that it might be convenient and reasonable to solve the equations of motion considering the geometric contraint $\epsilon = 0$. See [AAP10, p. 98] for a detailed discussion

adapted to the centerline during deformation, or equivalently that transverse shear strains are neglected.[25] The extension of the centerline is characterized by ϵ defined such that :

$$\bar{\boldsymbol{x}}' = \boldsymbol{d}_3 \tag{5.19a}$$

$$\boldsymbol{x}' = (1+\epsilon)\boldsymbol{d}_3 \tag{5.19b}$$

However, one can parametrized the deformed centerline by its own arc length parameter, denoted s_t. Let's call L_t the length of the deformed centerline and Ψ_t the $\mathcal{C}^1$ diffeomorphism that maps s onto s_t ($s_t = \Psi_t(s) \Leftrightarrow s = \Psi_t^{-1}(s_t)$). Thus, the centerline is equivalently described by :

$$\begin{array}{rccc} \gamma_t : & [0, L_t] & \longrightarrow & \mathbb{R}^3 \\ & s_t & \longmapsto & \boldsymbol{x}(s_t) \end{array} \tag{5.20}$$

Because s_t is the arc length parameter of γ_t the following relations hold :

$$\frac{\partial \boldsymbol{x}}{\partial s_t} = \boldsymbol{d}_3 \tag{5.21a}$$

$$\frac{\partial s_t}{\partial s} = \eta_3 = 1 + \epsilon \tag{5.21b}$$

Thus, one can deduced that the derivation with respect to s is proportional to the derivation with respect to s_t by a factor $1+\epsilon$. This factor has to be taken into account when computing the material curvatures, which are no more equivalent to their geometric counterparts in the deformed configuration. This is detailed in the next section.

5.3.3 Strains

This section, introduces the material force and moment strains of a Kirchhoff rod. It shows how they are related – yet distinct if $\epsilon \neq 0$ – to the geometric curvatures of the centerline.

Reference configuration

Since the material frame is orthonormal and adapted to the centerline, its evolution along the undeformed centerline is described thanks to the *reference material curvature vector* $\bar{\boldsymbol{\kappa}}$ defined as :

$$\bar{\boldsymbol{d}}_i' = \bar{\boldsymbol{\kappa}} \times \bar{\boldsymbol{d}}_i \tag{5.22}$$

of the subject.

[25] This is also known as the "unsherable" assumption. Indeed, if $\frac{\partial \boldsymbol{x}}{\partial s} = \eta_k \boldsymbol{d}_k = (1+\epsilon)\boldsymbol{d}_3 \Leftrightarrow \eta_1 = \eta_2 = 0$.

In the reference configuration, because s is the centerline's arc length parameter, the strain vector components expressed in the material frame basis take the form : [26]

$$\bar{\varkappa}_1 = \bar{k}_1 = \bar{\boldsymbol{\kappa b}} \cdot \bar{\boldsymbol{d}}_1 \tag{5.23a}$$
$$\bar{\varkappa}_2 = \bar{k}_2 = \bar{\boldsymbol{\kappa b}} \cdot \bar{\boldsymbol{d}}_2 \tag{5.23b}$$
$$\bar{\varkappa}_3 = \bar{\tau} \ = \bar{\boldsymbol{d}}_1{}' \cdot \bar{\boldsymbol{d}}_2 \tag{5.23c}$$

where $\bar{\boldsymbol{\kappa b}}$ is the curvature binormal vector of $\bar{\gamma}$:

$$\bar{\boldsymbol{\kappa b}} = \bar{\boldsymbol{t}} \times \frac{\partial \bar{\boldsymbol{t}}}{\partial s} = \bar{\boldsymbol{t}} \times \bar{\boldsymbol{t}}' \tag{5.24}$$

$\bar{\varkappa}_1$ and $\bar{\varkappa}_2$ are called the *material* reference curvatures. $\bar{\varkappa}_3$ is called the *material* reference twist. In this configuration, $\bar{\varkappa}_1$ and $\bar{\varkappa}_2$ are simply computed as the projection of the curvature binormal vector along $\bar{\boldsymbol{d}}_1$ and $\bar{\boldsymbol{d}}_2$.

Note the important distinction between the material reference twist ($\bar{\tau}$) and the torsion of Frenet (τ_f) of the centerline, as defined in **??**.

Deformed configuration

Since the material frame is orthonormal, it's evolution along the *deformed* centerline is described thanks to the *actual strains vector* $\boldsymbol{\varkappa}$ defined as :

$$\frac{\partial \boldsymbol{d}_k}{\partial s} = \boldsymbol{\varkappa} \times \boldsymbol{d}_k \tag{5.25}$$

Note that the strains vector is defined relatively to the arc length s of the *reference* configuration and not the arc length s_t of the *actual* configuration. Thus the strains vector components expressed in the material frame basis are given by :

$$\varkappa_1 = \boldsymbol{d}_3' \cdot \boldsymbol{d}_2 = (1+\epsilon) k_1 = (1+\epsilon) \boldsymbol{\kappa b} \cdot \boldsymbol{d}_1 \tag{5.26a}$$
$$\varkappa_2 = \boldsymbol{d}_1' \cdot \boldsymbol{d}_3 = (1+\epsilon) k_2 = (1+\epsilon) \boldsymbol{\kappa b} \cdot \boldsymbol{d}_2 \tag{5.26b}$$
$$\varkappa_3 = \boldsymbol{d}_1' \cdot \boldsymbol{d}_2 = (1+\epsilon) \tau = (1+\epsilon) \frac{\partial \boldsymbol{d}_1}{\partial s_t} \cdot \boldsymbol{d}_2 \tag{5.26c}$$

where $\boldsymbol{\kappa b}$ is the curvature binormal vector of γ_t given by :

$$\boldsymbol{\kappa b} = \boldsymbol{t} \times \frac{\partial \boldsymbol{t}}{\partial s_t} = (1+\epsilon) \boldsymbol{t} \times \boldsymbol{t}' \tag{5.27}$$

$\varkappa_1$ and $\varkappa_2$ are called the *material* curvatures. $\varkappa_3$ is called the *material* twist. Note this time the dependence of the material strains ($\varkappa_1$, $\varkappa_2$, $\varkappa_3$) regarding the extension of the rod. These are the strains employed in the classical constitutive laws that lead to the determination of the internal axial force ($N = ES\epsilon$), internal bending moments ($M_1 = EI_1(\varkappa_1 - \bar{\varkappa}_1)$, $M_2 = EI_2(\varkappa_2 - \bar{\varkappa}_2)$) and internal twisting moment ($Q = GJ((\varkappa_3 - \bar{\varkappa}_3))$).

[26] Recall the following result for an adapted frame : eq. (3.34).

In the case of an inextensible rod ($\epsilon = 0$) there is no need to make the distinction between s_t and s. The same parameter is the arc length parameter for all configurations at all time.

5.3.4 Balance of momentum

Let $\boldsymbol{\mathcal{P}}$ be the first *Piola-Kirchhoff* stress tensor. $\boldsymbol{\mathcal{P}}$ expresses how contact forces are acting in a *deformed* body, referring to its (known) *reference* configuration. Let $\boldsymbol{dS} = \boldsymbol{n}dS$ be an elementary oriented surface of the rod in the *reference* configuration of centroid $\boldsymbol{p}(X_1, X_2, s, t) \in \mathcal{S}(s)$.[27] The contact forces exerted on $\boldsymbol{dS}$ are given by :

$$\boldsymbol{dF}(X_1, X_2, s, t) = \boldsymbol{\sigma_n}(X_1, X_2, s, t)\, dS \tag{5.28a}$$

$$\boldsymbol{\sigma_n}(X_1, X_2, s, t) = \boldsymbol{\mathcal{P}}(X_1, X_2, s, t) \cdot \boldsymbol{n} \tag{5.28b}$$

We have introduce the *Piola stress vector* ($\boldsymbol{\sigma_n}$) which expresses the contact forces exerted on the body per unit area of the *reference* configuration.[28]

The generic laws for the balance of linear and angular momentums are obtained by summation over the reference configuration, where $\boldsymbol{b}$ are the body forces per unit volume of the *reference* configuration :

$$\iiint_{\mathcal{V}} \rho \ddot{\boldsymbol{p}}\, dV = \iint_{\partial\mathcal{V}} \boldsymbol{\sigma_n}\, dS + \iiint_{\mathcal{V}} \rho \boldsymbol{b}\, dV \tag{5.29a}$$

$$\iiint_{\mathcal{V}} \rho(\boldsymbol{p} \times \ddot{\boldsymbol{p}})\, dV = \iint_{\partial\mathcal{V}} \boldsymbol{p} \times \boldsymbol{\sigma_n}\, dS + \iiint_{\mathcal{V}} \rho(\boldsymbol{p} \times \boldsymbol{b})\, dV \tag{5.29b}$$

Here, and subsequently, $\mathcal{V}$ denotes the volume of a slice of the rod in the *reference* configuration, encompassed between two cross-sections ($\mathcal{S}_1 = \mathcal{S}(s_1)$, $\mathcal{S}_2 = \mathcal{S}(s_2)$, $s_1 < s_2$). We also denote $\mathcal{L}_{12}$ the lateral surface of the rod in the *reference* configuration so that the exterior surface of the volume is : $\partial\mathcal{V} = \mathcal{S}_1 \bigcup \mathcal{L}_{12} \bigcup \mathcal{S}_2$.

The cross-section $\mathcal{S}(s)$ splits the rod in two parts. Hereafter, the upstream part of the rod over $[s, L]$ we will called the "right part". Reciprocally, the downstream part of the rod over $[0, s]$ will be called the "left part".

Internal forces and moments

At the cross-section $\mathcal{S}(s)$, the contact forces applied by the right part onto the left part of the rod yield the following resultant force $\boldsymbol{F}$ and resultant moment $\boldsymbol{M}$ about the point $\boldsymbol{x}(s, t)$:

$$\boldsymbol{F}(s, t) = \iint_{\mathcal{S}(s)} \boldsymbol{\sigma_n}(X_1, X_2, s, t)\, dX_1 dX_2 \tag{5.30a}$$

$$\boldsymbol{M}(s, t) = \iint_{\mathcal{S}(s)} \boldsymbol{r}(X_1, X_2, s, t) \times \boldsymbol{\sigma_n}(X_1, X_2, s, t)\, dX_1 dX_2 \tag{5.30b}$$

[27] dS is the area and $\boldsymbol{n}$ is the unit normal of the elementary oriented surface $\boldsymbol{dS}$.
[28] For a detailed introduction to the Piola-Kirchhoff stress tensor, refer to [AAP10, p. 52].

$\boldsymbol{F}$ and $\boldsymbol{M}$ are commonly known as the *internal forces* and the *internal moments* of the rod.

External forces and moments

We assume that the resultant distributed force and moment of the contact forces on $\mathcal{L}_{12}$ and the body forces on $\mathcal{V}$ reduced to the following forms :

$$\iint_{\mathcal{L}} \boldsymbol{\sigma_n}\, dS + \iiint_{\mathcal{V}} \rho \boldsymbol{b}\, dV = \int_s \overline{\boldsymbol{f}} + (1+\epsilon)\boldsymbol{f}_t\, ds \tag{5.31a}$$

$$\iint_{\mathcal{L}} \boldsymbol{p} \times \boldsymbol{\sigma_n}\, dS + \iiint_{\mathcal{V}} \rho(\boldsymbol{p} \times \boldsymbol{b})\, dV = \int_s \overline{\boldsymbol{m}} + (1+\epsilon)\boldsymbol{m}_t + \boldsymbol{x} \times \left(\overline{\boldsymbol{f}} + (1+\epsilon)\boldsymbol{f}_t\right) ds \tag{5.31b}$$

where $\overline{\boldsymbol{f}}$ (resp. $\boldsymbol{f_t}$) is the distributed resultant force per unit length of the reference (resp. deformed) configuration ; and $\overline{\boldsymbol{m}}$ (resp. $\boldsymbol{m}_t$) is the distributed resultant moment per unit length of the reference (resp. deformed) configuration. For instance, these distributed forces and moments include external and body loads such as weight, snow, wind, ... [29]

Note that Kirchhoff's theory require that the stress components on the sides of the rod are small [Dil92, p. 11] – that is $\boldsymbol{\sigma_n} \cdot \boldsymbol{n} = O(\alpha^2)$ over $\mathcal{L}$. Thus, the first two terms in the above expression will be neglected :

$$\iint_{\mathcal{L}} \boldsymbol{\sigma_n}\, dS \simeq 0 \tag{5.32a}$$

$$\iint_{\mathcal{L}} \boldsymbol{p} \times \boldsymbol{\sigma_n}\, dS \simeq 0 \tag{5.32b}$$

Although the continuous model does not account formally for punctual loads,[30] they will be introduced seamlessly in the discrete model as the dynamical equations for the motion of the rod will translate into rigid body equations for the discrete segments composing the rod.

[29] At this stage, although this is uncommon in the literature, it has been found convenient to mark the distinction between loads referring to the reference configuration and loads referring to the actual configuration. Indeed, various distributed loads depend on the actual length of an element such as pressure and wind loads. On the other hand, some loads are independent of the extension of the rod, such as its weight.

[30] This is possible but would require more math. However, local effects of such loads would not be properly modeled in the theory of Kirchhoff (Saint-Venant's Principle).

Inertial forces

The inertial forces for a volume of the rod encompassed between cross-sections $\mathcal{S}_1$ and $\mathcal{S}_2$ are obtained by summation as :

$$\iiint_{\mathcal{V}} \rho \ddot{\boldsymbol{p}}\, dV = \iiint_{\mathcal{V}_t} \rho_t \ddot{\boldsymbol{p}}\, dV_t \tag{5.33a}$$

$$\iiint_{\mathcal{V}} \rho(\boldsymbol{p} \times \ddot{\boldsymbol{p}})\, dV = \iiint_{\mathcal{V}_t} \rho_t(\boldsymbol{p} \times \ddot{\boldsymbol{p}})\, dV_t \tag{5.33b}$$

Here, ρ (resp. ρ_t) is the mass density of the rod in the reference (resp. deformed) configuration. Expressions are given in both coordinate systems.[31]

In the context of Kirchhoff's approximation, the local deformations of the cross-sections can be neglected in the computation of the inertial forces [Dil92, p. 16]. This yields :

$$\boldsymbol{p} \simeq \boldsymbol{x} + X_1\boldsymbol{d}_1 + X_2\boldsymbol{d}_2 \tag{5.34a}$$

$$\dot{\boldsymbol{p}} = \dot{\boldsymbol{x}} + \boldsymbol{\omega} \times (X_1\boldsymbol{d}_1 + X_2\boldsymbol{d}_2) \tag{5.34b}$$

$$\ddot{\boldsymbol{p}} = \ddot{\boldsymbol{x}} + \dot{\boldsymbol{\omega}} \times (X_1\boldsymbol{d}_1 + X_2\boldsymbol{d}_2) + \boldsymbol{\omega} \times (\boldsymbol{\omega} \times (X_1\boldsymbol{d}_1 + X_2\boldsymbol{d}_2)) \tag{5.34c}$$

Since X_1 and X_2 are the coordinates with respect to the centroid ($\boldsymbol{x}$) and the principal axes of the cross-section ($\boldsymbol{d}_1$, $\boldsymbol{d}_2$), the cross-section area (S) and principal moments of inertia (I_1, I_2) are given by : [32,33]

$$0 = \iint_{\mathcal{S}(s)} (X_1X_2)\ dX_1dX_2 \tag{5.35a}$$

$$S = \iint_{\mathcal{S}(s)} dX_1dX_2 \tag{5.35b}$$

$$I_1 = \iint_{\mathcal{S}(s)} {X_2}^2\, dX_1dX_2 \tag{5.35c}$$

$$I_2 = \iint_{\mathcal{S}(s)} {X_1}^2\, dX_1dX_2 \tag{5.35d}$$

More over, for a given cross-section the definition of the centroid yields :

$$\boldsymbol{0} = \iint_{\mathcal{S}(s)} (X_1\boldsymbol{d}_1 + X_2\boldsymbol{d}_2)\ dX_1dX_2 \tag{5.36a}$$

$$0 = \iint_{\mathcal{S}(s)} X_1\ dX_1dX_2 \tag{5.36b}$$

$$0 = \iint_{\mathcal{S}(s)} X_2\ dX_1dX_2 \tag{5.36c}$$

[31] In [Dil92] the change in volume and the conservation of mass is expressed through the determinants of the metric tensors of the reference and deformed configurations. Recall that this determinant is the square of the volume of the elementary cell defined by $\frac{\partial \boldsymbol{p}}{\partial s}$, $\frac{\partial \boldsymbol{p}}{\partial X_1}$, $\frac{\partial \boldsymbol{p}}{\partial X_2}$ in the reference configuration, which is convected to the elementary cell defined by $\frac{\partial \boldsymbol{p}_t}{\partial s}$, $\frac{\partial \boldsymbol{p}_t}{\partial X_1}$, $\frac{\partial \boldsymbol{p}_t}{\partial X_2}$ in the reference configuration.

[32] This is exact in the reference configuration but only approximately true in the deformed configuration as the theory consider only small deformations of cross-sections.

[33] eq. (5.36a) is nothing but the definition of the centroid position. eq. (5.35a) holds because the tensor of inertia of the cross-section is diagonal in the basis $\{\boldsymbol{d}_1, \boldsymbol{d}_2, \boldsymbol{d}_3\}$ and thus $I_{12} = I_{21} = 0$.

For a thin slice of the rod ($\delta\mathcal{V}$) between cross-sections $\mathcal{S}(s)$ and $\mathcal{S}(s+ds)$, eq. (5.33a) and (5.33b) yield respectively : [34]

$$\iiint_{\delta\mathcal{V}} \rho\ddot{\boldsymbol{p}}\, dV = (\rho S\ddot{\boldsymbol{x}})ds \tag{5.37a}$$

$$\iiint_{\delta\mathcal{V}} \rho(\boldsymbol{p}\times\ddot{\boldsymbol{p}})\, dV = \left(\rho S\ddot{\boldsymbol{x}} + \rho\iint_{\mathcal{S}(s)} \boldsymbol{r}\times\ddot{\boldsymbol{r}}\, dX_1dX_2\right) ds \tag{5.37b}$$

Finally, remark that :

$$\boldsymbol{r}\times\ddot{\boldsymbol{r}} = (X_1)^2\boldsymbol{d}_1\times\ddot{\boldsymbol{d}}_1 + (X_2)^2\boldsymbol{d}_2\times\ddot{\boldsymbol{d}}_2 + X_1X_2(\boldsymbol{d}_1\times\ddot{\boldsymbol{d}}_2 + \boldsymbol{d}_2\times\ddot{\boldsymbol{d}}_1) \tag{5.38}$$

Thus, reminding eq. (5.35) and (5.36), one can conclude that the inertial forces reduce to :

$$\iiint_{\delta\mathcal{V}} \rho\ddot{\boldsymbol{x}}\, dV = (\rho S\ddot{\boldsymbol{x}})ds \tag{5.39a}$$

$$\iiint_{\delta\mathcal{V}} \rho(\boldsymbol{p}\times\ddot{\boldsymbol{p}})\, dV = (\rho S\ddot{\boldsymbol{x}} + \rho I_1\boldsymbol{d}_1\times\ddot{\boldsymbol{d}}_1 + \rho I_2\boldsymbol{d}_2\times\ddot{\boldsymbol{d}}_2)ds \tag{5.39b}$$

Balance of linear momentum

For a thin slice of the rod ($\delta\mathcal{V}$) between cross-sections $\mathcal{S}(s)$ and $\mathcal{S}(s+ds)$, using eq. (5.30a) and (5.31a), the balance of linear momentum referring to the *reference* configuration expressed in eq. (5.29a) yields :

$$\begin{aligned}
\iiint_{\delta\mathcal{V}} \rho\ddot{\boldsymbol{p}}\, dV &= \iint_{\partial\mathcal{V}} \boldsymbol{\sigma_n}\, dS + \iiint_{\delta\mathcal{V}} \rho\boldsymbol{b}\, dV \\
&= \iint_{\mathcal{S}(s)} \boldsymbol{\sigma_n}\, dS + \iint_{\mathcal{S}(s+ds)} \boldsymbol{\sigma_n}\, dS + \left(\iint_{\delta\mathcal{L}} \boldsymbol{\sigma_n}\, dS + \iiint_{\delta\mathcal{V}} \rho\boldsymbol{b}\, dV\right) \\
&= -\boldsymbol{F}(s) + \boldsymbol{F}(s+ds) + \Big(\overline{\boldsymbol{f}}(s) + (1+\epsilon)\boldsymbol{f}_t(s)\Big)ds \\
&= \left(\frac{\partial\boldsymbol{F}}{\partial s} + \overline{\boldsymbol{f}} + (1+\epsilon)\boldsymbol{f}_t\right)(s)ds
\end{aligned} \tag{5.40}$$

Thus, using eq. (5.39a), the equation for the balance of linear momentum reduce to either equations :

$$\frac{\partial\boldsymbol{F}}{\partial s} + \overline{\boldsymbol{f}} + (1+\epsilon)\boldsymbol{f}_t = \rho S\ddot{\boldsymbol{x}} \tag{5.41a}$$

$$(1+\epsilon)\frac{\partial\boldsymbol{F}}{\partial s_t} + \overline{\boldsymbol{f}} + (1+\epsilon)\boldsymbol{f}_t = \rho S\ddot{\boldsymbol{x}} \tag{5.41b}$$

[34] Indeed, since $\iint_{\mathcal{S}(s)} \boldsymbol{r}\, dX_1dX_2 = \boldsymbol{0}$ from eq. (5.36a) we have $\iint_{\mathcal{S}(s)} \ddot{\boldsymbol{r}}\, dX_1dX_2 = \iint_{\mathcal{S}(s)} \dot{\boldsymbol{\omega}}\times\boldsymbol{r} + \boldsymbol{\omega}\times(\boldsymbol{\omega}\times\boldsymbol{r})\, dX_1dX_2 = \boldsymbol{0}$ and $\iint_{\mathcal{S}(s)} \boldsymbol{r}\times\ddot{\boldsymbol{x}}\, dX_1dX_2 = \boldsymbol{0}$ as $\boldsymbol{w}$ and $\boldsymbol{x}$ are independent of X_1 and X_2.

Balance of angular momentum

Similarly, for a thin slice of the rod ($\delta\mathcal{V}$) between cross-sections $\mathcal{S}(s)$ and $\mathcal{S}(s+ds)$, using eq. (5.30a) and (5.30b) yields :

$$\begin{aligned}\iint_{\mathcal{S}(s)\bigcup\mathcal{S}(s+ds)} \boldsymbol{p}\times\boldsymbol{\sigma_n}\,dS &= \iint_{\mathcal{S}(s)\bigcup\mathcal{S}(s+ds)} (\boldsymbol{x}+\boldsymbol{r})\times\boldsymbol{\sigma_n}\,dS \\ &= -(\boldsymbol{x}\times\boldsymbol{F})(s)+(\boldsymbol{x}\times\boldsymbol{F})(s+ds)-\boldsymbol{M}(s)+\boldsymbol{M}(s+ds) \\ &= \frac{\partial}{\partial s}\Big(\boldsymbol{M}+\boldsymbol{x}\times\boldsymbol{F}\Big)(s)ds\end{aligned} \tag{5.42}$$

Using eq. (5.31b), the balance of linear momentum referring to the *reference* configuration expressed in eq. (5.29b) yields :

$$\begin{aligned}\iiint_{\delta\mathcal{V}} \rho(\boldsymbol{p}\times\ddot{\boldsymbol{p}})\,dV &= \iint_{\partial\delta\mathcal{V}} \boldsymbol{p}\times\boldsymbol{\sigma_n}\,dS+\iiint_{\delta\mathcal{V}}\rho(\boldsymbol{p}\times\boldsymbol{b})\,dV \\ &= \frac{\partial}{\partial s}\Big(\boldsymbol{M}+\boldsymbol{x}\times\boldsymbol{F}\Big)(s)ds+\bar{\boldsymbol{m}}+(1+\epsilon)\boldsymbol{m}_t+\boldsymbol{x}\times\Big(\bar{\boldsymbol{f}}+(1+\epsilon)\boldsymbol{f}_t\Big)\,ds\end{aligned} \tag{5.43}$$

Finally, combining eq. (5.43) with eq. (5.39b) and (5.41a), the equation for the balance of angular momentum reduce to either equations : [35]

$$\frac{\partial\boldsymbol{M}}{\partial s}+\frac{\partial\boldsymbol{x}}{\partial s}\times\boldsymbol{F}+\bar{\boldsymbol{m}}+(1+\epsilon)\boldsymbol{m}_t=\rho I_1\boldsymbol{d}_1\times\ddot{\boldsymbol{d}}_1+\rho I_2\boldsymbol{d}_2\times\ddot{\boldsymbol{d}}_2 \tag{5.44a}$$

$$(1+\epsilon)\frac{\partial\boldsymbol{M}}{\partial s_t}+(1+\epsilon)\frac{\partial\boldsymbol{x}}{\partial s_t}\times\boldsymbol{F}+\bar{\boldsymbol{m}}+(1+\epsilon)\boldsymbol{m}_t=\rho I_1\boldsymbol{d}_1\times\ddot{\boldsymbol{d}}_1+\rho I_2\boldsymbol{d}_2\times\ddot{\boldsymbol{d}}_2 \tag{5.44b}$$

5.3.5 Equations of motion

With some scaling arguments [Dil92] shows that terms in ω_1 and ω_2 should be negligible in the inertial forces of the rod given in eq. (5.39b), which yields to : [36]

$$\rho I_1(\dot{\omega}_1+\omega_2\omega_3)\simeq 0 \tag{5.45a}$$

$$\rho I_2(\dot{\omega}_2-\omega_1\omega_3)\simeq 0 \tag{5.45b}$$

$$\rho(I_1+I_2)\dot{\omega}_3+\rho(I_1-I_1)\omega_1\omega_2\simeq\rho(I_1+I_2)\dot{\omega}_3 \tag{5.45c}$$

[35] Note the simplification of the term $\rho S\ddot{\boldsymbol{x}}$. Alternatively, the balance equations could be written for the slice as for a rigid body. In the barycentric frame of the slice : $\frac{d}{dt}(dI_G)=\boldsymbol{M}(s+ds)-\boldsymbol{M}(s)+\boldsymbol{m}(s)ds+(\frac{1}{2}ds\boldsymbol{x}')\times\boldsymbol{F}(s+ds)+(-\frac{1}{2}ds\boldsymbol{x}')\times-\boldsymbol{F}(s)=\big(\frac{\partial\boldsymbol{M}}{\partial s}(s)+\boldsymbol{m}(s)+\boldsymbol{x}'\times\boldsymbol{F}(s)\big)\,ds$ with $dI_G\simeq\rho ds(I_1\boldsymbol{d}_1+I_2\boldsymbol{d}_2+(I_1+I_2)\boldsymbol{d}_3)$.

[36] "It follows that $\varkappa_1$ and $\varkappa_2$ can be neglected in the kinetic energy [...]. However, $\varkappa_3$, which provides the angular momentum about the axis of the rod, must be retained, This assumption of Kirchhoff is consistent with the technical theory of beams where rotary inertia is known to provide corrections to the natural frequencies of vibration of $O(\alpha^2)$ if the length measure is the half-wave length" [Dil92, p. 17]. This assumption is made in numerous publications but often with ambiguous or no justifications, as of instance : "neglecting inertial momentum due to the vanishing cross-section lead to the following dynamic equations for a Kirchhoff rod" [CBd13].

For our application – a beam model for quasi-static analysis of gridshell structures – this approximation is clearly sufficient as what matters is the quasi-static response of the structural system and there is no need for a too accurate modeling of the transient phase. More over, the quasi-static response will be determined through a fictitious dynamic process appropriately damped to speed up the convergence to the steady state, and so there is no reason that the transient phase has any real physical meaning. This means that its is enough to keep only the twisting dynamic of the rod around its centerline.

Thus, the final dynamical equations for the motion of the rod to be retained are :

$$\frac{\partial \boldsymbol{F}}{\partial s} + \overline{\boldsymbol{f}} + (1+\epsilon)\boldsymbol{f}_t = \rho S \ddot{\boldsymbol{x}} \tag{5.46a}$$

$$\frac{\partial \boldsymbol{M}}{\partial s} + \frac{\partial \boldsymbol{x}}{\partial s} \times \boldsymbol{F} + \overline{\boldsymbol{m}} + (1+\epsilon)\boldsymbol{m}_t \simeq \rho(I_1 + I_2)\dot{\omega}_3 \boldsymbol{d}_3 \tag{5.46b}$$

5.3.6 Hookean elasticity

From now on we consider that the rod material is isotropic and linear elastic.[37] This is the framework of the so called *Hookean Elasticity*. This assumption allows the determination of the local displacement field ($\boldsymbol{u}$), the strain tensor ($\boldsymbol{\mathcal{E}}$), the stress tensor ($\boldsymbol{\mathcal{S}}$) and the constitutive equations that link the axial force ($\boldsymbol{F}_1$), the bending moments ($\boldsymbol{M}_1$, $\boldsymbol{M}_2$) and the twisting moment ($\boldsymbol{M}_3$) to the strains (ϵ, $\boldsymbol{\varkappa}$, $\overline{\boldsymbol{\varkappa}}$).

Such a material is characterized by a linear relation between the strain and stress tensors that takes the form : [38]

$$\boldsymbol{\mathcal{S}} = 2\mu\boldsymbol{\mathcal{E}} + \lambda Tr(\boldsymbol{\mathcal{E}})\boldsymbol{\mathcal{I}} \tag{5.47}$$

where λ and μ are known as the elastic coefficients of Lamé. This coefficients are related to the elastic (E) and shear (G) modulus and to the Poisson ratio (η) :

$$\mu = \frac{E}{2(1+\eta)} = G \tag{5.48a}$$

$$\lambda = \frac{2\mu\eta}{1-2\eta} \tag{5.48b}$$

A worthwhile presentation of the theory of elasticity in the specific context of rods can be found in [AAP10].

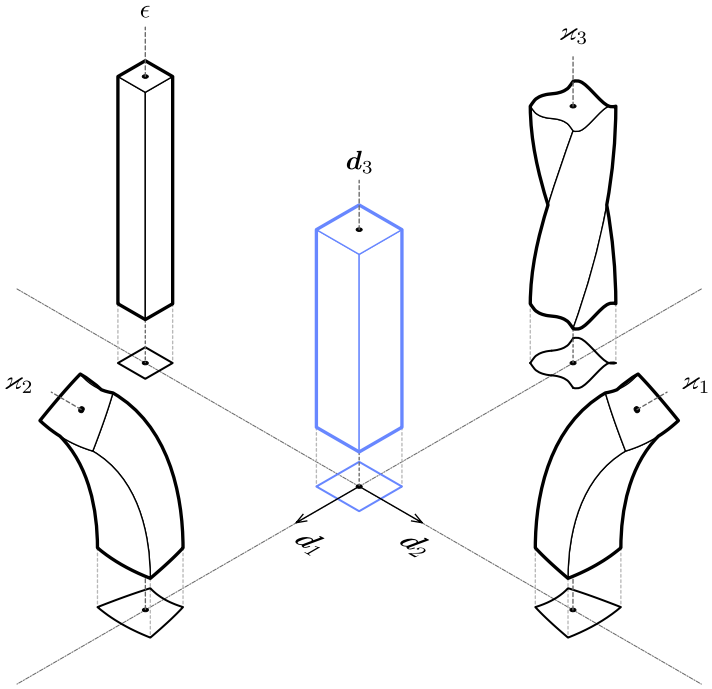

Figure 5.4 – Typical deformation modes of cross-sections in Kirchhoff's theory. Flexion around $\boldsymbol{d}_1$ (resp. $\boldsymbol{d}_2$) is measured through the material curvature $\varkappa_1$ (resp. $\varkappa_2$) ; torsion around $\boldsymbol{d}_3$ is measured through the material twist $\varkappa_3$; and ϵ measures the axial extension. Remark that cross-sections are subjected to both in-plane deformations ($\varkappa_1$, $\varkappa_2$, ϵ) and out-of-plane deformations ($\varkappa_3$).

5.3.7 Deformation of cross-sections

In this paragraph, we simply recall the canonical form of the local displacement field ($\boldsymbol{u}$) for the cross-section $\mathcal{S}(s)$ in the context of Kirchhoff's approximation : [39]

$$u_1 = -\nu\epsilon X_1 - \nu(\varkappa_1 - \bar{\varkappa}_1)X_1X_2 + \tfrac{1}{2}\nu(\varkappa_2 - \bar{\varkappa}_2)({X_1}^2 - {X_2}^2) \tag{5.49a}$$

$$u_2 = -\nu\epsilon X_2 + \nu(\varkappa_2 - \bar{\varkappa}_2)X_1X_2 + \tfrac{1}{2}\nu(\varkappa_1 - \bar{\varkappa}_1)({X_1}^2 - {X_2}^2) \tag{5.49b}$$

$$u_3 = (\varkappa_3 - \bar{\varkappa}_3)\varphi_s(X_1, X_2) \tag{5.49c}$$

[37] This is true at first order for small strains anyway.

[38] Using Einstein notation this expression yields : $\sigma_{ij} = \lambda\epsilon_{kk}\delta_{ij} + 2\mu\epsilon_{ij}$.

[39] Remark that the local displacement field results from the superposition of the three displacement fields obtained for pure and uniform extension, flexion and twist. For a detailed analysis of pure and uniform flexion and twist of rods; refer to [AAP10, ch. 3].

where φ_s is the warping function (in torsion) of $\mathcal{S}(s)$, determined by the differential equation and the boundary condition over the contour of the cross-section : [40]

$$0 = \frac{\partial^2 \varphi_s}{\partial {X_1}^2} + \frac{\partial^2 \varphi_s}{\partial {X_2}^2} \qquad \forall (X_1, X_2) \in \mathcal{S}(s) \tag{5.50a}$$

$$0 = \frac{\partial f_s}{\partial X_1}\left(\frac{\partial \varphi_s}{\partial X_1} - X_2\right) + \frac{\partial f_s}{\partial X_2}\left(\frac{\partial \varphi_s}{\partial X_2} + X_1\right) \forall (X_1, X_2) \in \mathcal{S}(s) \ / \ f_s(X_1, X_2) = 0 \tag{5.50b}$$

These equations have known analytical solutions for classical shapes such as circles, ellipses, squares or rectangles. For other shapes, when it is not easy to find analytical solutions, the membrane analogy introduced by Prandtl [Pra03] is employed.[41]

5.3.8 Strain tensor

In this paragraph, we simply recall the canonical form of the strain tensor ($\boldsymbol{\mathcal{E}}$) for the cross-section $\mathcal{S}(s)$ in the context of Kirchhoff's approximation :

$$\epsilon_{33} = \epsilon + (\varkappa_1 - \bar{\varkappa}_1)X_2 - (\varkappa_2 - \bar{\varkappa}_2)X_1 \tag{5.51a}$$

$$\epsilon_{11} = \epsilon_{22} = -\nu\epsilon_{33} \tag{5.51b}$$

$$\epsilon_{12} = 0 \tag{5.51c}$$

$$\epsilon_{31} = \tfrac{1}{2}(\varkappa_3 - \bar{\varkappa}_3)\left(\frac{\partial \varphi_s}{\partial X_1} - X_2\right) \tag{5.51d}$$

$$\epsilon_{32} = \tfrac{1}{2}(\varkappa_3 - \bar{\varkappa}_3)\left(\frac{\partial \varphi_s}{\partial X_2} + X_1\right) \tag{5.51e}$$

5.3.9 Stress tensor

In this paragraph, we simply recall the canonical form of the strain tensor ($\boldsymbol{\mathcal{E}}$) for the cross-section $\mathcal{S}(s)$ in the context of Kirchhoff's approximation :

$$\sigma_{33} = E\epsilon_{33} \tag{5.52a}$$

$$\sigma_{11} = \sigma_{22} = \sigma_{12} = 0 \tag{5.52b}$$

$$\sigma_{31} = 2G\epsilon_{31} \tag{5.52c}$$

$$\sigma_{32} = 2G\epsilon_{32} \tag{5.52d}$$

Thus, the Piola stress vector defined in eq. (5.28b) becomes :

$$\boldsymbol{\sigma_n} = \sigma_{31}\boldsymbol{d}_1 + \sigma_{32}\boldsymbol{d}_2 + \sigma_{33}\boldsymbol{d}_3 \tag{5.53}$$

[40] $\boldsymbol{n} = (\partial f_s/\partial X_1, \partial f_s/\partial X_1)^T$ is the unit normal vector to the boundary curve of $\mathcal{S}(s)$ defined implicitly by the equation $f_s(X_1, X_2) = 0$.

[41] Recent advances [Koo14] in the formfinding of soap films with the force density method might be of practical use to evaluate the warping function.

5.3.10 Constitutive equations for internal forces and moments

In Kirchhoff's theory, constitutive equations for internal forces and moments should not be considered as assumptions. Indeed, as shown hereafter, they are somehow consequences of the assumptions made on the motion – that is the rod remains close to a motion where cross-sections remain planar, undistorted and perpendicular to the centerline – and on the material – the Hookean elasticity – of the rod.

From eq. (5.30a), (5.51a), (5.52a) and (5.53) we deduce the constitutive equation for the axial component of the internal forces : [42]

$$\begin{aligned} F_3 &= \iint_{\mathcal{S}(s)} \boldsymbol{\sigma_n}(X_1, X_2, s, t) \cdot \boldsymbol{d}_3 \, dX_1 dX_2 \\ &= ES\epsilon - (\varkappa_2 - \bar{\varkappa}_2) \iint_{\mathcal{S}(s)} X_1 \, dX_1 dX_2 + (\varkappa_1 - \bar{\varkappa}_1) \iint_{\mathcal{S}(s)} X_2 \, dX_1 dX_2 \\ &= ES\epsilon \end{aligned} \tag{5.54}$$

From eq. (5.30b), (5.51d), (5.51e), (5.52c), (5.52d) and (5.53) we deduce the constitutive equation for the axial component of the internal moments :

$$\begin{aligned} M_3 &= \iint_{\mathcal{S}(s)} (\boldsymbol{r} \times \boldsymbol{\sigma_n}(X_1, X_2, s, t)) \cdot \boldsymbol{d}_3 \, dX_1 dX_2 \\ &= \iint_{\mathcal{S}(s)} -X_2\sigma_{31} + X_1\sigma_{32} \, dX_1 dX_2 \\ &= G(\varkappa_3 - \bar{\varkappa}_3) \iint_{\mathcal{S}(s)} X_1 \left(\frac{\partial \varphi_s}{\partial X_2} + X_1 \right) - X_2 \left(\frac{\partial \varphi_s}{\partial X_1} - X_2 \right) \, dX_1 dX_2 \end{aligned} \tag{5.55}$$

From eq. (5.30b), (5.51a), (5.52a) and (5.53) we deduce the constitutive equation for the first component of the internal moments :

$$\begin{aligned} M_1 &= \iint_{\mathcal{S}(s)} (\boldsymbol{r} \times \boldsymbol{\sigma_n}(X_1, X_2, s, t)) \cdot \boldsymbol{d}_1 \, dX_1 dX_2 \\ &= \iint_{\mathcal{S}(s)} X_2\sigma_{33} \, dX_1 dX_2 \\ &= E(\varkappa_1 - \bar{\varkappa}_1) \iint_{\mathcal{S}(s)} {X_2}^2 \, dX_1 dX_2 \end{aligned} \tag{5.56}$$

From eq. (5.30b), (5.51a), (5.52a) and (5.53) we deduce the constitutive equation for the

[42] Also recall from eq. (5.36) that $\iint_{\mathcal{S}(s)} X_1 \, dX_1 dX_2 = 0$ and $\iint_{\mathcal{S}(s)} X_2 \, dX_1 dX_2 = 0$.

second component of the internal moments :

$$\begin{aligned} M_2 &= \iint_{\mathcal{S}(s)} (\boldsymbol{r} \times \boldsymbol{\sigma_n}(X_1, X_2, s, t)) \cdot \boldsymbol{d}_2 \; dX_1 dX_2 \\ &= \iint_{\mathcal{S}(s)} -X_1 \sigma_{33} \; dX_1 dX_2 \\ &= E(\varkappa_2 - \bar{\varkappa}_2) \iint_{\mathcal{S}(s)} {X_1}^2 \; dX_1 dX_2 \end{aligned} \tag{5.57}$$

5.3.11 Summary of the theory

Let's summarize the assumptions and results of Kirchhoff's theory of rods on which our discret beam model will be based on.

In the reference configuration the rod is described by its reference strains :

$$\bar{\boldsymbol{d}}_i{}' = \bar{\boldsymbol{\varkappa}} \times \bar{\boldsymbol{d}}_i \tag{5.58}$$

In the actual configuration the rod is described by its strains and spin vector :

$$\boldsymbol{x}' = (1+\epsilon)\boldsymbol{t} \tag{5.59a}$$
$$\boldsymbol{d}_i' = \boldsymbol{\varkappa} \times \boldsymbol{d}_i \tag{5.59b}$$
$$\dot{\boldsymbol{d}}_i = \boldsymbol{\omega} \times \boldsymbol{d}_i \tag{5.59c}$$

The rod is subjected to internal forces and moments :

$$\boldsymbol{F} = F_1\boldsymbol{d}_1 + F_2\boldsymbol{d}_2 + F_3\boldsymbol{d}_3 \tag{5.60a}$$
$$\boldsymbol{M} = M_1\boldsymbol{d}_1 + M_2\boldsymbol{d}_2 + M_3\boldsymbol{d}_3 \tag{5.60b}$$

The rod is subjected to external and body loads described as distributed forces and moments acting on the centerline – either given per unit length of the reference configuration ($\bar{\boldsymbol{f}}$, $\bar{\boldsymbol{m}}$) or per unit length of the actual configuration ($\boldsymbol{f}_t$, $\boldsymbol{m}_t$) – and given in the condensed form :

$$\boldsymbol{f} = \bar{\boldsymbol{f}} + (1+\epsilon)\boldsymbol{f}_t = f_1\boldsymbol{d}_1 + f_2\boldsymbol{d}_2 + f_3\boldsymbol{d}_3 \tag{5.61a}$$
$$\boldsymbol{m} = \bar{\boldsymbol{m}} + (1+\epsilon)\boldsymbol{m}_t = m_1\boldsymbol{d}_1 + m_2\boldsymbol{d}_2 + m_3\boldsymbol{d}_3 \tag{5.61b}$$

The internal axial force, the internal bending moments and the internal twisting moment are computed with the following constitutive equations :

$$F_3 = ES\epsilon \tag{5.62a}$$
$$M_1 = EI_1(\varkappa_1 - \bar{\varkappa}_1) \tag{5.62b}$$
$$M_2 = EI_2(\varkappa_2 - \bar{\varkappa}_2) \tag{5.62c}$$
$$M_3 = GJ(\varkappa_3 - \bar{\varkappa}_3) \tag{5.62d}$$

where S, I_1, I_2, J are respectively the area, the second moments of inertia and the torsional stiffness of the cross-section :

$$S = \iint_{\mathcal{S}(s)} dX_1 dX_2 \tag{5.63a}$$
$$I_1 = \iint_{\mathcal{S}(s)} {X_2}^2\, dX_1 dX_2 \tag{5.63b}$$
$$I_2 = \iint_{\mathcal{S}(s)} {X_1}^2\, dX_1 dX_2 \tag{5.63c}$$
$$J = \iint_{\mathcal{S}(s)} X_1\left(\frac{\partial \varphi_s}{\partial X_2} + X_1\right) - X_2\left(\frac{\partial \varphi_s}{\partial X_1} - X_2\right)\, dX_1 dX_2 \tag{5.63d}$$

and φ_s is the warping fonction of the cross-section that satisfies the differential system :

$$0 = \frac{\partial^2 \varphi_s}{\partial {X_1}^2} + \frac{\partial^2 \varphi_s}{\partial {X_2}^2} \qquad , \forall (X_1, X_2) \in \mathcal{S}(s) \tag{5.64a}$$

$$0 = \frac{\partial f_s}{\partial X_1}\left(\frac{\partial \varphi_s}{\partial X_1} - X_2\right) + \frac{\partial f_s}{\partial X_2}\left(\frac{\partial \varphi_s}{\partial X_2} + X_1\right) \qquad , \forall (X_1, X_2) \,/\, f_s(X_1, X_2) = 0 \tag{5.64b}$$

The dynamical equations for the motion of the rod are :

$$\frac{\partial \boldsymbol{F}}{\partial s} + \boldsymbol{f} = \rho S \ddot{\boldsymbol{x}} \tag{5.65a}$$

$$\frac{\partial \boldsymbol{M}}{\partial s} + \frac{\partial \boldsymbol{x}}{\partial s} \times \boldsymbol{F} + \boldsymbol{m} = \rho I_1 \boldsymbol{d}_1 \times \ddot{\boldsymbol{d}}_1 + \rho I_2 \boldsymbol{d}_2 \times \ddot{\boldsymbol{d}}_2 \tag{5.65b}$$

Neglecting the rotational dynamics around $\boldsymbol{d}_1$ and $\boldsymbol{d}_2$ the components of the above equations are written :

$$F_1' + \varkappa_2 F_3 - \varkappa_3 F_2 + f_1 = \rho S \ddot{x}_1 \tag{5.66a}$$

$$F_2' + \varkappa_3 F_1 - \varkappa_1 F_3 + f_2 = \rho S \ddot{x}_2 \tag{5.66b}$$

$$F_3' + \varkappa_1 F_2 - \varkappa_2 F_1 + f_3 = \rho S \ddot{x}_3 \tag{5.66c}$$

$$M_1' + \varkappa_2 M_3 - \varkappa_3 M_2 - (1+\epsilon) F_2 + m_1 \simeq 0 \tag{5.66d}$$

$$M_2' + \varkappa_3 M_1 - \varkappa_1 M_3 + (1+\epsilon) F_1 + m_2 \simeq 0 \tag{5.66e}$$

$$M_3' + \varkappa_1 M_2 - \varkappa_2 M_1 + m_3 \simeq \rho (I_1 + I_2) \dot{\omega}_3 \tag{5.66f}$$

The local displacements of the cross-sections are given by :

$$u_1 = -\nu\epsilon X_1 - \nu(\varkappa_1 - \bar{\varkappa}_1) X_1 X_2 + \tfrac{1}{2}\nu(\varkappa_2 - \bar{\varkappa}_2)({X_1}^2 - {X_2}^2) \tag{5.67a}$$

$$u_2 = -\nu\epsilon X_2 + \nu(\varkappa_2 - \bar{\varkappa}_2) X_1 X_2 + \tfrac{1}{2}\nu(\varkappa_1 - \bar{\varkappa}_1)({X_1}^2 - {X_2}^2) \tag{5.67b}$$

$$u_3 = (\varkappa_3 - \bar{\varkappa}_3)\varphi_s(X_1, X_2) \tag{5.67c}$$

The non-zero components of the strain tensor are given by :

$$\epsilon_{33} = \epsilon + (\varkappa_1 - \bar{\varkappa}_1) X_2 - (\varkappa_2 - \bar{\varkappa}_2) X_1 \tag{5.68a}$$

$$\epsilon_{31} = \tfrac{1}{2}(\varkappa_3 - \bar{\varkappa}_3)\left(\frac{\partial \varphi_s}{\partial X_1} - X_2\right) \tag{5.68b}$$

$$\epsilon_{32} = \tfrac{1}{2}(\varkappa_3 - \bar{\varkappa}_3)\left(\frac{\partial \varphi_s}{\partial X_2} + X_1\right) \tag{5.68c}$$

$$\epsilon_{11} = \epsilon_{22} = -\nu\epsilon_{33} \tag{5.68d}$$

The non-zero components of the stress tensor are given by :

$$\sigma_{33} = E\epsilon_{33} \tag{5.69a}$$

$$\sigma_{31} = 2G\epsilon_{31} \tag{5.69b}$$

$$\sigma_{32} = 2G\epsilon_{32} \tag{5.69c}$$

5.3.12 Comments

- The internal shear forces are reacting parameters and are given by the balance equations. Transverse shear deformations and stresses are not given by the present theory.
- There is a noticeable symmetry in the equations between the roles played by F_1, F_2 and M_1, M_2 and by the roles played by F_2 and M_3.
- Warping is supposed to happen freely.

5.4 Geometric interpretation of Kirchhoff's equations

The previous equations for the motion of the rod (see eq. (5.66a) to (5.66f)) have been established expressing the fundamental principles of balance of linear and angular momentums. An alternative approach, leading to the same results, consists in differentiating the elastic energy of a given configuration of the rod – assumed to be stationary – with respect to the degrees of freedom of the mechanical system (principle of virtual work).[43]
However, the approach through equilibrium seems easier to understood as it is (almost) just a matter of balance between forces and moments on infinitesimal slices of the rods (see fig. 5.5). This is of obvious pedagogical interest as it allows to understand how the geometry of the rod influence the splitting of the elastic energy between extension, flexion and torsion of the rod.
To emphasis this, we provide the proper drawings (see figures 5.6 to 5.8) and computations for the contribution of internal forces and moments to the balance of linear and angular momentums. This is what we call the "geometric interpretation" of Kirchhoff's equations.

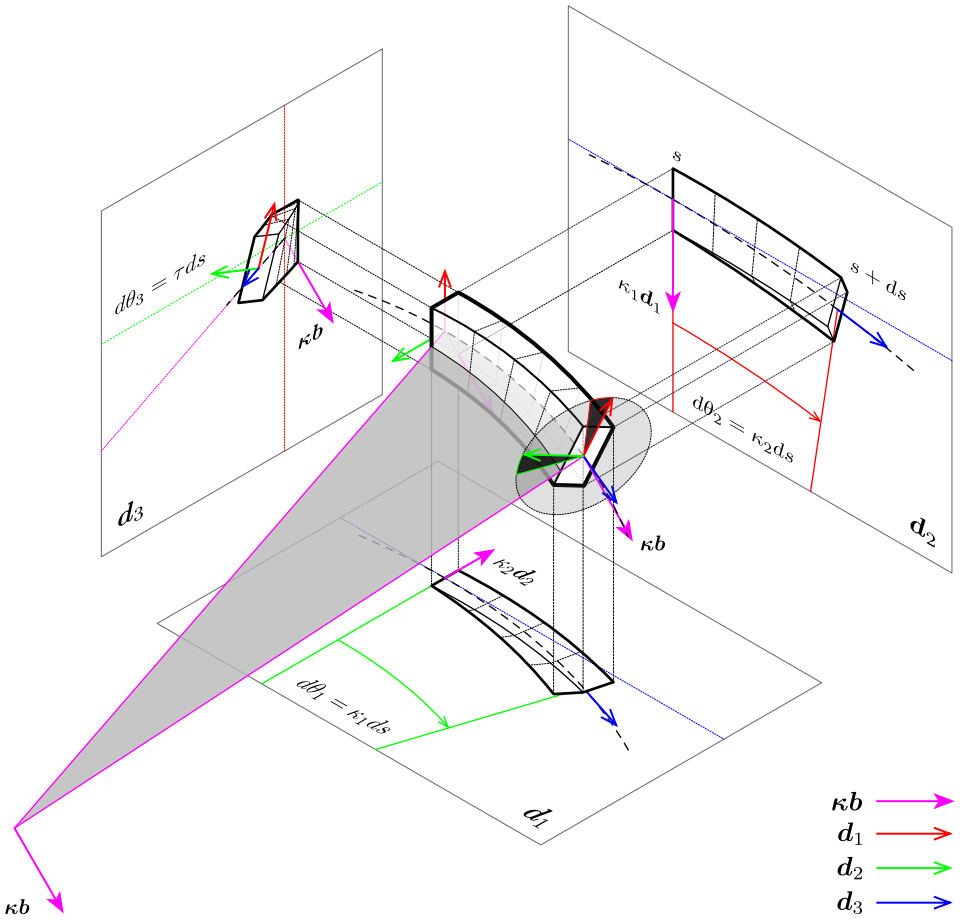

Figure 5.5 – Flexion and torsion of an elementary slice of a Kirchhoff rod of length ds. Projections of the deformations are given in the material planes defined by $\boldsymbol{d}_1$, $\boldsymbol{d}_2$, $\boldsymbol{d}_3$.

[43] This is the approach employed in the theory presented in **??** and is also the one developed in [AAP10], for strictly inextensible rods.

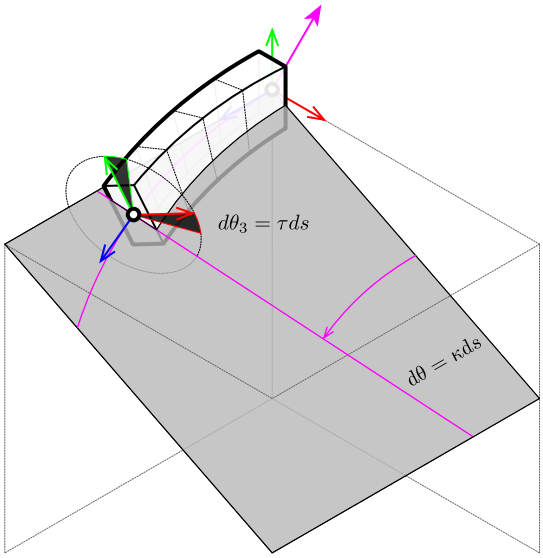

(a) Infinitesimal deformation.

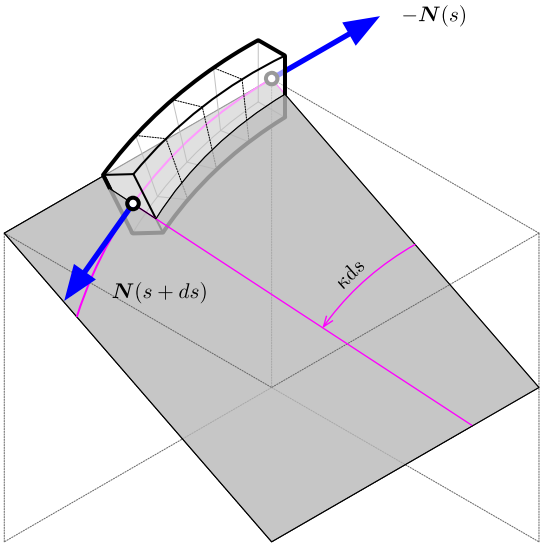

(b) Contributions of the internal forces.

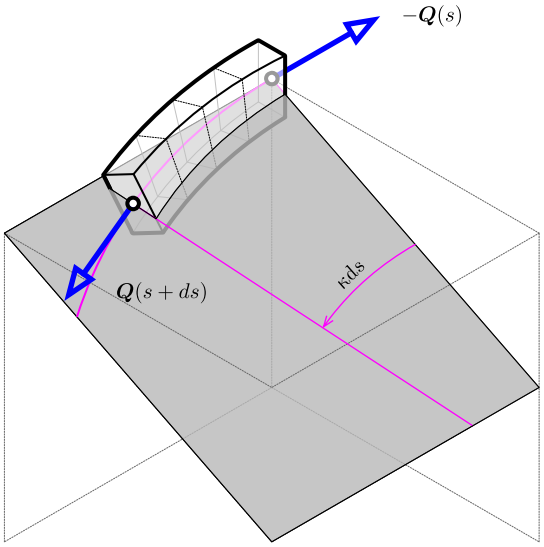

(c) Contributions of the internal moments.

Figure 5.6 – Influence of the curvature (κ) in the deflection of internal forces and moments along the centerline.

Contributions to the balance of forces

$\boldsymbol{N}(s+ds)$ is deflected from $\boldsymbol{d}_3(s)$ by the rotation of angle κds around $\boldsymbol{\kappa b}$ (fig. 5.6b). Thus, its contribution to the balance of forces onto $\boldsymbol{d}_3(s)$ is :

$$N(s+ds)\cos(\kappa ds) - N(s) = N'(s)ds + o(ds)$$

Contributions to the balance of moments

$\boldsymbol{Q}(s+ds)$ is deflected from $\boldsymbol{d}_3(s)$ by the rotation of angle κds around $\boldsymbol{\kappa b}$ (fig. 5.6c). Thus, its contribution to the balance of moments onto $\boldsymbol{d}_3(s)$ is :

$$Q(s+ds)\cos(\kappa ds) - Q(s) = Q'(s)ds + o(ds)$$

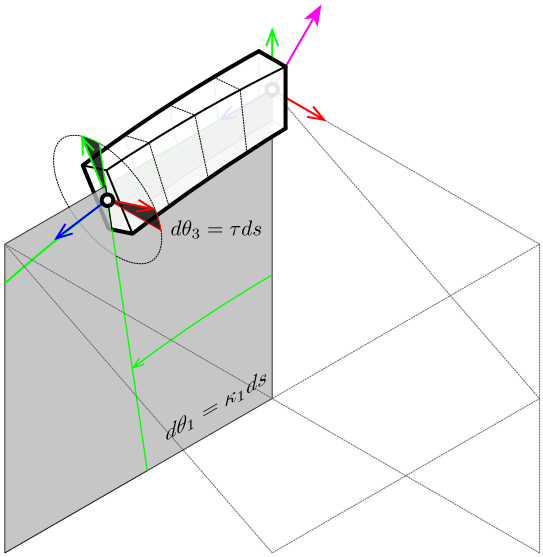

(a) Infinitesimal deformation.

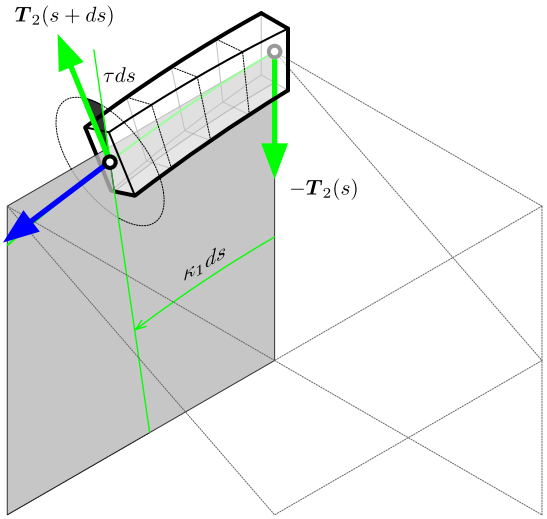

(b) Contributions of the internal forces.

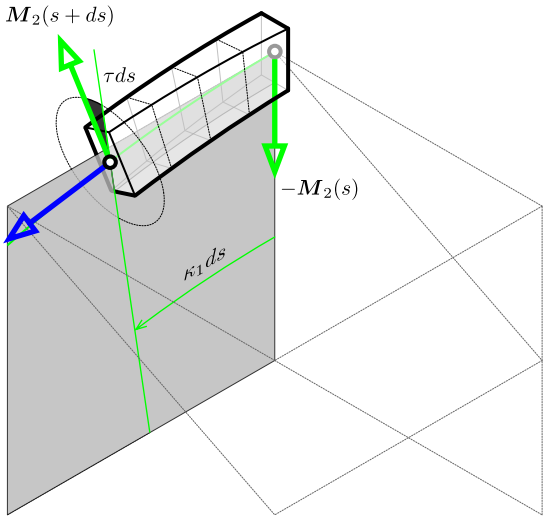

(c) Contributions of the internal moments.

Figure 5.7 – Influence of the first material curvature (κ_1) in the deflection of internal forces and moments along the centerline.

Contributions to the balance of forces

$\boldsymbol{T}_2(s+ds)$ is deflected from $\boldsymbol{d}_2(s)$ by the combined rotations of angle τds around $\boldsymbol{d}_3$ and $\kappa_2 ds$ around $\boldsymbol{d}_2$ (fig. 5.7b). Thus, its contribution to the balance of forces onto $\boldsymbol{d}_1(s)$ is :

$$-T_2(s+ds)\sin(\tau ds)\cos(\kappa_2 ds) = -\tau T_2(s)ds + o(ds)$$

$\boldsymbol{T}_2(s+ds)$ is deflected from $\boldsymbol{d}_2(s)$ by the combined rotations of angle τds around $\boldsymbol{d}_3$ and $\kappa_1 ds$ around $\boldsymbol{d}_1$ (fig. 5.7b). Thus, its contribution to the balance of forces onto $\boldsymbol{d}_2(s)$ is :

$$-T_2(s) + T_2(s+ds)\cos(\tau ds)\cos(\kappa_1 ds) = T_2'(s)ds + o(ds)$$

$\boldsymbol{T}_2(s+ds)$ is deflected from $\boldsymbol{d}_2(s)$ by the combined rotations of angle τds around $\boldsymbol{d}_3$ and $\kappa_1 ds$ around $\boldsymbol{d}_1$ (fig. 5.7b). Thus, its contribution to the balance of forces onto $\boldsymbol{d}_3(s)$ is :

$$T_2(s+ds)\cos(\tau ds)\sin(\kappa_1 ds) = \kappa_1 T_2(s)ds + o(ds)$$

$\boldsymbol{N}(s+ds)$ is deflected from $\boldsymbol{d}_3(s)$ by the combined rotations of angle $\kappa_2 ds$ around $\boldsymbol{d}_2$ and $\kappa_1 ds$ around $\boldsymbol{d}_1$ (fig. 5.7b). Thus, its contribution to the balance of forces onto $\boldsymbol{d}_2(s)$ is :

$$-N(s+ds)\cos(\kappa_2 ds)\sin(\kappa_1 ds) = -\kappa_1 N(s)ds + o(ds)$$

Contributions to the balance of moments

$\boldsymbol{T}_2(s+ds)$ is deflected from the plane normal to $\boldsymbol{d}_1(s)$ by a rotation of angle τds around $\boldsymbol{d}_3$ (fig. 5.7b). It produces a moment around $\boldsymbol{d}_1$ with the lever arm $b = \cos(\kappa_2 ds)ds$. Thus, its contribution to the balance of moments onto $\boldsymbol{d}_1(s)$ is :

$$-T_2(s+ds)\cos(\tau ds)(\cos(\kappa_2 ds)ds) = -T_2(s)ds + o(ds)$$

$\boldsymbol{M}_2(s+ds)$ is deflected from $\boldsymbol{d}_2(s)$ by the combined rotations of angle τds around $\boldsymbol{d}_3$ and $\kappa_2 ds$ around $\boldsymbol{d}_2$ (fig. 5.7c). Thus, its contribution to the balance of moments onto $\boldsymbol{d}_1(s)$ is :

$$-M_2(s+ds)\sin(\tau ds)\cos(\kappa_2 ds) = -\tau M_2(s)ds + o(ds)$$

$\boldsymbol{M}_2(s+ds)$ is deflected from $\boldsymbol{d}_2(s)$ by the combined rotations of angle τds around $\boldsymbol{d}_3$ and $\kappa_1 ds$ around $\boldsymbol{d}_1$ (fig. 5.7c). Thus, its contribution to the balance of moments onto $\boldsymbol{d}_2(s)$ is :

$$-M_2(s) + M_2(s+ds)\cos(\tau ds)\cos(\kappa_1 ds) = M_2'(s)ds + o(ds)$$

$\boldsymbol{M}_2(s+ds)$ is deflected from $\boldsymbol{d}_2(s)$ by the combined rotations of angle τds around $\boldsymbol{d}_3$ and $\kappa_1 ds$ around $\boldsymbol{d}_1$ (fig. 5.7c). Thus, its contribution to the balance of moments onto $\boldsymbol{d}_3(s)$ is :

$$M_2(s+ds)\cos(\tau ds)\sin(\kappa_1 ds) = \kappa_1 M_2(s)ds + o(ds)$$

$\boldsymbol{Q}(s+ds)$ is deflected from $\boldsymbol{d}_3(s)$ by the combined rotations of angle $\kappa_2 ds$ around $\boldsymbol{d}_2$ and $\kappa_1 ds$ around $\boldsymbol{d}_1$ (fig. 5.7c). Thus, its contribution to the balance of moments onto $\boldsymbol{d}_2(s)$ is :

$$-Q(s+ds)\cos(\kappa_2 ds)\sin(\kappa_1 ds) = -\kappa_1 Q(s)ds + o(ds)$$

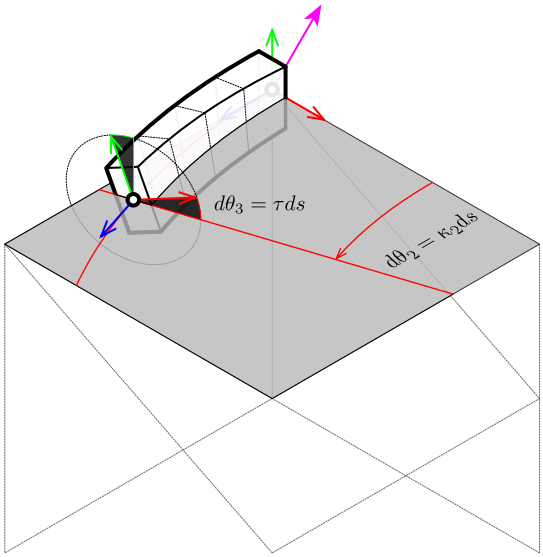

(a) Infinitesimal deformation.

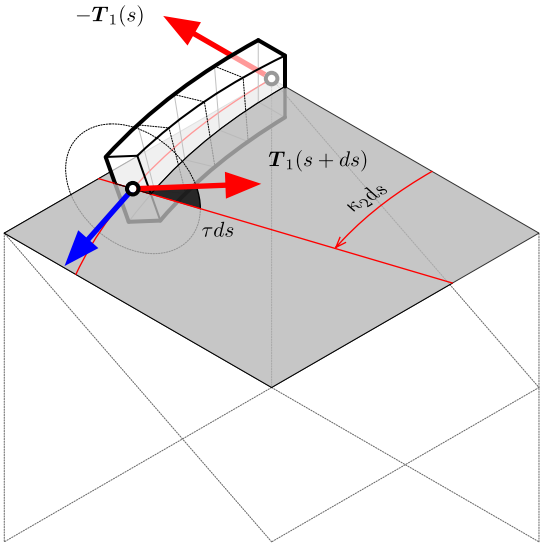

(b) Contributions of the internal forces.

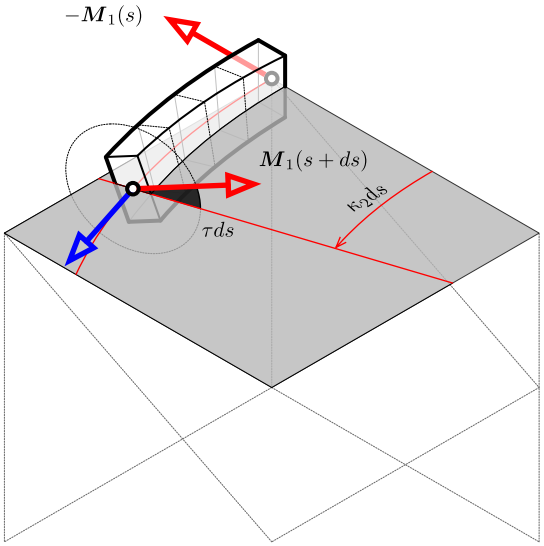

(c) Contributions of the internal moments.

Figure 5.8 – Influence of the second material curvature (κ_2) in the deflection of internal forces and moments along the centerline.

Contributions to the balance of forces

$\boldsymbol{T}_1(s+ds)$ is deflected from $\boldsymbol{d}_1(s)$ by the combined rotations of angle τds around $\boldsymbol{d}_3$ and $\kappa_2 ds$ around $\boldsymbol{d}_2$ (fig. 5.8b). Thus, its contribution to the balance of forces onto $\boldsymbol{d}_1(s)$ is :

$$-T_1(s) + T_1(s+ds)\cos(\tau ds)\cos(\kappa_2 ds) = T_1'(s)ds + o(ds)$$

$\boldsymbol{T}_1(s+ds)$ is deflected from $\boldsymbol{d}_1(s)$ by the combined rotations of angle τds around $\boldsymbol{d}_3$ and $\kappa_1 ds$ around $\boldsymbol{d}_1$ (fig. 5.8b). Thus, its contribution to the balance of forces onto $\boldsymbol{d}_2(s)$ is :

$$T_1(s+ds)\sin(\tau ds)\cos(\kappa_1 ds) = \tau T_1(s)ds + o(ds)$$

$\boldsymbol{T}_1(s+ds)$ is deflected from $\boldsymbol{d}_1(s)$ by the combined rotations of angle τds around $\boldsymbol{d}_3$ and $\kappa_2 ds$ around $\boldsymbol{d}_2$ (fig. 5.8b). Thus, its contribution to the balance of forces onto $\boldsymbol{d}_3(s)$ is :

$$-T_1(s+ds)\cos(\tau ds)\sin(\kappa_2 ds) = -\kappa_2 T_1(s)ds + o(ds)$$

$\boldsymbol{N}(s+ds)$ is deflected from $\boldsymbol{d}_3(s)$ by the combined rotations of angle $\kappa_1 ds$ around $\boldsymbol{d}_1$ and $\kappa_2 ds$ around $\boldsymbol{d}_2$ (fig. 5.8b). Thus, its contribution to the balance of forces onto $\boldsymbol{d}_1(s)$ is :

$$N(s+ds)\cos(\kappa_1 ds)\sin(\kappa_2 ds) = \kappa_2 N(s)ds + o(ds)$$

Contributions to the balance of moments

$\boldsymbol{T}_1(s+ds)$ is deflected from the plane normal to $\boldsymbol{d}_2(s)$ by the angle τds around $\boldsymbol{d}_3$ along ds (fig. 5.8b). It produces a moment around $\boldsymbol{d}_2$ with the lever arm $b = \cos(\kappa_1 ds)ds$. Thus, its contribution to the balance of moments onto $\boldsymbol{d}_2(s)$ is :

$$T_1(s+ds)\cos(\tau ds)(\cos(\kappa_1 ds)ds) = T_1(s)ds + o(ds)$$

$\boldsymbol{M}_1(s+ds)$ is deflected from $\boldsymbol{d}_1(s)$ by the combined rotations of angle τds around $\boldsymbol{d}_3$ and $\kappa_2 ds$ around $\boldsymbol{d}_2$ (fig. 5.8c). Thus, its contribution to the balance of moments onto $\boldsymbol{d}_1(s)$ is :

$$-M_1(s) + M_1(s+ds)\cos(\tau ds)\cos(\kappa_2 ds) = M_1'(s)ds + o(ds)$$

$\boldsymbol{M}_1(s+ds)$ is deflected from $\boldsymbol{d}_1(s)$ by the combined rotations of angle τds around $\boldsymbol{d}_3$ and $\kappa_2 ds$ around $\boldsymbol{d}_2$ (fig. 5.8c). Thus, its contribution to the balance of moments onto $\boldsymbol{d}_2(s)$ is :

$$M_1(s+ds)\sin(\tau ds)\cos(\kappa_2 ds) = \tau M_1(s)ds + o(ds)$$

$\boldsymbol{M}_1(s+ds)$ is deflected from $\boldsymbol{d}_1(s)$ by the combined rotations of angle τds around $\boldsymbol{d}_3$ and $\kappa_2 ds$ around $\boldsymbol{d}_2$ (fig. 5.8c). Thus, its contribution to the balance of moments onto $\boldsymbol{d}_3(s)$ is :

$$-M_1(s+ds)\cos(\tau ds)\sin(\kappa_2 ds) = -\kappa_2 M_1(s)ds + o(ds)$$

$\boldsymbol{Q}(s+ds)$ is deflected from $\boldsymbol{d}_3(s)$ by the combined rotations of angle $\kappa_1 ds$ around $\boldsymbol{d}_1$ and $\kappa_2 ds$ around $\boldsymbol{d}_2$ (fig. 5.8c). Thus, its contribution to the balance of moments onto $\boldsymbol{d}_1(s)$ is :

$$Q(s+ds)\cos(\kappa_1 ds)\sin(\kappa_2 ds) = \kappa_2 Q(s)ds + o(ds)$$

5.5 Numerical resolution

5.5.1 Main hypothesis

On néglige les forces d'inertie liées à la rotation de l'élément (devant quoi ?? traitement quasi-statique par rapport à la rotation). Cette hypothèse est faite explicitement chez Florence Bertail :

Cette hypothèse est faite mais passée sous silence chez Douthe, Adriaenssen, D'Amico lorsqu'ils déduisent l'effort tranchant du moment de flexion.

Principe :

- les équations constitutives permettent le calcul de M_1, M_2, Q à partir de la géométrie $\{\boldsymbol{x}, \theta\}$.

- La seconde loi de kirchhoff projetée sur les axes matériels 1 et 2 de la section me donnent accès aux efforts tranchants T_1 et T_2.

- La seconde loi de kirchhoff projetée sur les axes matériel 3 (tangente à la centerline) de la section me donnent l"hypothèse quasi-statique de Audoly.

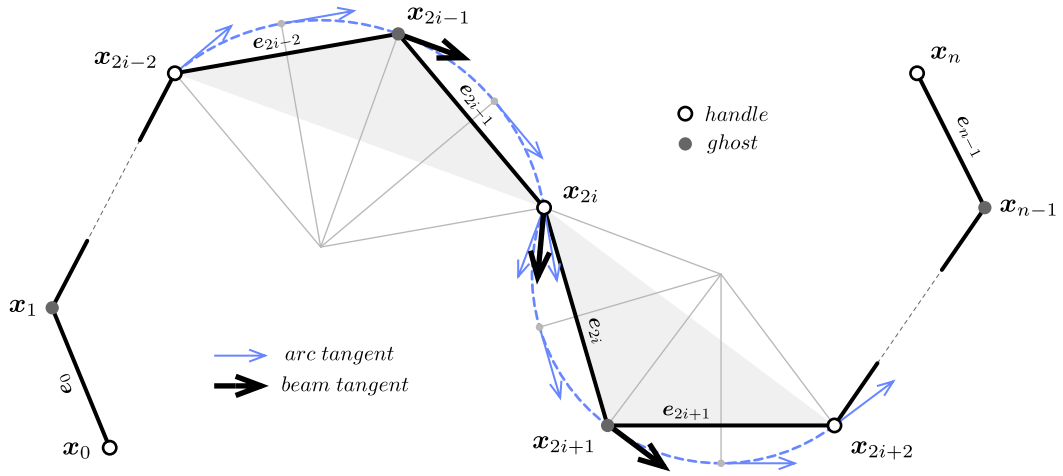

(a) Centerline of the discrete biarc model.

		open	closed
segments	n_s	n_s	n_s
edges	n_e	$2n_s$	$2n_s$
vertices	n	$2n_s + 1$	$2n_s$
ghosts	n_g	n_s	n_s
handles	n_h	$n_s + 1$	n_s

(b) Number of segments, edges and vertices whether the centerline is closed or open.

Figure 5.9 – Biarc model for a discrete beam. The centerline is divided into curved segments (grey solid hatch). Each segment is defined as a three-noded element with uniform material and section properties. It has two end vertices (white) called *handle* as they are used to interact with the model, for instance to apply loads or restrains. It has one mid vertex (grey) called *ghost* as it is used only to enrich the segment kinematics and is not accessible to the end user.

5.5.2 Discret beam model

Let's introduce the discrete biarc model to describe the configuration of a beam. It is composed of a discrete curve called *centerline* and a discrete adapted frame called *material frame* as its axes are chosen to be the principal axes of the beam cross-section (fig. 5.9a). The centerline itself is organized in n_s consecutive adjacent segments which are three-vertices and two-edges elements with uniform material and section properties.

Beams can either be closed or open. The corresponding number of vertices, edges and segments are reported in fig. 5.9b.

Centerline

The discrete centerline is a polygonal space curve (fig. 5.9a) defined as an ordered sequence of $n+1$ pairwise disjoint *vertices* : $\Gamma = (\boldsymbol{x}_0, \boldsymbol{x}_1, \dots, \boldsymbol{x}_n) \in \mathbb{R}^{3(n+1)}$. Consecutive pairs of vertices define n straight segments $(\boldsymbol{e}_0, \boldsymbol{e}_1, \dots, \boldsymbol{e}_{n-1})$ called *edges* and pointing from one vertex to the next one : $\boldsymbol{e}_i = \boldsymbol{x}_{i+1} - \boldsymbol{x}_i$:

$$\begin{cases} \boldsymbol{e}_i = \boldsymbol{x}_{i+1} - \boldsymbol{x}_i \\ l_i = \|\boldsymbol{e}_i\| \\ \boldsymbol{u}_i = \boldsymbol{e}_i / l_i \end{cases} \tag{5.70}$$

The length of the ith edge is denoted l_i and its normalized direction vector is denoted $\boldsymbol{u}_i$. The arc length of the ith vertex is denoted s_i and is given by :

$$\begin{cases} s_0 = 0 & i = 0 \\ s_i = \displaystyle\sum_{k=0}^{i-1} l_k & i \in [\![1, n-1]\!] \\ s_n = L & i = n \end{cases} \tag{5.71}$$

Thus, the centerline is parametrized by arc length and $\Gamma(s_i) = \boldsymbol{x}_i$. Additionally, we define the vertex-based mean length at vertex $\boldsymbol{x}_i$:

$$\begin{cases} \overline{l_0} = \frac{1}{2} l_0 & i = 0 \\ \overline{l_i} = \frac{1}{2}(l_{i-1} + l_i) & i \in [\![1, n-1]\!] \\ \overline{l_n} = \frac{1}{2} l_{n-1} & i = n \end{cases} \tag{5.72}$$

Segments

The discrete centerline is divided into n_s curved segments. Each segment is a three-noded element – see fig. 5.9a where the area covered by a segment is represented as a grey solid hatch. The ith segment is composed of three vertices $(\boldsymbol{x}_{2i}, \boldsymbol{x}_{2i+1}, \boldsymbol{x}_{2i+2})$ spanning two edges $(\boldsymbol{e}_{2i}, \boldsymbol{e}_{2i+1})$. The (i-1)th segment and the ith segment share the same vertex $\boldsymbol{x}_{2i}$ at arc length s_{2i}.

Each segment has two end vertices called *handle* ($\boldsymbol{x}_{2i}, \boldsymbol{x}_{2i+2}$) and one mid vertex called *ghost* ($\boldsymbol{x}_{2i+1}$) as this one is not accessible to the end user in order to interact with the model (link, restrain, loading, ...). Ghost vertices are used only for internal purpose to give a higher richness in the kinematic description of a segment than a two-noded segment would.

We define the *chord length* of the ith segment as the distance between $\boldsymbol{x}_{2i}$ and $\boldsymbol{x}_{2i+2}$: $L_i = \|\boldsymbol{e}_{2i} + \boldsymbol{e}_{2i+1}\|$.

Material and section properties

In addition, the model assumes that a segment has uniform section (S, I_1, I_2, J)[44] and material (E, G)[45] properties over its length : $s \in]s_{2i}, s_{2i+2}[$. For the sake of simplicity, we introduce for further calculations the *material stiffness matrix* ($\boldsymbol{B}_i$) attached to each segment. It has the following form in the material frame basis :

$$\boldsymbol{B}_i = \begin{bmatrix} EI_1 & 0 & 0 \\ 0 & EI_2 & 0 \\ 0 & 0 & GJ \end{bmatrix}_i \tag{5.73}$$

External loads

Also, the model assumes that each segment can be loaded with uniform external distributed forces ($\boldsymbol{f}_{ext}$) and moments ($\boldsymbol{m}_{ext}$).

External loads

External concentrated forces ($\boldsymbol{F}_{ext}$) and moments ($\boldsymbol{M}_{ext}$) are applied to the segment end vertices ($\boldsymbol{x}_{2i}$, $\boldsymbol{x}_{2i+2}$).

This discret model involves that axial, bending and torsion strains, section and material properties will be continuous fonctions of the arc length over each segment $]\boldsymbol{x}_{2i}, \boldsymbol{x}_{2i+2}[$. Discontinuities in strains, internal and external forces, internal and external moments will be located at handle vertices. The left and right limits of this fonctions at handle vertices will be denoted respectively by f^- and f^+. Possibly they are continuous at handle nodes that is the left and right limits agree ($f^- = f^+$).

Lets call : $l_i = \|\boldsymbol{e}_i\|$ with $i \in [0, n_e]$. Lets call : $u_i = \frac{e_i}{l_i}$ with $i \in [0, n_e]$.

Lets call : $L_i = \|\boldsymbol{e}_{2i} + \boldsymbol{e}_{2i+1}\|$ with $i \in [0, n_g]$.

We have : $\boldsymbol{d}_{3,i+1/2} = \boldsymbol{u}_i$

Let $\boldsymbol{B}_i$ be the material stiffness matrix along the principal axes of inertia, uniform over

[44] S is the cross-section area ; I_1, I_2 and J are the cross-section principal moments of inertia.
[45] E is the elastic modulus and G is the shear modulus for the considered material

the slice $]\boldsymbol{x}_{2i}, \boldsymbol{x}_{2i+2}[$. Thus, it has the following form in the material basis :

$$\boldsymbol{B}_i = \begin{bmatrix} EI_1 & 0 & 0 \\ 0 & EI_2 & 0 \\ 0 & 0 & GJ \end{bmatrix}_i \tag{5.74}$$

Thus, one will write the constitutive equations for the bending moment in matrix notation as :

$$\boldsymbol{M}_i = \boldsymbol{B}_i(\boldsymbol{\kappa b}_i - \bar{\boldsymbol{\kappa b}}_i) \tag{5.75}$$

With $\boldsymbol{\kappa b} = \begin{bmatrix} \kappa_1 & \kappa_2 & \tau \end{bmatrix}^T$ expressed in the material frame.

5.5.3 Discret extension and axial force

We assume the axial force ($\boldsymbol{N}$) to vary linearly over $]\boldsymbol{x}_{2i}, \boldsymbol{x}_{2i+2}[$. The variation occurs if the segment is subject to a distributed load f_3, uniform over the segment. Consequently, the axial strain $(1+\epsilon)$ is also required to vary linearly. The value of the axial force and the extension at mid span of each edge are given by :

$$\epsilon_{i+1/2} = \frac{l_i}{\overline{l}_i} - 1 \tag{5.76a}$$

$$\boldsymbol{N_{i+1/2}} = [ES]_i \epsilon_i \boldsymbol{d}_{3,i+1/2} \tag{5.76b}$$

Remark the sign convention : as expected, when edge $\boldsymbol{e}_i$ suffers a positive extension, vertex $\boldsymbol{x}_i$ "attracts" vertex $\boldsymbol{x}_{i-1}$ to it as $\boldsymbol{d}_{3,i+1/2}$ is pointing from $\boldsymbol{x}_i$ towards $\boldsymbol{x}_{i+1}$. Remark also that $\epsilon_{i+1/2} = 0 \Leftrightarrow l_i = \overline{l}_i$ when the rod is not stretched.

5.5.4 Discret bending moments and curvatures

We assume that the internal bending moment and curvature are quadratic functions of the arc length over $]\boldsymbol{x}_{2i}, \boldsymbol{x}_{2i+2}[$. While they must be continuous over this interval, they might be discontinuous at handle vertices and be subjected to jump discontinuities in direction and magnitude.

Curvature at ghost vertices

For a given geometry of the centerline, the curvature binormal vector at ghost vertex $\boldsymbol{x}_{2i-1}$ (resp. $\boldsymbol{x}_{2i+1}$) is computed considering the circumscribed osculating circle passing through the vertices $(\boldsymbol{x}_{2i-2}, \boldsymbol{x}_{2i-1}, \boldsymbol{x}_{2i})$ of the $(i-1)th$ segment – resp. through the vertices $(\boldsymbol{x}_{2i}, \boldsymbol{x}_{2i+1}, \boldsymbol{x}_{2i+2})$ of the *i-th* segment.

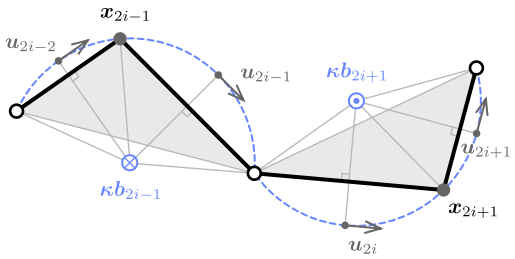

$$\kappa b_{2i-1} = \frac{2}{L_{i-1}} u_{2i-2} \times u_{2i-1}$$

$$\kappa b_{2i+1} = \frac{2}{L_i} u_{2i} \times u_{2i+1}$$

Unit tangent vectors at ghost vertices

This definition of the curvature leads to a natural definition of the unit tangent vector at ghost vertex x_{2i-1} (resp. x_{2i+1}), as the unit vector tangent to the osculating circle of the $(i-1)th$ segment (resp. i-th segment) at that point.

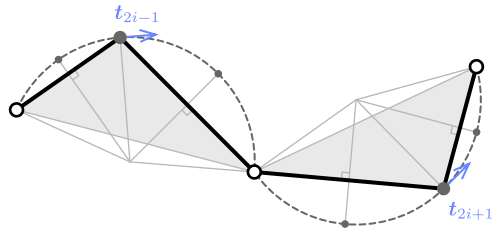

$$t_{2i-1} = \frac{l_{2i-1}}{L_{i-1}} u_{2i-2} + \frac{l_{2i-2}}{L_{i-1}} u_{2i-1}$$

$$t_{2i+1} = \frac{l_{2i+1}}{L_i} u_{2i} + \frac{l_{2i}}{L_i} u_{2i+1}$$

Left/right unit tangent vectors at handle vertices

Equivalently, the definition of the osculating circles of the $(i-1)th$ and i-th segments leads to a natural definition of the left (t^-_{2i}) and right (t^+_{2i}) unit tangent vectors at handle vertex x_{2i}, for segments of uniform curvature. When both segments have the same curvature, left and right vectors agree.

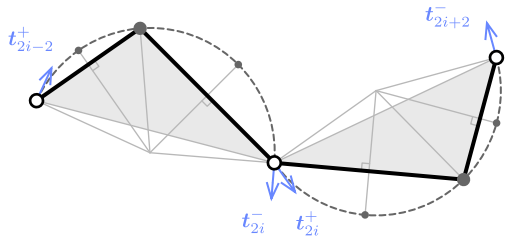

$$t^-_{2i} = 2(t_{2i-1} \cdot u_{2i-1}) u_{2i-1} - t_{2i-1}$$

$$t^+_{2i} = 2(t_{2i+1} \cdot u_{2i}) u_{2i} - t_{2i+1}$$

Unit tangent vectors at handle vertices

The unit tangent vector t_{2i} – that is the beam section normal – at handle vertex x_{2i} is chosen to be the mean of the left and right unit tangent vectors at that vertex.[46]

[46] Consequently, this model assumes that the field of tangents along the centerline is continuous and is thus unable to model cases where the centerline is not at least $\mathcal{C}^1$. In such case the beam must be considered as two parts glued together.

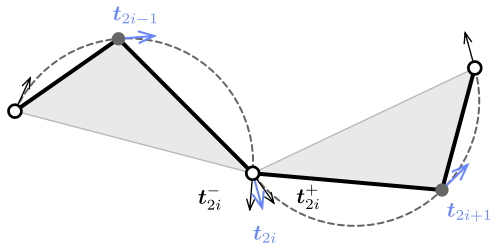

$$\boldsymbol{t}_{2i} = \frac{\boldsymbol{t}_{2i}^- + \boldsymbol{t}_{2i}^+}{\|\boldsymbol{t}_{2i}^- + \boldsymbol{t}_{2i}^+\|}$$

This way, the determination of the tangent vectors – or equivalently the section normals – in the static equilibrium configuration will be done in the flow of the dynamic relaxation process, without the need of introducing any additional degrees of freedom (for instance the usual Euler angles). The position of the vertices rules the orientation of the section normals.

Left/right bending moments at handle vertices

Given the unit tangent vector $\boldsymbol{t}_{2i}$, one can define the left ($\boldsymbol{\kappa}_{2i}^-$) and right ($\boldsymbol{\kappa}_{2i}^+$) curvatures at handle vertex $\boldsymbol{x}_{2i}$. The left curvature is initially evaluated from the left osculating circle, defined as the circle passing through $\boldsymbol{x}_{2i-1}$ and $\boldsymbol{x}_{2i}$ and tangent to $\boldsymbol{t}_{2i}$ at $\boldsymbol{x}_{2i}$. The right curvature is initially evaluated from the right osculating circle, defined as the circle passing through $\boldsymbol{x}_{2i}$ and $\boldsymbol{x}_{2i+1}$ and tangent to $\boldsymbol{t}_{2i}$ at $\boldsymbol{x}_{2i}$.[47,48]

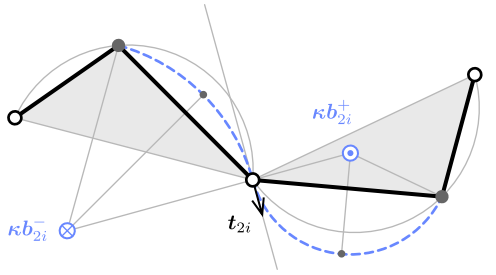

$$\boldsymbol{\kappa b}_{2i}^- = \frac{2}{l_{2i-1}} \boldsymbol{u}_{2i-1} \times \boldsymbol{t}_{2i}$$

$$\boldsymbol{\kappa b}_{2i}^+ = \frac{2}{l_{2i}} \boldsymbol{t}_{2i} \times \boldsymbol{u}_{2i}$$

However, this values need to be adjusted so that the static condition for rotational equilibrium ($\boldsymbol{M}^{ext} + \boldsymbol{M}^+ - \boldsymbol{M}^- = 0$) is satisfied at all time. Then, this condition will be satisfied – in particular – at the end of the solving process. To achieve this goal, we first compute a realistic mean value ($\boldsymbol{M}_{2i}$) for the internal bending moment as :

$$\boldsymbol{M}_{2i} = \frac{1}{2}\boldsymbol{B}_{i-1}(\boldsymbol{\kappa b}_{2i}^- - \bar{\boldsymbol{\kappa b}}_{2i}^-) + \frac{1}{2}\boldsymbol{B}_i(\boldsymbol{\kappa b}_{2i}^+ - \bar{\boldsymbol{\kappa b}}_{2i}^+) \tag{5.77}$$

To enforce the jump discontinuity in bending moment ($\boldsymbol{M}^{ext} = \boldsymbol{M}^- - \boldsymbol{M}^+$) across the

[47] Remark that the centerline is now approximated with a biarc in the vicinity of $\boldsymbol{x}_{2i}$. This is the reason why this model is called the "biarc model".

[48] This model offers the ability to represent discontinuities in curvature – thus in bending moment – at handle vertices as the left and right curvatures does not necessarily agree. This is quite different from the classical 3-dof element [Bar99, ABW99, DBC06] which assumes that the curvature – thus the bending moment – is $\mathcal{C}^0$ and can be evaluated at every vertices from the circumscribed osculating circle.

handle vertex, we define the left and right bending moments at $\boldsymbol{x}_{2i}$ as :

$$\boldsymbol{M}_{2i}^{-} = \boldsymbol{M}_{2i} + \frac{1}{2}\boldsymbol{M}_{2i}^{ext} \tag{5.78a}$$

$$\boldsymbol{M}_{2i}^{+} = \boldsymbol{M}_{2i} - \frac{1}{2}\boldsymbol{M}_{2i}^{ext} \tag{5.78b}$$

Note that in the case where no external concentrated bending moment is applied to the handle vertex, the internal bending moment is continuous across the vertex.

Left/right curvatures at handle vertices

Finally, the left and right curvatures at handle vertex $\boldsymbol{x}_{2i}$ are computed back with the constitutive law :

$$\boldsymbol{\kappa b}_{2i}^{-} = \boldsymbol{B}_{i-1}^{-1}\boldsymbol{M}_{2i}^{-} + \boldsymbol{\kappa}\bar{\boldsymbol{b}}_{2i}^{-} \tag{5.79a}$$

$$\boldsymbol{\kappa b}_{2i}^{+} = \boldsymbol{B}_{i}^{-1}\boldsymbol{M}_{2i}^{+} + \boldsymbol{\kappa}\bar{\boldsymbol{b}}_{2i}^{+} \tag{5.79b}$$

Bending moment at ghost vertices

The internal bending moment at ghost vertices is simply given by the constitutive law as :

$$\boldsymbol{M}_{2i-1} = \boldsymbol{B}_{i-1}(\boldsymbol{\kappa b}_{2i-1} - \boldsymbol{\kappa}\bar{\boldsymbol{b}}_{2i-1}) \tag{5.80a}$$

$$\boldsymbol{M}_{2i+1} = \boldsymbol{B}_{i}(\boldsymbol{\kappa b}_{2i+1} - \boldsymbol{\kappa}\bar{\boldsymbol{b}}_{2i+1}) \tag{5.80b}$$

5.5.5 Discret twisting moment

We assume the twisting moment and the rate of twist to vary linearly over $]\boldsymbol{x}_{2i}, \boldsymbol{x}_{2i+2}[$. Thus, the rate of twist at mid edge is given by :

$$\tau_{i+1/2} = \frac{\Delta\theta_i}{l_i} \tag{5.81}$$

And $\theta_{i+1} - \theta_i$ is the additional twisting angle between two frames with parallel transport.

$$Q_{i+1/2} = GJ(\tau_{i+1/2} - \overline{\tau}_{i+1/2}) \tag{5.82}$$

5.5.6 Discret axial force

We assume the axial force and the axial strain to vary linearly over $]\boldsymbol{x}_{2i}, \boldsymbol{x}_{2i+2}[$. Thus, the axial strain at mid edge is given by :

$$\epsilon_{i+1/2} = \frac{l_i}{\overline{l}_i} - 1 \tag{5.83}$$

$$N_{i+1/2} = ES\epsilon_{i+1/2} \tag{5.84}$$

5.5.7 Discret shear force

Shear forces are computed from the second Kirchhoff law, considering that the inertial term is negligible.

$$\boldsymbol{F}_{i+1/2} = \boldsymbol{d}_{3,i+1/2} \times (\boldsymbol{M}'_{i+1/2} + \boldsymbol{m}_{ext,i}) + Q_{i+1/2}\boldsymbol{\kappa b}_{i+1/2} - \tau_{i+1/2}\boldsymbol{M}_{i+1/2} \tag{5.85}$$

5.5.8 Interpolation

5.6 Conclusion

Remind that the beam is subject to a distributed external force $\boldsymbol{f}_{ext}$ and a distributed external moment $\boldsymbol{m}_{ext}$.

We neglect rotational inertial effects on $\boldsymbol{d}_1$ et $\boldsymbol{d}_2$ in (**??**) and (**??**) which leads to the following shear force :

$$\boldsymbol{F}^{\perp}(s) = \boldsymbol{d}_3 \times (\boldsymbol{M}' + \boldsymbol{\varkappa} \times \boldsymbol{M} + \boldsymbol{m}_{ext}) \tag{5.86}$$

$$\boldsymbol{F}^{\parallel}(s) = N\boldsymbol{d}_3 \tag{5.87}$$

We may neglect as well the last term ($\tau\boldsymbol{M}$) and get back to the shear force obtained by the variational approach.The total internal force acting on the beam is hence given by :

$$\boldsymbol{F}(s) = \boldsymbol{N}(s) + \boldsymbol{T}(s) \tag{5.88}$$

Sections are subject to the following rotational moment around the centerline :

$$\boldsymbol{\Gamma}(s) = Q' + \boldsymbol{d}_3 \cdot (\kappa\boldsymbol{b} \times \boldsymbol{M} + \boldsymbol{m}_{ext}) \tag{5.89}$$

Bibliography

[AAP10] Basile Audoly, M Amar, and Yves Pomeau. *Elasticity and geometry*. 2010.

[ABW99] Sigrid Adriaenssens, Michael Barnes, and Christopher Williams. A new analytic and numerical basis for the form-finding and analysis of spline and gridshell structures. In B Kumar and B H V Topping, editors, *Computing Developments in Civil and Structural Engineering*, pages 83–91. Civil-Comp Press, Edinburgh, 1999.

[Alv14] João Manuel Alves. *Dynamic analysis of bridge girders subjected to moving loads : Numerical and analytical beam models considering warping effects*. PhD thesis, Tecnico Lisboa, 2014.

[Ant74] Stuart Antman. Kirchhoff's problem for nonlinearly elastic rods. *Quarterly of Applied Mathematics*, XXXIV(3):221–240, 1974.

[Ant05] Stuart Antman. *Nonlinear problems of elasticity*. Applied mathematical sciences. Springer, New York, 2005.

[BAK13] Michael Barnes, Sigrid Adriaenssens, and Meghan Krupka. A novel torsion/bending element for dynamic relaxation modeling. *Computers & Structures*, 119:60–67, apr 2013.

[Bar99] Michael Barnes. Form finding and analysis of tension structures by dynamic relaxation. *International Journal of Space Structures*, 14(2):89–104, 1999.

[BAV+10] Miklós Bergou, Basile Audoly, Etienne Vouga, Max Wardetzky, and Eitan Grinspun. Discrete viscous threads. *ACM Transactions on ...*, pages 1–10, 2010.

[Ben91a] Edoardo Benvenuto. *An introduction to the history of structural mechanics : statics and resistance of solids*. Springer Verlag, New York, 1991.

[Ben91b] Edoardo Benvenuto. *An introduction to the history of structural mechanics : vaulted structures and elastic systems*. Springer Verlag, New York, 1991.

[CBd13] Romain Casati and Florence Bertails-descoubes. Super space clothoids. In *SIGGRAPH*, 2013.

[CDL+93] Bernard Coleman, Ellis Harold Dill, Mazario Lembo, Lu Zheng, and Irwin Tobias. On the dynamics of rods in the theory of Kirchhoff and Clebsch. *Archive for Rational Mechanics and Analysis*, 121(4):339–359, 1993.

[CH02] J Cisternas and P Holmes. Buckling of extensible thermoelastic rods. *Mathematical and Computer Modelling*, 36(3):233–243, 2002.

[Cle83] Alfred Clebsch. *Théorie de l'élasticité des corps solides*. Dunod, Paris, 1883.

[CMPP09] A Campanile, M Mandarino, V Piscopo, and A Pranzitelli. On the exact solution of non-uniform torsion for beams with asymmetric cross-section. *World Academy of Science, Engineering and Technology*, 31:36–45, 2009.

[DA14] Marcelo A. Dias and Basile Audoly. A non-linear rod model for folded elastic strips. *Journal of the Mechanics and Physics of Solids*, 62(1):57–80, 2014.

[DA15] Marcelo A. Dias and Basile Audoly. "Wunderlich, meet kirchhoff" : a general and unified description of elastic ribbons and thin rods. *Journal of Elasticity*, 119(1):49–66, 2015.

[Day65] Alister Day. An Introduction to dynamic relaxation. *The Engineer*, 1965.

[DBC06] Cyril Douthe, Olivier Baverel, and Jean-François Caron. Formfinding of a grid shell in composite materials. *Journal of the IASS*, 47:53–62, 2006.

[Dil92] Ellis Harold Dill. Kirchhoff's theory of rods. *Archive for History of Exact Sciences*, page 23, 1992.

[DKZ14] B. D'Amico, A. Kermani, and H. Zhang. Form finding and structural analysis of actively bent timber grid shells. *Engineering Structures*, 81:195–207, 2014.

[DLP13] Ye Duan, Dong Li, and P. Frank Pai. Geometrically exact physics-based modeling and computer animation of highly flexible 1D mechanical systems. *Graphical Models*, 75(2):56–68, 2013.

[dPTL+15] Lionel du Peloux, Frédéric Tayeb, Baptiste Lefevre, Olivier Baverel, and Jean-François Caron. Formulation of a 4-DoF torsion / bending element for the formfinding of elastic gridshells. In *Proceedings of the International Association for Shell and Spatial Structures*, number August, pages 1–14, Amsterdam, 2015.

[DZK16] B. D'Amico, H. Zhang, and A. Kermani. A finite-difference formulation of elastic rod for the design of actively bent structures. *Engineering Structures*, 117:518–527, 2016.

[Elt84] Edit Elter. Two formuli of the shear center. *Periodica Polytechnica Mechanical Engineering*, 28(2-3):179–193, 1984.

[Hoo06] P C J Hoogenboom. 7 Vlasov torsion theory. (October):1–12, 2006.

[Kir50] Gustav Kirchhoff. *Über das gleichgewicht und die bewegung einer elastischen scheibe*. Berlin, 1850.

[Kir76] Gustav Kirchhoff. *Vorlesungen über mathematische, physik, mechanik*. Leipzig, 1876.

[Koo14] K Koohestani. Nonlinear force density method for the form-finding of minimal surface membrane structures. *Communications in Nonlinear Science and Numerical Simulation*, 19(6):2071–2087, 2014.

[LL09] Holger Lang and Joachim Linn. Lagrangian field theory in space-time for geometrically exact Cosserat rods. 150:21, 2009.

[Lov92] Augustus Love. *A treatise on the mathematical theory of elasticity*. Cambridge University Press, first edition, 1892.

[LS96] Joel Langer and David Singer. Lagrangian Aspects of the Kirchhoff elastic rod. *Society for Industrial and Applied Mathematics Review*, 38(4):605–618, 1996.

[MG16] David Manta and Rodrigo Gonçalves. A geometrically exact Kirchhoff beam model including torsion warping. *Computers and Structures*, 177:192–203, 2016.

[MLG13] D.E. Moulton, Th. Lessinnes, and A Goriely. Morphoelastic rods. Part I : A single growing elastic rod. *Journal of the Mechanics and Physics of Solids*, 61(2):398–427, 2013.

[MPW14] Christoph Meier, Alexander Popp, and Wolfgang A. Wall. An objective 3D large deformation finite element formulation for geometrically exact curved Kirchhoff rods. *Computer Methods in Applied Mechanics and Engineering*, 278(August):445–478, 2014.

[Neu09] S. Neukirch. *Enroulement, contact et vibrations de tiges élastiques*. PhD thesis, 2009.

[Pra03] Ludwig Prandtl. Zur torsion von prismatischen stäben. *Physikalische Zeitschrift*, 4:758–770, 1903.

[Rei73] E. Reissner. On one-dimensional large-fisplacement finite-strain beam theory. *Studies in Applied Mathematics*, 52(2):87–95, 1973.

[Rei81] E Reissner. On the effect of shear center location on the values of axial and lateral cantilever buckling loads for singly symmetric cross-section beams. *Journal of Applied Mathematics and Physics*, 32(1):182–188, 1981.

[SBH95] Yaoming Shi, Andrey E. Borovik, and John E. Hearst. Elastic rod model incorporating shear and extension, generalized nonlinear Schrödinger equations, and novel closed-form solutions for supercoiled DNA. *The Journal of Chemical Physics*, 103(8):3166–3183, 1995.

[Spi08] Jonas Spillmann. *CORDE : Cosserat rod elements for the animation of interacting elastic rods*. PhD thesis, 2008.

[TG51] Stephen Timoshenko and James Norman Goodier. *Theory of elasticity*. McGraw-Hill, New York, second edition, 1951.

[The07] Adrien Theetten. *Splines dynamiques géométriquement exactes : simulation haute performance et interaction*. PhD thesis, Université des Sciences et Technologies de Lille, 2007.

[Tim21] Stephen Timoshenko. On the correction for shear of the differential equation for transverse vibrations of prismatic bars. *Philosophical Magazine Series 6*, 41(245):744–746, 1921.

[Tim22] Stephen Timoshenko. On the transverse vibrations of bars of uniform cross-section. *Philosophical Magazine Series 6*, 43(253):125–131, 1922.

[Tim45a] Stephen Timoshenko. Theory of bending, torsion and buckling of thin-walled members of open cross section : Part I. *Journal of The Franklin Institute*, 239(3):201–219, 1945.

[Tim45b] Stephen Timoshenko. Theory of bending, torsion and buckling of thin-walled members of open cross section : Part II. *Journal of The Franklin Institute*, 249(4):249–268, 1945.

[Tim45c] Stephen Timoshenko. Theory of bending, torsion and buckling of thin-walled members of open cross section : Part III. *Journal of The Franklin Institute*, 239(5):343–336, 1945.

[Vet14] Yury Vetyukov. *Nonlinear mechanics of thin-walled structures : asymptotics, direct approach and numerical analysis*. 1 edition, 2014.

[Vil97] Piero Villaggio. *Mathematical models for elastic structures*. Cambridge University Press, 1997.

[Vla61] Vasilii Zakharovich Vlasov. *Thin-walled elastic beams*. National Technical Information Service, second edition, 1961.

[Wak80] David Wakefield. *Dynamic relaxation analysis of pretensioned networks supported by compression arches*. PhD thesis, City University London, 1980.

[Wei02] H Weiss. Dynamics of geometrically nonlinear rods : Mechanical models and equations of motion. *Nonlinear Dynamics*, 30:357–381, 2002.

A Calculus of variations

A.1 Introduction

In this appendix we drawback essential mathematical concepts for the calculus of variations. Recall how the notion of energy, gradients are extended to function spaces.

[AMR02]

A.2 Spaces

A.2.1 Normed space

A *normed space* $V(\mathbb{K})$ is a vector space V over the scalar field $\mathbb{K}$ with a norm $\|.\|$.

A *norm* is a map $\|.\| : V \times V \longmapsto \mathbb{K}$ which satisfies :

$$\forall x \in V, \qquad \|x\| = 0_{\mathbb{K}} \Rightarrow x = 0_V \tag{A.1a}$$

$$\forall x \in V, \forall \lambda \in \mathbb{K}, \qquad \|\lambda x\| = |\lambda| \, \|x\| \tag{A.1b}$$

$$\forall (x, y) \in V^2, \qquad \|x + y\| \leqslant \|x\| + \|y\| \tag{A.1c}$$

A.2.2 Inner product space

A *inner product space* or *pre-hilbert space* $E(\mathbb{K})$ is a vector space E over the scalar field $\mathbb{K}$ with an inner product.

An *inner product* is a map $\langle \, ; \, \rangle : E \times E \longmapsto \mathbb{K}$ which is bilinear, symmetric and positive-

definite :

$$\forall (x,y,z) \in E^3, \forall (\lambda,\mu) \in \mathbb{K}^2, \quad \begin{aligned} &\langle \lambda x \ + \mu y \,;\, z\rangle = \lambda\langle x \,;\, z\rangle + \mu\langle y \,;\, z\rangle \\ &\langle x \,;\, \lambda y + \mu z\rangle = \lambda\langle x \,;\, y\rangle + \mu\langle x \,;\, z\rangle \end{aligned} \tag{A.2a}$$

$$\forall (x,y) \in E^2, \quad \langle x \,;\, y\rangle = \langle y \,;\, x\rangle \tag{A.2b}$$

$$\forall x \in E, \quad \langle x \,;\, x\rangle \geqslant 0_{\mathbb{K}} \tag{A.2c}$$

$$\forall x \in E, \quad \langle x \,;\, x\rangle = 0_{\mathbb{K}} \Rightarrow x = 0_E \tag{A.2d}$$

Moreover, an inner product naturally induces a norm on E defined by :

$$\forall x \in E, \quad \|x\| = \sqrt{\langle x \,;\, x\rangle} \tag{A.3}$$

Thus, an inner product vector space is also naturally a normed vector space.

A.2.3 Euclidean space

An *Euclidean space* $\mathcal{E}(\mathbb{R})$ is a finite-dimensional real vector space with an inner product. Thus, distances and angles between vectors could be defined and measured regarding to the norm associated with the chosen inner product.

An Euclidean space is nothing but a finite-dimensional real pre-hilbert space.

A.2.4 Banach space

A *Banach space* $\mathcal{B}(\mathbb{K})$ is a complete normed vector space, which means that it is a normed vector space in which every Cauchy sequence of $\mathcal{B}$ converges in $\mathcal{B}$ for the given norm.

Thus, a Banach space is a vector space with a metric that allows the computation of vector length and distance between vectors and is complete in the sense that a Cauchy sequence of vectors always converges to a well defined limit in that space.

A.2.5 Hilbert space

A *Hilbert space* is an inner product vector space $\mathcal{H}(\mathbb{K})$ such that the natural norm induced by the inner product turns $\mathcal{H}$ into a complete metric space (i.e. every Cauchy sequence of $\mathcal{H}$ converges in $\mathcal{H}$).

The Hilbert space concept is a generalization of the Euclidean space concept. In physics it's common to encounter Hilbert spaces as infinite-dimensional function spaces.

Hilbert spaces are Banach spaces, but the converse does not hold generally.

For example, $\mathcal{L}^2([a,b])$ is an infinite-dimensional Hilbert space with the canonical inner product $\langle f \,;\, g\rangle = \int_a^b fg$.

Note that $\mathcal{L}^2$ is the only Hilbert space among the $\mathcal{L}^p$ spaces.

A.3 Derivative

The well known notion of function derivative in $\mathbb{R}^{\mathbb{R}}$ can be extended to maps between Banach spaces. This is useful in physics when formulating problems as variational problems, usually in terms of energy minimization. Indeed, energy is generally defined over a functional vector space and not simply over the real line.

In this case, the research of minimal values of a potential energy rests on the calculus of variations of the energy function compared to variations to other functions defining the problem (geometry, materials, boundary conditions, ...).

Mathematical concepts extended well-known notions of derivative, jacobian and hessian in Euclidean spaces (typically $\mathbb{R}^2$ or $\mathbb{R}^3$) for Banach functional spaces.

A.3.1 Fréchet derivative

Differentiability

Let $\mathcal{B}_V$ and $\mathcal{B}_W$ be two Banach spaces and $U \subset \mathcal{B}_V$ an open subset of $\mathcal{B}_V$. Let $f : u \longmapsto f(u)$ be a function of $U^{\mathcal{B}_W}$. f is said to be *Fréchet differentiable* at $u_0 \in U$ if there exists a continious linear operator $\boldsymbol{D}f(u_0) \in \mathcal{L}(\mathcal{B}_V, \mathcal{B}_W)$ such that :

$$\lim_{h \to 0} \frac{f(u_0 + h) - f(u_0) - \boldsymbol{D}f(u_0) \cdot h}{\|h\|} = 0 \tag{A.4a}$$

Or, equivalently :

$$f(u_0 + h) = f(u_0) + \boldsymbol{D}f(u_0) \cdot h + o(h) \quad , \quad \lim_{h \to 0} \frac{o(h)}{\|h\|} = 0 \tag{A.4b}$$

In the literature, it is common to found the following notations : $df = \boldsymbol{D}f(u_0) \cdot h = \boldsymbol{D}f_{u_0}(h) = \boldsymbol{D}f(u_0, h)$ for the differential of f, which means nothing but $\boldsymbol{D}f(u_0)$ is linear regarding h. The dot denotes the evaluation of $\boldsymbol{D}f(u_0)$ at h. This notation can be ambiguous as far as the linearity of $\boldsymbol{D}f(u_0)$ in h is denoted as a product which is not explicitly defined.

Derivative

If f is Fréchet differentiable at $u_0 \in U$, the continous linear operator $\boldsymbol{D}f(u_0) \in \mathcal{L}(\mathcal{B}_V, \mathcal{B}_W)$ is called the *Fréchet derivative* of f at u_0 and is also denoted :

$$f'(u_0) = \boldsymbol{D}f(u_0) \tag{A.5}$$

f is said to be $\mathcal{C}^1$ in the sens of Fréchet if f is Fréchet differentiable for all $u \in U$ and the function $\boldsymbol{D}f : u \longmapsto f'(u)$ of $U^{\mathcal{L}(\mathcal{B}_V, \mathcal{B}_W)}$ is continuous.

Differential or total derivative

$df = \boldsymbol{D}f(u_0) \cdot h$ is sometimes called the *differential* or *total derivative* of f and represents the change in the function f for a perturbation h from u_0.

Higer derivatives

Because the differential of f is a linear map from $\mathcal{B}_V$ to $\mathcal{L}(\mathcal{B}_V, \mathcal{B}_W)$ it is possible to look for the differentiability of $\boldsymbol{D}f$. If it exists, it is denoted $\boldsymbol{D}^2 f$ and maps $\mathcal{B}_V$ to $\mathcal{L}(\mathcal{B}_V, \mathcal{L}(\mathcal{B}_V, \mathcal{B}_W))$.

A.3.2 Gâteaux derivative

Directional derivative

Let $\mathcal{B}_V$ and $\mathcal{B}_W$ be two Banach spaces and $U \subset \mathcal{B}_V$ an open subset of $\mathcal{B}_V$. Let $f : u \longmapsto f(u)$ be a function of $U^{\mathcal{B}_W}$. f is said to have a *derivative in the direction* $h \in \mathcal{B}_V$ at $u_0 \in U$ if :

$$\frac{d}{d\lambda} f(u_0 + \lambda h)\Big|_{\lambda=0} = \lim_{\lambda \to 0} \frac{f(u_0 + \lambda h) - f(u_0)}{\lambda} \tag{A.6}$$

exists. This element of $\mathcal{B}_W$ is called the *directional derivative* of f in the direction h at u_0.

Differentiability

Let $\mathcal{B}_V$ and $\mathcal{B}_W$ be two Banach spaces and $U \subset \mathcal{B}_V$ an open subset of $\mathcal{B}_V$. Let $f : u \longmapsto f(u)$ be a function of $U^{\mathcal{B}_W}$. f is said to be *Gâteaux differentiable* at $u_0 \in U$ if there exists a continious linear operator $\boldsymbol{D}f(u_0) \in \mathcal{L}(\mathcal{B}_V, \mathcal{B}_W)$ such that :

$$\forall h \in \mathcal{U}, \quad \lim_{\lambda \to 0} \frac{f(u_0 + \lambda h) - f(u_0)}{\lambda} = \frac{d}{d\lambda} f(u_0 + \lambda h)\Big|_{\lambda=0} = \boldsymbol{D}f(u_0) \cdot h \tag{A.7a}$$

Or, equivalently :

$$\forall h \in \mathcal{U}, \quad f(u + \lambda h) = f(u) + \lambda \boldsymbol{D}f(u_0) \cdot h + o(\lambda) \quad , \quad \lim_{\lambda \to 0} \frac{o(\lambda)}{\lambda} = 0 \tag{A.7b}$$

In other words, it means that all the directional derivatives of f exist at u_0.

Derivative

If f is Gâteaux differentiable at $u_0 \in U$, the continous linear operator $\boldsymbol{D}f(u_0) \in \mathcal{L}(\mathcal{B}_V, \mathcal{B}_W)$ is called the *Gâteaux derivative* of f at u_0 and is also denoted :

$$f'(u_0) = \boldsymbol{D}f(u_0) \tag{A.8}$$

f is said to be $\mathcal{C}^1$ in the sens of Gâteaux if f is Gâteaux differentiable for all $u \in U$ and the function $\boldsymbol{D}f : u \longmapsto f'(u)$ of $U^{\mathcal{L}(\mathcal{B}_V, \mathcal{B}_W)}$ is continuous.

The Gâteaux derivative is a weaker form of derivative than the Fréchet derivative. If f is Fréchet differentiable, then it is also Gâteaux differentiable and its Fréchet and Gâteaux derivatives agree, but the converse does not hold generally.

A.3.3 Useful properties

Let $\mathcal{B}_V$, $\mathcal{B}_W$ and $\mathcal{B}_Z$ be three Banach spaces. Let $f, g : \mathcal{B}_V \longmapsto \mathcal{B}_W$ and $h : \mathcal{B}_W \longmapsto \mathcal{B}_Z$ be three Gâteaux differentiable functions. Then, the following useful properties holds :

$$\boldsymbol{D}(f+g)(u) = \boldsymbol{D}f(u) + \boldsymbol{D}g(u) \tag{A.9}$$

$$\boldsymbol{D}(f \circ h)(u) = \boldsymbol{D}h(f(u)) \circ \boldsymbol{D}f(u) = \boldsymbol{D}h(f(u)) \cdot \boldsymbol{D}f(u) \tag{A.10}$$

Recall that the composition of $\boldsymbol{D}h(f(u))$ with $\boldsymbol{D}f(u)$ means "$\boldsymbol{D}h(f(u))$ applied to $\boldsymbol{D}f(u)$" and is also denoted by $\cdot$ as explained previously.

A.3.4 Partial derivative

Following [AMR02] the main results on partial derivatives of two-variables functions are presented here. They are generalizable to n-variables functions.

Definition

Let $\mathcal{B}_{V_1}$, $\mathcal{B}_{V_2}$ and $\mathcal{B}_W$ be three Banach spaces and $U \subset \mathcal{B}_{V_1} \oplus \mathcal{B}_{V_2}$ an open subset of $\mathcal{B}_{V_1} \oplus \mathcal{B}_{V_2}$. Let $f : u \longmapsto f(u)$ be a function of $U^{\mathcal{B}_W}$. Let $u_0 = (u_{01}, u_{02}) \in U$. If the derivatives of the following functions exist :

$$f_1 : \begin{array}{ccc} \mathcal{B}_{V_1} & \longrightarrow & \mathcal{B}_W \\ u_1 & \longmapsto & f(u_1, u_{02}) \end{array} \quad , \quad f_2 : \begin{array}{ccc} \mathcal{B}_{V_2} & \longrightarrow & \mathcal{B}_W \\ u_2 & \longmapsto & f(u_{01}, u_2) \end{array} \tag{A.11}$$

they are called *partial derivatives* of f at u_0 and are denoted $\boldsymbol{D}_1 f(u_0) \in \mathcal{L}(\mathcal{B}_{V_1}, \mathcal{B}_W)$ and $\boldsymbol{D}_2 f(u_0) \in \mathcal{L}(\mathcal{B}_{V_2}, \mathcal{B}_W)$.

Differentiability

Let $\mathcal{B}_{V_1}$, $\mathcal{B}_{V_2}$ and $\mathcal{B}_W$ be three Banach spaces and $U \subset \mathcal{B}_{V_1} \oplus \mathcal{B}_{V_2}$ an open subset of $\mathcal{B}_{V_1} \oplus \mathcal{B}_{V_2}$. Let $f : u \longmapsto f(u)$ be a function of $U^{\mathcal{B}_W}$. If f is differentiable, then the partial derivatives exist and satisfy for all $h = (h_1, h_2) \in \mathcal{B}_{V_1} \oplus \mathcal{B}_{V_2}$:

$$\boldsymbol{D}_1 f(u) \cdot h_1 = \boldsymbol{D} f(u) \cdot (h_1, 0) \tag{A.12}$$

$$\boldsymbol{D}_2 f(u) \cdot h_2 = \boldsymbol{D} f(u) \cdot (0, h_2) \tag{A.13}$$

$$\boldsymbol{D} f(u) \cdot (h_1, h_2) = \boldsymbol{D}_1 f(u) \cdot h_1 + \boldsymbol{D}_2 f(u) \cdot h_2 \tag{A.14}$$

A.4 Gradient vector

Let $\mathcal{H}$ be a Hilbert space with the inner product denoted $\langle \, , \rangle$. Let $U \subset \mathcal{H}$ an open subset of $\mathcal{H}$. Let $F : u \longmapsto F(u)$ be a scalar function of $U^{\mathbb{R}}$. The *gradient* of F is the map $grad\ F : x \longmapsto (grad\ F)(x)$ of $U^{\mathcal{H}}$ such that :

$$\forall h \in \mathcal{H}, \quad \langle (grad\ F)(x) \, , h \rangle = \boldsymbol{D} F(x) \cdot h \tag{A.15}$$

Note that the gradient vector depends on the chosen inner product. For $\mathcal{H} = \mathbb{R}^n$ with the canonical inner product, one can recall the usual definition of the gradient vector and the corresponding linear approximation of F :

$$\boldsymbol{F}_{x+h} = \boldsymbol{F}_x + (grad\ F)_x^T H + \boldsymbol{o}(H) \quad , \quad grad\ F_x = \begin{bmatrix} \frac{\partial F}{\partial x_1} \\ \vdots \\ \frac{\partial F}{\partial x_n} \end{bmatrix} \in \mathbb{R}^n \tag{A.16}$$

Recall that the canonical inner product on $\mathbb{R}^n$ is such that $\langle x \, , y \rangle = X^T Y$ in a column vector representation. In this case it is common to denote $grad\ F = \nabla F$.

For function spaces the usual definition of the gradient can be extended. For instance if F is a scalar function on $\mathcal{L}^2$, the gradient of F is the unique function (if it exists) from $\mathcal{L}^2$ which satisfies :

$$\forall h \in \mathcal{L}^2, \quad \boldsymbol{D} F(x) \cdot h = \langle (grad\ F)(x) \, , h \rangle = \int (grad\ F) h \tag{A.17}$$

In this case it is common to denote $grad\ F = \frac{\delta F}{\delta x}$. The gradient is also known as the *functional derivative*. The existence and unicity of $grad\ F$ is ensured by the *Riesz representation theorem*.

A.5 Jacobian matrix

Let f be a differentiable function from $\mathbb{R}^n$ to $\mathbb{R}^m$. The *differential* or *total derivative* of such a fonction is a linear application from $\mathbb{R}^n$ to $\mathbb{R}^m$ which could be represented with the

following matrix called the *jacobian matrix* :

$$\boldsymbol{D}f(x) = \boldsymbol{J}_x = \frac{df}{dx} = \begin{bmatrix} \frac{\partial f}{\partial x_1} & \cdots & \frac{\partial f}{\partial x_n} \end{bmatrix} = \begin{bmatrix} \frac{\partial f_1}{\partial x_1} & \cdots & \frac{\partial f_1}{\partial x_n} \\ \vdots & \ddots & \vdots \\ \frac{\partial f_m}{\partial x_1} & \cdots & \frac{\partial f_m}{\partial x_n} \end{bmatrix} \in \mathcal{M}_{m,n}(\mathbb{R}) \tag{A.18}$$

Thus, with the matrix notation, the Taylor expansion takes the following form :

$$\boldsymbol{F}_{x+h} = \boldsymbol{F}_x + \boldsymbol{J}_x H + \boldsymbol{o}(H) \tag{A.19}$$

In the cas $m = 1$, the jacobian matrix of the functional F is nothing but the gradient vector transpose itself :

$$\boldsymbol{D}F(x) = \boldsymbol{J}_x = \frac{dF}{dx} = \begin{bmatrix} \frac{\partial F}{\partial x_1} & \cdots & \frac{\partial F}{\partial x_n} \end{bmatrix} = \nabla F^T \tag{A.20}$$

A.6 Hessian

Let F be a differentiable scalar function from $\mathbb{R}^n$ to $\mathbb{R}$. The second order differential of such a fonction is a linear application from $\mathbb{R}^n$ to $\mathbb{R}^n$ which could be represented with the following matrix called the *hessian matrix* :

$$\boldsymbol{D}^2F(x) = \boldsymbol{H}_x = \frac{d^2F}{dx}(x) = \begin{bmatrix} \frac{\partial F_1^2}{\partial x_1^2} & \frac{\partial F_1^2}{\partial x_1 \partial x_2} & \cdots & \frac{\partial F_1^2}{\partial x_1 \partial x_n} \\ \frac{\partial F_1^2}{\partial x_2 \partial x_1} & \frac{\partial F_1^2}{\partial x_2^2} & \cdots & \frac{\partial F_1^2}{\partial x_2 \partial x_n} \\ \vdots & & \ddots & \vdots \\ \frac{\partial F_p^2}{\partial x_n \partial x_1} & \frac{\partial F_p^2}{\partial x_n \partial x_2} & \cdots & \frac{\partial F_p^2}{\partial x_n^2} \end{bmatrix} \in \mathcal{M}_{n,n}(\mathbb{R}) \tag{A.21}$$

Thus, with the matrix notation, the Taylor expansion takes the following form :

$$\boldsymbol{F}_{x+h} = \boldsymbol{F}_x + \boldsymbol{J}_x H + \tfrac{1}{2} H^T \boldsymbol{H}_x H + \boldsymbol{o}(H) \tag{A.22}$$

A.7 Functional

A *functional* is a map from a vector space $E(\mathbb{K})$ into its underlying scalar field $\mathbb{K}$. Here $\mathcal{E}_p[\boldsymbol{x}, \theta]$ is a functional depending over $\boldsymbol{x}$ and θ.

Bibliography

[AMR02] Ralph Abraham, Jerrold E. Marsde, and Tudor Ratiu. *Manifolds, Tensor Analysis, and Applications (Ralph Abraham, Jerrold E. Marsden and Tudor Ratiu)*. 2002.